An unbiased template of the *Drosophila* brain and ventral nerve cord

John A Bogovic[1*], Hideo Otsuna[1], Larissa Heinrich[1], Masayoshi Ito[1], Jennifer Jeter[1], Geoffrey Meissner[1], Aljoscha Nern[1], Jennifer Colonell[1], Oz Malkesman[1], Kei Ito[2], and Stephan Saalfeld[1*]

[1]Janelia Research Campus, HHMI, Ashburn, VA, USA
[2]Institute of Zoology, University of Cologne, Germany
[*]bogovicj@janelia.hhmi.org, saalfelds@janelia.hhmi.org

July 24, 2018

Abstract

The fruit fly *Drosophila melanogaster* is an important model organism for neuroscience with a wide array of genetic tools that enable the mapping of individuals neurons and neural subtypes. Brain templates are essential for comparative biological studies because they enable analyzing many individuals in a common reference space. Several central brain templates exist for *Drosophila*, but every one is either biased, uses sub-optimal tissue preparation, is imaged at low resolution, or does not account for artifacts. No publicly available *Drosophila* ventral nerve cord template currently exists. In this work, we created high-resolution templates of the *Drosophila* brain and ventral nerve cord using the best-available technologies for imaging, artifact correction, stitching, and template construction using groupwise registration. We evaluated our central brain template against the four most competitive, publicly available brain templates and demonstrate that ours enables more accurate registration with fewer local deformations in shorter time.

1 Introduction and Related work

Canonical templates (or "atlases") of stereotypical anatomy are vital in inter-subject biological studies. In neuroscience, atlases of the central nervous

system have become an important tool for cumulative and comparative studies. Neuroanatomical templates for humans (Talairach and Tournoux, 1988; Lancaster et al., 2000), mouse (Allen Institute for Brain Science, 2015; Lein et al., 2007), C. *elegans* (Long et al., 2009), and *Drosophila* (Jenett et al., 2012; Aso et al., 2014; Arganda-Carreras et al., 2018) have been valuable and influential for studies of anatomy, function, and behavior (Ashburner et al., 1998; Aso et al., 2014; Panser et al., 2016; Robie et al., 2017).

For a template space to be useful, one must be able to reliably find spatial transformations between individual subjects and that template. The transformation must be capable of expressing the biological variability so that stereotypical anatomical features of many transformed subjects are well aligned in template space. This serves to normalize for "irrelevant" sources of variability while comparing across a population. Early templates used simple affine spatial transformations (Talairach and Tournoux, 1988), for which identifying a small number of stereotypical landmarks was sufficient. More recently, image registration has enabled the computation of more flexible (elastic, diffeomorphic, etc. Sotiras et al., 2013) transformations to be found between pairs of images. As a result, modern templates consist of a representative digital image of the anatomy and imaging modality of interest, which is used as the target (or "fixed" image) for image registration, which generates the spatial transformation (Maurer and Fitzpatrick, 1993).

Transforming individual subjects' anatomy to a template space enables the comparison and analysis of a cohort of individuals in a common reference space. Typical registration approaches are either feature/landmark-based, as in Peng et al. (2011), or pixel based, using generic image registration software libraries, such as ANTs (Avants et al., 2009) or CMTK (Rohlfing and Maurer, 2003). If the template itself has anatomical labels superimposed, then it also enables an individual's anatomy to be labeled via the spatial transformation to the template (Cabezas et al., 2011).

The fruit fly *Drosophila melanogaster* is an important model organism for neuroscience. The availability of powerful genetic tools that enable precise imaging and manipulation of specific neuronal populations (Luan et al., 2006; Pfeiffer et al., 2010; Tirian and Dickson, 2017) have made possible many important biological experiments. For example, the Fly-circuit database by Chiang et al. (2011) reconstructed approximately 16,000 neurons in *Drosophila* from light microscopy. Jenett et al. (2012) produced and imaged 6,650 GAL4 lines that have enabled the cataloging of a wide array of neurons in the *Drosophila* central nervous system. Among other advances, these resources enabled the creation of a spatial map of projec-

tion neurons for the lateral horn and mushroom body of *Drosophila* (Jefferis et al., 2007). Panser et al. (2016) generated a spatial clustering of the *Drosophila* brain into functional units on the basis of enhancer expression. Using over 2,000 GAL4 lines, Robie et al. (2017) created a whole brain map linking behavior to brain regions. Yu et al. (2013) explore *Drosophila* development, analyzing the connectivity of neuronal lineages by neuropil compartment.

Canonical templates and spatial alignment are an important aspect of the above studies that leverage genetic tools and imagery in *Drosophila*. Any given line labels a different neuronal population, and so it is necessary to perform comparisons in a canonical space. Many brain templates exist for *Drosophila*, a summary of which we give below:

Rein et al. (2002) generated a template starting with 28 individual brains, stained with nc82 (Kittel et al., 2006) and imaged at $0.6 \times 0.6 \times 1.1\,\mu\text{m}$ resolution. The template brain was chosen as the individual with "the average volume for each substructure." Registration was done by first estimating a global rigid, then estimating a per-structure rigid or similarity transformation which was interpolated over space.

Jenett et al. (2012) selected a representative confocal image of a female fly brain, imaged at $0.62 \times 0.62 \times 1.0\,\mu\text{m/px}$ as a standard brain for their GAL4 driver line resource, and was later resampled in z to an isotropic resolution of $0.62\,\mu\text{m/px}$. We will refer to this template as JFRC 2010.

Aso et al. (2014) selected another single female brain as their JFRC 2013 template. It comprises five stitched tiles, imaged at $0.19 \times 0.19 \times 0.38\,\mu\text{m/px}$, then down-sampled to an isotropic resolution of $0.38 \times 0.38 \times 0.38\,\mu\text{m/px}$. Since the JFRC 2010 and JFRC 2013 templates consist of a brain image of a single individual fly, we will call these "individual templates."

Ito et al. (2014) introduced the "Ito half-brain" as their reference standard. It includes a rich set of compartment labels for neuropil boundaries and fiber bundles but automatic registration of whole brains to this standard is not straightforward.

The female, male, and unisex FCWB templates by Ostrovsky and Jefferis (2014) were generated from images manually selected from the FlyCircuit database (Chiang et al., 2011), imaged at $0.32 \times 0.32 \times 1.0\,\mu\text{m/px}$, using groupwise registration (Avants and Gee, 2004) with the CMTK tool. Groupwise registration is the process of co-registering a set of images without specifying one particular image as the registration target and thereby avoids bias. Seventeen brain samples were used for the female template and nine for the male template. The two gendered average brain templates were themselves registered and averaged with equal weight to create a uni-

sex template.

Arganda-Carreras et al. (2018) recently used groupwise registration with the ANTs tool to generate an improved unbiased *Drosophila* brain template from ten individual fly brains, imaged at $0.6 \times 0.6 \times 0.98$ µm/px and labeled with the nc82 antibody. We call this the "Tefor" template. To measure registration performance, the authors compare overlap of anatomical labels of individuals after registration, and conclude that templates generated by groupwise registration outperform templates consisting of an individual brain image.

Given the abundance of brain templates for *Drosophila*, Manton et al. (2014) created "bridging transformations" that align many of these templates, including JFRC 2010, JFRC 2013, FCWB, and the Ito half-brain. Bridging transformations link previously disparate data-sets and thereby enable comparisons across all datasets in the space of any of these templates. The combination of neuronal database, image registration, and brain template has made neuron matching with NBLAST (Costa et al., 2016) an important technology. NBLAST has also recently found success matching neurons obtained from different, complementary data-sets (Schlegel et al., 2017), including the first complete electron microscopy (EM) volume of the female adult fly brain (FAFB) generated by Zheng et al. (2017). This image volume enables the complete tracing of every neuron and identification of synapses spanning the central brain in a single individual, and is potentially a very useful reference standard brain.

Meinertzhagen (2018) describes how neurons identified from LM will offer an important form of validation for neurons traced in EM, either manually or automatically. This capability depends on spatial alignment between the two modalities. A plugin for Fiji (Schindelin et al., 2012) called ELM (`github.com/saalfeldlab/elm`) is a custom wrapper of the BigWarp (Bogovic et al., 2016) plugin, and was used to manually place landmark point correspondences between the LM template and generate a spatial transformation from the EM space to the JFRC 2013 template space.

Using this registration, Zheng et al. (2017) showed that neurons traced in FAFB can be matched with neurons cataloged from light microscopy (LM), a capability that will enable researchers to simultaneously leverage the advantages of each modality: dense connectivity from EM, and cell type, neurotransmitter, gene expression, etc. information from LM (Schlegel et al., 2017).

While studies of the *Drosophila* ventral nerve cord (VNC) are numerous and ongoing (Prokop and Technau, 1991; Stockinger et al., 2005; Lacin and Truman, 2016), efforts in generating a standard anatomical coordinate

system are somewhat lacking. Brner and Duch (2010) created a standard *Drosophila* VNC, but to our knowledge, the data are not publicly available; thus its impact is limited. Recently, Court et al. (2017) developed a standard nomenclature for the ventral nervous system.

In summary, all existing *Drosophila* brain templates lack certain desirable characteristics. Some consist of a individual samples and are therefore biased. Those that use groupwise registration to avoid bias use a small number of subjects, imaged at relatively low resolution and do not leverage new advances in tissue preparation, imaging, and artifact correction. No publicly available groupwise averaged ventral nerve cord template exists.

1.1 Contributions

We generated unbiased, symmetric, high-resolution, male, female, and unisex templates for the *Drosophila* brain and ventral nerve cord using the newest advances in tissue preparation, imaging, artifact correction, and image stitching. The images of individual samples that comprised the template were acquired at high resolution of $0.19 \times 0.19 \times 0.38\,\mu\text{m/px}$. We used groupwise image registration to ensure that the shape of the resulting template is not biased toward our choice of subject. Figure 1 shows the female, unisex, and male templates for the *Drosophila* central brain and ventral nerve cord. We call this set of templates "JRC 2018."

We performed a thorough comparison using the four most competitive publicly available *Drosophila* brain templates, measuring registration quality, amount of deformation, and computational cost. Each template was evaluated using six different choices of registration algorithms/parameter settings. We show that *Drosophila* brain samples register significantly *better*, *faster*, and with *less local deformation* to our JRC 2018 template than to any prior template, enabling more accurate comparison studies than previously possible.

We also generated a new, automatic registration between the female full adult fly brain (FAFB) electron microscopy data-set of Zheng et al. (2017) using automated synapse predictions (Heinrich et al., 2018). This registration is more data-driven, less likely to suffer from variable error, and potentially better regularized than the existing manual registration generated with ELM (Zheng et al., 2017; Bogovic et al., 2016).

The templates and transformations can be found on-line at `https://www.janelia.org/lab/saalfeld-lab/resources/jrc-2018-templates`.

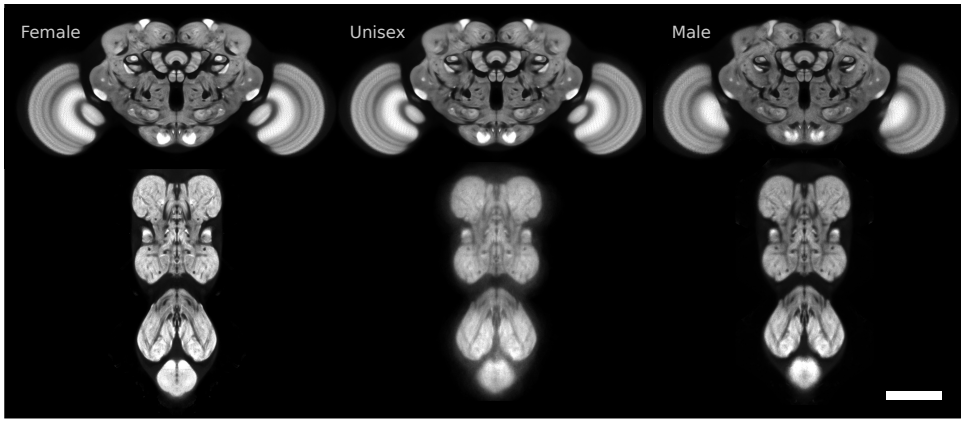

Figure 1: Slices of the six templates we created for female, unisex, and male *Drosophila* central brains and ventral nerve cords. Scale bar 100 µm.

2 Materials and Methods

2.1 Sample Preparation and Image Acquisition

2.1.1 Template data

All samples were based on the transgene brp-SNAP (Kohl et al., 2014) and labeled with 2 µM Cy2 SNAP-tag ligand (Grimm et al., 2017). Samples were fixed for 55 minutes in 2% PFA at room temperature, SNAP-tag labeled for 15 minutes at room temperature, then fixed for 4 hours in 4% PFA at room temperature. Samples were dehydrated in ethanol, cleared in xylene, and mounted in DPX, as described at `https://www.janelia.org/project-team/flylight/protocols` (Aso et al., 2014; Nern et al., 2015). Samples were imaged unidirectionally on six Zeiss 710 LSM confocal microscopes with Plan Apo 63×/1.4 Oil DIC 420780/2-9900 lenses, at a resolution of 0.19 µm/px, in tiles of 1024 × 1024 px (192.6 × 192.6 µm), a pixel dwell time of 1.27 µm, a z-interval of 0.38 µm, and a pinhole of 1 AU to 488 nm. Brains were imaged in five overlapping tiles, VNCs in three. Scanning was controlled by Zeiss ZEN 2010 software and a custom MultiTime macro, as described by Jenett et al. (2012).

Tiles were corrected for lens-distortion and chromatic aberration (see Section 2.2) and stitched with Fiji's (Schindelin et al., 2012) stitching plugin (Preibisch et al., 2009). Custom scripts were used to parallelize processing on the Janelia CPU cluster. For template construction, 62 central brains (36 female) and 75 ventral nerve cords (36 female) were acquired.

2.1.2 Evaluation data

For evaluation, we chose 20 female flies imaged with both an nc82 channel and a channel in which neuronal membrane of a split GAL4 driver line were labeled with a myristoylated FLAG reporter, as described by Aso et al. (2014). We selected four split GAL4 lines that label neurons with broad arborization, that together, cover nearly the whole brain. Maximum intensity projections of the neuronal membrane channel for these lines are shown in Figure 2. Our testing cohort consisted of 20 individuals in total, summarized in Table 1. As a result, our evaluation includes measurements across the whole brain and does not focus on a particular subset of the anatomy.

Line		#
JRC_SS23204	GMR_13F04-p65ADZp in attP40 and GMR_13B05-ZpGDBD in attP2	2
JRC_SS23206	GMR_28F06-p65ADZp in attP40 and GMR_13B05-ZpGDBD in attP2	2
JRC_SS23208	GMR_40F04-p65ADZp in attP40 and GMR_13B05-ZpGDBD in attP2	2
JRC_SS30756	GMR_15C12-p65ADZp in attP40 and GMR_64B11-ZpGDBD in attP2	3
JRC_SS30777	GMR_70D06-p65ADZp in attP40 and GMR_64B11-ZpGDBD in attP2	2
JRC_SS33007	GMR_54H04-p65ADZp in attP40 and GMR_10D10-ZpGDBD in attP2	3
JRC_SS33017	GMR_67A07-p65ADZp in attP40 and GMR_35G08-ZpGDBD in attP2	3
JRC_SS32529	GMR_21G11-p65ADZp in attP40 and GMR_78H08-ZpGDBD in attP2	3

Table 1: Split GAL4 driver lines chosen for evaluation with the count of the number of subjects per line (#).

2.2 Lens Distortion and Chromatic Aberration Correction

2.2.1 Re-usable Calibration Slides

Measurements to establish and update the calibration models were made by imaging multicolor beads mounted, like the tissue samples, on #1.5H cover slips. The beads are 1 µm silica (Polysciences 24326-15), functionalized through reaction with tri-ethoxy-sliane-PEG biotin (Nanocs #PEG6-0023). The biotinylated surface was labeled with a mixture of dye-labeled streptavidin. The dyes were Alexa 488 (ThermoFisher S32354), cy3 (Jackson Immunoresearch 016-160-084), Alexa 594 (ThermoFisher S32356), and Atto647N (Sigma-Aldrich 94149-1MG). The beads were deposited out of tris-buffered saline onto plasma cleaned coverslips, dried, and mounted in DPX according to the same tissue mounting protocol described above.

2.2.2 Distortion Correction

Image stack mosaics of 4×4 tiles with 50–60% overlap were taken using the same settings as described above. Image stacks were acquired in two passes, first at 488 nm and 594 nm, then at 488 nm, 561 nm, and 647 nm.

Channels were separated and max-intensity projections for each single channel tile were created with a custom Fiji script. Single channel 4×4 mosaics were imported as individual layers in TrakEM2 (Cardona et al., 2012). Channel mosaics were pre-stitched to account for stage shift. A non-linear lens-distortion correction model for each channel was estimated with a new extended version of the method by Kaynig et al. (2010) that we made available in TrakEM2. Lens-corrected channel mosaics were stitched and then all channels were globally aligned with an affine transformation model. The composition of the non-linear lens-correction model and the affine alignment transformation correct for both lens-deformation and chromatic aberration. These correction models were generated and exported, for all confocal microscopes (five Zeiss LSM 710's and one Zeiss LSM 780). Finally, they were applied to individual 3D image stacks of *Drosophila* brain samples prior to stitching.

We recorded detailed video instructions to reproduce the calibration protocol and made them available on Youtube: `https://www.youtube.com/watch?v=lPt-WQuniUs`. Code can be found on-line at `https://github.com/saalfeldlab/confocal-lens`.

2.3 Neuron skeletonization

We computed skeletons from the neuron channel by first applying 3D direction-selective local-thresholding (DSLT) (Kawase et al., 2015) to each raw image tile. DLST convolves the image with multiple scaled and rotated cylindrical kernels. We used kernel radii of 2, 6, and 10 voxels. The maximum response was thresholded to give a neuron mask. This mask was transformed along with the tile during image stitching, and then skeletonized using the 3D Skeletonization plugin in Fiji (Schindelin et al., 2012).

2.4 Template construction

We constructed our template using groupwise registration, which seeks to find both an average shape and average intensity across all individuals in a cohort and is described in Avants and Gee (2004) and Avants et al. (2011) The script `buildtemplateparallel.sh` that is part of the ANTs library, im-

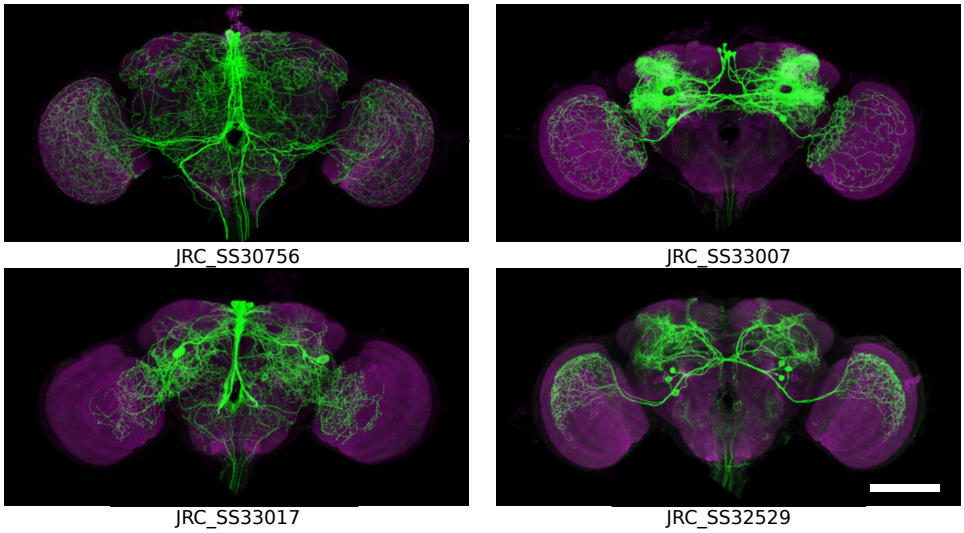

Figure 2: Maximum intensity projections of individuals from four of the GAL4 driver lines used to evaluate registration accuracy (magenta nc82, green GAL4). Notice the broad arborization spanning most of the central brain and optic lobes. Scale bar 100 µm.

plements this. Our modifications, descried below, can be found on-line at https://github.com/saalfeldlab/template-building.

Groupwise registration begins with an initial template - often a single individual or the average of the unregistered cohort of images is selected (we chose the latter). Next, every individual is registered to that initial template using a particular registration algorithm (transformation model, similarity measure, optimization scheme) and then transformed to the template space. Next, the set of transformed individuals are averaged and the transformations are averaged. This yields new mean intensities as well as a mean transformation from subject to the current template estimate. Finally, the new mean intensity image is transformed through the inverse of the mean transformation to obtain a new template. This procedure of registration-averaging-transformation is iterated to transport the initial template toward the mean intensity and shape.

We made several changes seeking to reduce the amount of deformation possible during registration. First, we used the elastic transformation model rather than SyN diffeomorphic model (Avants et al., 2009). Second, we regularized the transform more strongly, the details of which can be found in our open source repository. We sought to generate a template with

left-right symmetry. Similar to the approach in Allen Institute for Brain Science (2015), we left-right flipped every individual brain and VNC in our cohort and included both the original and flipped images in the groupwise registration procedure. This doubled both our effective image count and computational expense during groupwise registration.

We down-sampled the raw and left-right flipped images to 0.76 µm/px isotropic resolution prior to running groupwise registration in order to reduce computational cost/runtime. We believe that this downsampling did not have an appreciable effect on the template construction. This is supported by experiments we performed showing that lower resolution templates can have similarly good performance as high resolution templates (see Appendix A.4). The final template was obtained by applying the transformation computed at low resolution to the original, high resolution images, resulting in a high resolution template. All templates were rendered at 0.19 µm/px isotropic resolution. This equals the xy-resolution of the original images, but has a higher z-resolution (by about a factor of 2). We chose this primarily for convenience, as the only downside is the additional storage space.

We applied this procedure to different subsets of our image data to produce female, male and unisex templates. For the central brain, we used 36 female individuals (72 images including left-right flips) for the female template, 26 male individuals (52 image with left-right flips) for the male template, and the union of both for the unisex brain template: 62 individuals (124 images with left-right flips). For the ventral nerve cord we used 36 female individuals (72 images including left-right flips) for the female template, 39 male individuals (78 image with left-right flips) for the male template, and the union of both for the unisex VNC template: 75 individuals (150 images with left-right flips).

2.5 Bridging registrations

Transformations between different template spaces have proven useful in neuroscience because they unify disparate sets of data that are each aligned to different templates (Manton et al., 2014). We computed forward and inverse bridging registrations between our template and the other templates we evaluated in this work: JFRC 2010, JFRC 2013, FCWB, and Tefor. We used the algorithm ("ANTs A") that we found performs best overall (see Appendix A.2). In Figure 3, we show these templates in the space of JRC 2018 and vice versa. Qualitatively, these registrations appear to be about as accurate as those from individuals to templates. We used the

transformation to normalize distances measured across templates (see Section 3.2). We also provide transformations between the unisex template and the male and female templates to facilitate inter-sex comparisons.

2.6 Registration with electron microscopy

We automatically aligned the FAFB EM volume and the JRC 2018 template (see Figure 3). We rendered and blurred (with a 1.0 µm Gaussian kernel) the synapse cleft distance predictions generated by Heinrich et al. (2018) at low resolution ($1.02 \times 1.02 \times 1.04$ µm) so that the resulting image has an appearance similar to an nc82 or brp-SNAP labeled confocal image (see Figure 3). We used ANTs A to find a transformation between the two images, the result of which produces a qualitatively accurate alignment. In Appendix A.6, we discuss additional motivation and tradeoffs, including additional visualizations and a quantitative evaluation. In particular, we show that this transformation reproduces scientific results by Zheng et al. (2017). The accuracy of the manual registration between FAFB and JFRC 2013 by Zheng et al. (2017) suffers from variable error caused by the preference of the human annotator for specific brain regions and spurious details. Our automatic registration does not have this preference and is potentially better regularized.

3 Results

We compared the registration tools ANTs (Avants et al., 2009), and CMTK (Rohlfing and Maurer, 2003) with three sets of parameters for each, giving a total of six different registration algorithms. We used images from 20 female flies for evaluation, the details of which are described in Section 2.1.2. Since all testing subjects were female, we used the female JRC 2018 template for the experiments below.

3.1 Qualitative comparison

In Figure 3, we visually compare slices through the JFRC 2010 (Jenett et al., 2012), JFRC 2013 (Aso et al., 2014), FCWB (Ostrovsky and Jefferis, 2014), Tefor (Arganda-Carreras et al., 2018), and our JRC 2018 brain templates. Note the improved contrast and sharpness of anatomical structures in our JRC 2018 template relative to the others. We describe possible reasons for this in the Section 4.

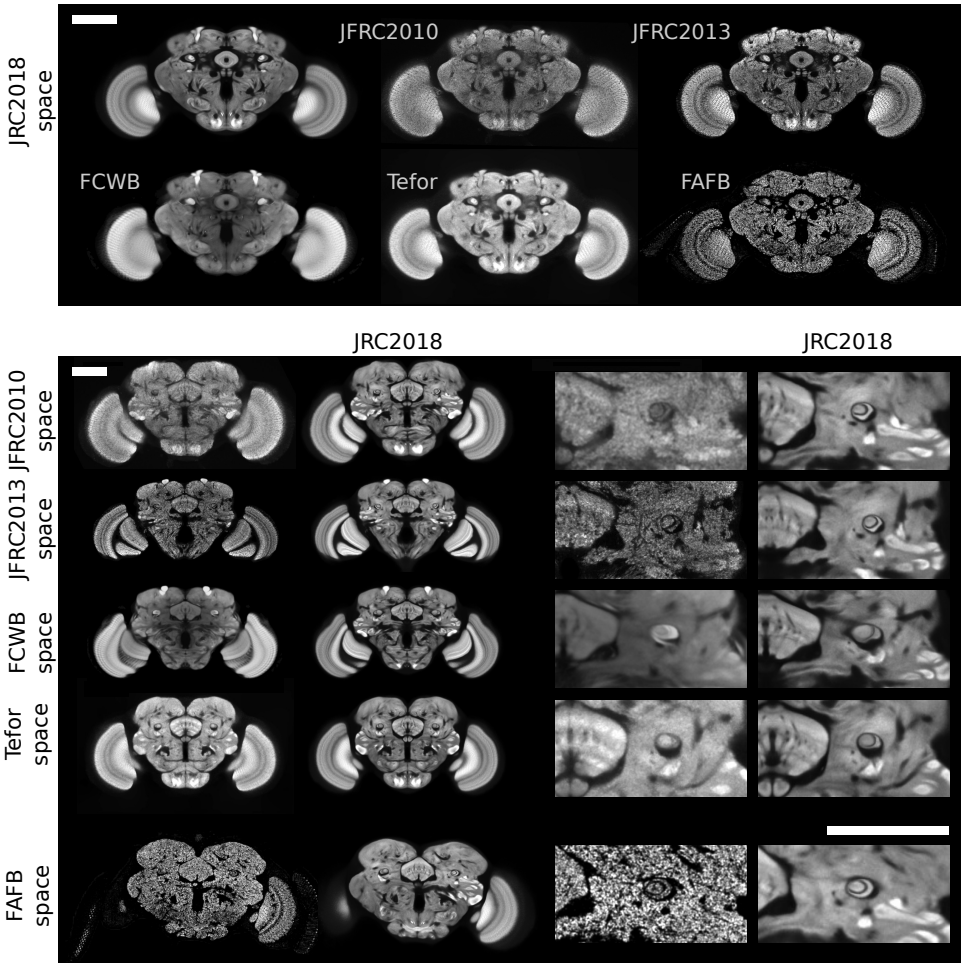

Figure 3: Visual comparison of *Drosophila* brain templates and bridging transformations. The top two rows show four existing templates registered to our JRC 2018 template, as well as synaptic cleft predictions derived from the FAFB EM volume, transformed into the space of JRC 2018. The middle four rows show JRC 2018 (second and fourth columns) registered to each of the three templates, along with a close-up around the fan-shaped body and the pedunculus of the mushroom body. The bottom row shows JRC 2018 transformed into the space of FAFB. Scale bars 100 µm.

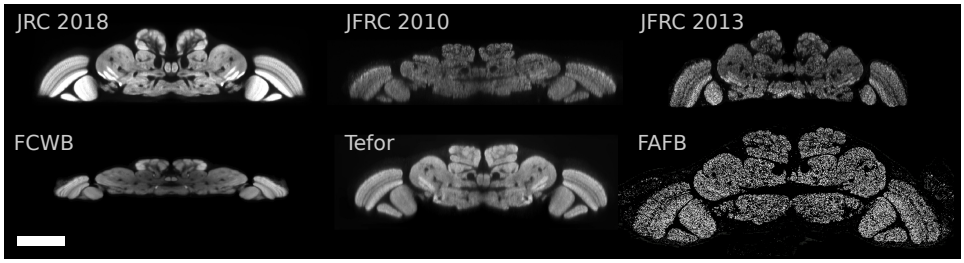

Figure 4: Horizontal (xz-slice) visualization of five brain templates and FAFB in physical coordinates. Note that the lower z-resolution is appreciable for individual templates (JFRC 2010 and JFRC 2013). Furthermore, observe the significant differences in physical sizes across these brain templates. Scale bars 100 µm.

Figure 4 shows xz-slices through the five templates and FAFB, where the x-axis is medial-lateral and the z-axis is anterior-posterior. Confocal imaging results in poorer z- than xy-resolution: 0.38 µm/px vs. 0.19 µm/px for our images. The brain templates vary notably in physical size and resolution (see Table 2). Specifically, the FCWB and JFRC 2010 templates are much smaller in the anterior-posterior direction. The affine part of the bridging transformations computed for Figure 3 indicate that the FCWB template is about 40% smaller than JRC 2018, and JFRC 2010 is about 20% smaller.

	JRC 2018	JFRC 2010	JFRC 2013	FCWB	Tefor	FAFB
xy	0.19	0.62	0.62	0.32	0.61	0.004
z	0.19	0.62	0.62	1.0	0.99	0.04

Table 2: The resolutions of all templates in µm/pixel. Evaluation against our JRC 2018 template was performed at a resolution of 0.62 µm/px or less. We added the resolution of the FAFB synapse cloud for comparison.

3.2 Quantitative comparison

Measuring and evaluating the accuracy of image registration is notoriously challenging (Rohlfing, 2012). Common measures include image similarity, distance between landmark points, or overlap of semantic (anatomical) regions, each of which come with their own disadvantages. Image similarity

can suffer from bias because the measurement may be the same quantity the registration algorithm is optimizing for and does not account for implausible deformation. Landmark points measure accuracy sparsely and are costly to generate (since they are usually manually placed). Region overlap is similarly costly and only sensitive to differences along or near boundaries of those regions. We discuss this in more detail in Section 4.1.

3.2.1 Registration accuracy measure

We measure registration accuracy with the naïve per node skeleton distance between the same neuronal arbor for different individual flies after registration to the template and normalizing for template size. Normalizing for size and shape is necessary given the observations from Figure 4 that some templates are physically smaller than others. Transforming skeletons to a physically smaller space would artificially decrease the distance measure. Similarly, if shape differs, regions with locally dense distributions of arbors could be compressed, leading to smaller distances for many point samples.

We compute this distance using the following procedure. Neurons are skeletonized using the methodology described in Section 2.3. Nc82 channels for two *Drosophila* individuals are independently registered to a template. The transformation found using the nc82 channel is then applied to the neuronal skeleton to bring them into template space. This is followed by an additional normalizing transformation that ensures all templates are at an equivalent scale and shape, that of JRC 2018 (see Section 2.5). The distance transform of both skeletons is computed and rendered at an isotropic resolution of 0.5 µm/px. For a given point (pixel) on one skeleton, the value of the distance transform of the other skeleton gives the naïve orthogonal distance between the skeletons. We report statistics of this skeleton-distance (in µm) both over the entire brain and split by compartment labels defined by JFRC 2010. Image processing was done using custom code based on ImgLib2 (Pietzsch et al., 2012). Statistics, analysis and visualization used pandas (McKinney, 2010) and matplotlib (Hunter, 2007). All evaluation code can be found on-line at `https://github.com/saalfeldlab/template-building`.

The skeleton distance is similar to landmark distance, but involves no manual human decision making or interaction since the structures of interest are directly specified by the anatomy. Our approach has the advantage of being fast and simple to compute as well as providing a distance for every point on the skeleton. It is limited in that it only measures distances perpendicular to the skeletons and assumes strict correspondence between

the nearest points on two skeletons. It will therefore tend to underestimate errors. See Section 4.1 in Section 4 for more details on the benefits and limitations of this performance measure.

We measured the skeleton distance between all pairs of individuals belonging to the same line, though we grouped the first five lines in Table 1 (JRC_SS23204, JRC_SS23206, JRC_SS23208, JRC_SS30756, JRC_SS30777) since they have very similar expression patterns. There exist 110 permutations of the 11 flies in the first line-group and 6 permutations each of the other three lines, making 128 pairwise comparisons in total. This distance is computed at every pixel for a given skeleton pair. When rendered at 0.5 µm resolution, each skeleton comprises about 250,000 pixels on average, yielding about 32 million points for which distance is estimated across all 128 skeleton pairs. This is repeated for each template and algorithm pair we evaluated.

We then compute several statistics of the distance across pairs of skeletons fixing a registration algorithm and template and report the results. Table 3 shows the mean and standard deviation of the distance distribution for different templates and algorithms. JRC 2018 has the lowest mean values of distance (indicating best performance) both when averaging across algorithms, and when choosing the best algorithm for a given template. Figure 5 and Figure 6 plot skeleton distance against a deformation measure (see Section 3.2.2), and CPU time, respectively.

	Mean (standard deviation) skeleton distance			
Template	All	Best	ANTs A	CMTK A
JRC 2018	4.17 (3.81)	3.97 (3.65)	3.97 (3.65)	4.03 (3.70)
JFRC 2013	4.79 (4.43)	4.15 (3.84)	4.15 (3.84)	4.73 (4.71)
Tefor	4.91 (4.91)	4.00 (3.68)	4.00 (3.68)	5.44 (5.75)
FCWB	5.08 (4.51)	4.35 (3.97)	4.35 (3.97)	5.52 (4.97)
JFRC 2010	5.42 (5.15)	4.59 (4.06)	6.31 (6.20)	5.69 (5.50)

Table 3: Mean (Standard deviation) of skeleton distance by template, in µm. Templates are ordered by decreasing performance for each template's best algorithm. Lower distances indicate better registration performance.

3.2.2 Registration deformation measure

In addition to measuring accuracy, we also report a scalar measure that approximates the "deformation" or distortion of a brain's shape after un-

dergoing a transformation, the standard deviation of the Jacobian determinant map (JSD). This is important if downstream analyses in template space rely on anatomical morphology, see Section 4.2 for a discussion. The Jacobian determinant of a transformation at a particular location describes the amount of local shrinking/stretching, where a value of 1.0 indicates that volume is locally preserved, less that 1.0 indicates shrinking, and greater than 1.0 indicates stretching. We claim that the standard deviation of the distribution of the Jacobian determinant map measures deformation, because the spread of this distribution (and not the mean) captures the extent to which a transformation is *simultaneously* stretching and shrinking space. A similarity transformation will have a single fixed value of the Jacobian determinant at all points equal to its scale parameter, and a mean Jacobian determinant equal to that value. Therefore, the mean value of the Jacobian determinant is not indicative of a deformation, but rather shows average scaling. We computed this quantity from displacement fields and do not include the affine component, to avoid confusing global scale changes with deformation.

In Figure 5, we plot the JSD against the mean skeleton distance described above. We observed that algorithms with stronger regularization (CMTK C, ANTs B) have a lower JSD, as we would expect. The mean distance between skeletons is lowest for the JRC 2018 template. Furthermore, for a fixed algorithm it also has lower JSD than other templates. For example, Table 4 shows the JSD for five templates when using ANTs A as the registration algorithm (the best algorithm on average, measured by mean skeleton distance). This suggests that the JRC 2018 template may be "closer" on average to the shape of individual brains (in our testing cohort) in the sense that less deformation is required to transform those brains to the template. Table 8 in section Appendix A.5, shows a complete listing of JSD statistics across templates and algorithms.

	JRC 2018	JFRC 2013	JFRC 2010	Tefor	FCWB
JSD	0.17	0.18	0.23	0.23	0.36

Table 4: Jacobian determinant standard deviation (JSD) sorted by templates for a fixed algorithm (ANTs A). This algorithm has the capability of producing large deformations (i.e. it is not overly regularized), as by the large value of JSD for the FCWB template. The smallest average amount of deformation was obtained after registration to our template, JRC 2018, followed closely by JFRC 2013.

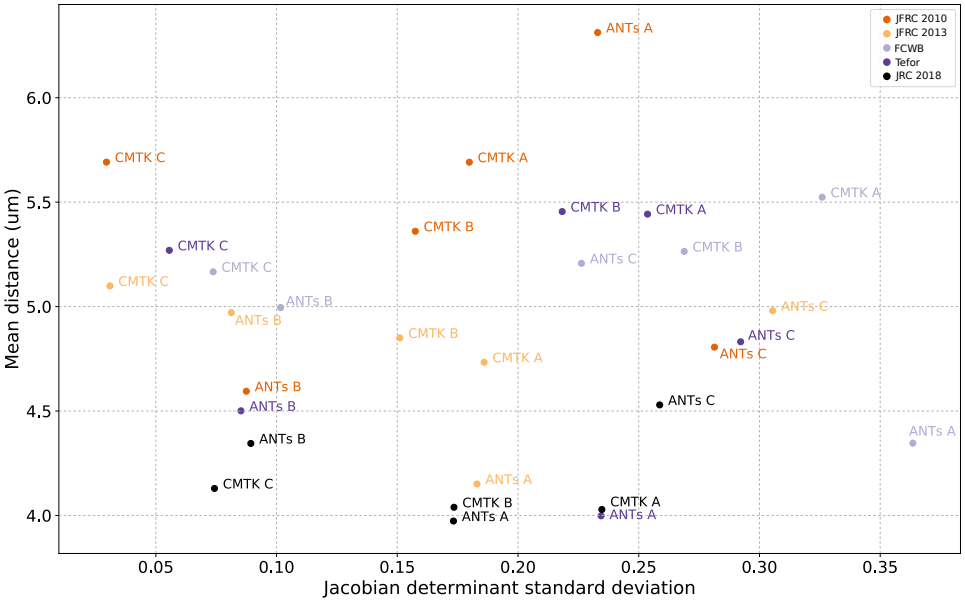

Figure 5: Scatterplot showing mean skeleton distance and standard deviation of Jacobian transform map for template-algorithm pairs.

3.3 Computation time and supplementary results

Figure 6 plots mean skeleton distance against mean computation time (in CPU-hours). The choice of algorithm and parameters influences computation expense more than the choice of template. Our particular parameter choices for CMTK are generally faster than ANTs. We see that the best performing algorithm (ANTs A) is also the most computationally demanding. Finally, for the fastest algorithms (CMTK B and CMTK C) mean distance is smallest using the JRC 2018 template.

Table 3 shows the mean and standard deviation of skeleton distances averaged across 128 pairs of flies (four driver lines). The second column gives the mean distance averaged also across six choices of registration algorithm/parameters, while the third and fourth columns give average distances for the "best" two algorithms (see Table 5). The JRC 2018 template performs best according to this measure, independent of the registration algorithm used.

We also performed experiments varying the resolution of the two best templates (JRC 2018 and Tefor), the details of which are in Appendix A.4. Finally, while the results shown here are averaged across the entire brain,

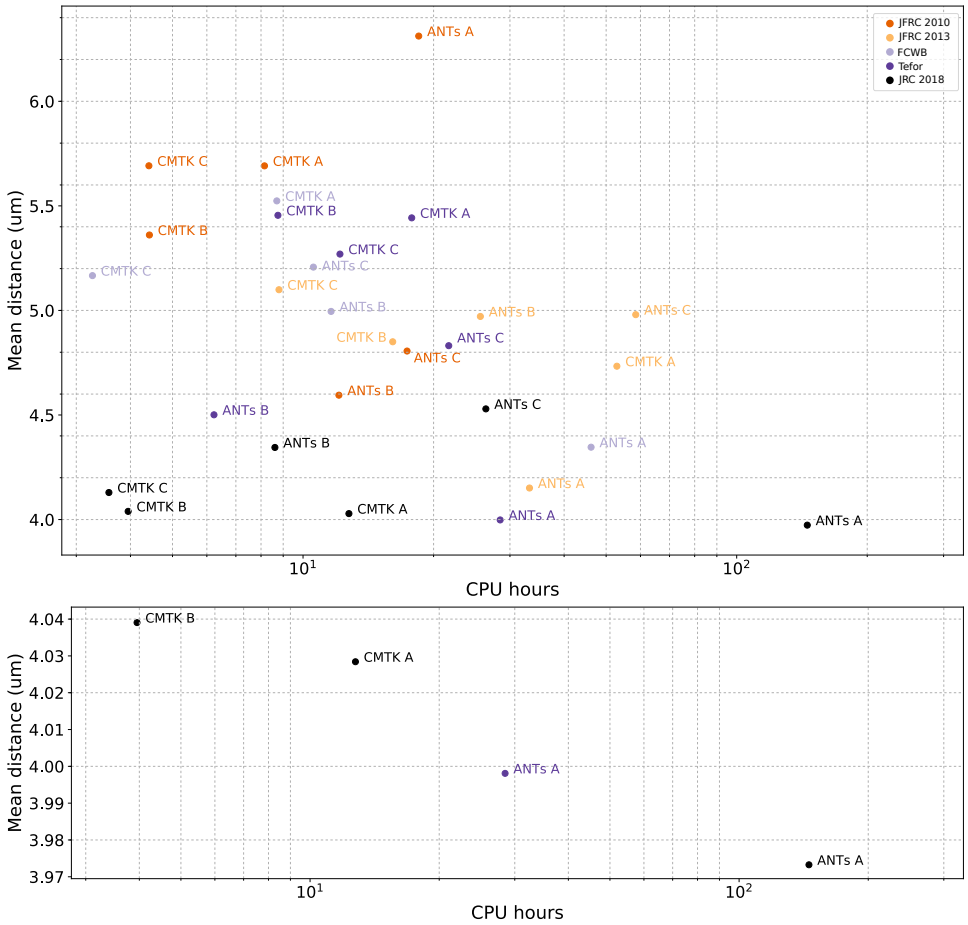

Figure 6: Scatterplot showing mean skeleton distance and the mean computation time in CPU-hours for all template-algorithm pairs (above), and the best performing pairs (below).

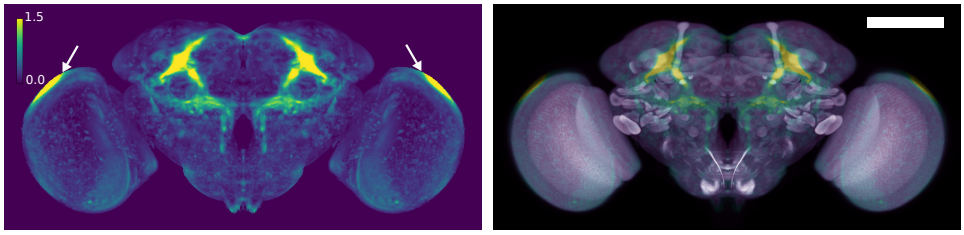

(A) Jacobian determinant map difference (B) Overlay

Figure 7: A visualization of female vs male morphological differences. (A) the maximum intensity projection (MIP) of the difference between male and female Jacobian determinant maps where values greater than 1 (yellow) indicate the male template is locally larger. (B) the MIP of the Jacobian determinant map overlayed with a MIP of the unisex template. Arrows indicate an artifact of this analysis in regions where the templates have no contrast, but the registration algorithm applies a strong deformation. Scale bar 100 µm.

we also performed a finer grain analysis, tabulating statistics of skeleton-distance for 75 anatomical compartment label, the results of which can be found in the Supplementary Tables S1-S76.

3.4 Sexual Dimorphism

Next, as a demonstration of efficacy, we briefly examine sexual dimorphism in the *Drosophila* brain, reproducing the results of Cachero et al. (2010), using the brain templates we created. Consistent with those previous findings, we observe enlargement of anatomy associated with *fruitless* gene expression in the male JRC 2018 template relative to the female JRC 2018 template.

We compared the Jacobian determinant maps of two transformations: the transformation between the male and unisex template and that between the female and unisex template. These transformations should reflect the differences between the mean female and male shapes, respectively. Figure 7 shows the differences of the Jacobian determinant map for the transformations between the male-to-unisex and female-to-unisex templates. This qualitatively agrees with the result in Cachero et al. (2010) that male enlarged regions correlate with *fruitless* gene expression.

4 Discussion

We created six *Drosophila* templates for female, male, and unisex central brains and ventral nerve cords. In Figure 1, we see that the unisex templates are generally more blurry than the single sex templates, likely because the unisex templates include inter-sex variation in addition to inter-individual variation. This is more pronounced for the VNC than for the central brain. Furthermore, male templates appear to be more blurry than the female templates both for the brain and VNC. This could be due to higher variability across male individuals, or poorer performance by registration algorithms for males, though we believe the former to be more likely.

It is difficult to determine the extent to which each aspect of template construction affects registration performance. Nevertheless, here we put our results in the context of other work attempting to estimate performance of various templates. We show in Figure 3 that in our template, anatomical features in the *Drosophila* brain are qualitatively more pronounced, having higher contrast than other existing templates. As a result, pixel-based similarity measures used by automatic registration algorithms may be more effective at optimization when the signal for the target image is less obscured by noise of different kinds (e.g., anatomical variability, imaging artifacts). This is potentially one of the reasons that our template, JRC 2018, outperforms others.

4.1 Estimating registration quality

In this work we chose pairwise neuronal skeleton distance as the primary measure of registration performance. Most templates are not explicitly evaluated for registration accuracy at time of publication (Jenett et al., 2012; Aso et al., 2014), though Arganda-Carreras et al. (2018) use the overlap of anatomical labels to compare performance. Unlike reference image similarity, both skeleton distance and label overlap are relevant in the sense that these measures are not directly optimized for by the registration algorithm which can lead to meaningless results (Rohlfing, 2012). Both of these measures have advantages and drawbacks.

Label overlap is sensitive to errors in the spatial location of anatomical compartments that are (usually manually) labeled by human annotators. Therefore, it specifically focuses on regions that are of potential interest to researchers. However, human annotation includes arbitrary choices, and therefore this measure may miss errors in biologically relevant areas that annotators overlook. Furthermore, annotating many individual images

can be costly and introduces the variability of manual labeling. On the other hand, having multiple individuals annotated is advantageous in that the anatomical labels themselves can also have uncertainty associated with them. Multiple labeled individuals enable multi-atlas segmentation (Iglesias and Sabuncu, 2015), an extension of single-atlas segmentation, at the cost of increased computational cost. Another potential drawback of using label overlap is that only changes near the boundaries of labels effects the overlap measure, and so it cannot differentiate methods that perform differently at the interior of labels. Registration errors parallel to or along the boundary are also not distinguishable.

The skeleton distance measure we use in this work evaluates registration using automatically extracted anatomy *directly* rather than indirectly as labeled by human annotators and so avoids manual effort in obtaining a registration accuracy measure. It instead requires that an additional independent image channel be acquired, and must deal with biological variability and algorithmic errors as confounding factors. Specifically, naïve skeletonization and pairwise matching rely on the assumption that the nearest points on two skeletons are in correspondence, and will result in underestimates of distance. This also means that skeleton distance cannot differentiate errors parallel to the skeleton. Furthermore, any errors in the automatic segmentation of the skeletons will affect the distance computation. Biological variability could also be a significant limitation if this variability is much larger than the differences between templates/registration algorithms. In this work, however, differences in the distributions of this measure between templates and algorithms was detectable, even in the presence of this noise.

Currently, the JRC 2018 templates do not have anatomical labels of their own superimposed, except for those that are inherited implicitly through bridging transformations to other templates. As a result, the accuracy of these labels depends on the accuracy of bridging transformation. In future work, we plan to develop a set of anatomical labels in the space of the JRC 2018 templates.

4.2 Deformation

As observed in Figure 5, one of the benefits of the JRC 2018 template is that an accurate registration can be obtained with less local deformation than for other brain templates. This is beneficial because the morphology of anatomy is better preserved, and therefore the influence of the transformation is less likely to be a confounding factor in downstream analyses.

For example, neuronal morphology is an important signal when searching across driver lines for a particular neuron or neurons of interest. This task benefits from normalizing spatial location (registration) and from comparing morphology. Therefore, minimizing deformation is beneficial for this task. For example, NBLAST (Costa et al., 2016) makes use of morphology of neurons in computing pairwise scores, and therefore any distortion in shape could prevent effective matching.

In the next sections we consider a few possible reasons for the improvements in performance we see when using JRC 2018 as a target for registration.

4.3 Influence of groupwise averaging

A potential concern in using an average of many individuals as a registration target is that some anatomical features are blurred or lost due to imperfect registration followed by averaging. In this case, it could be that the loss or blurring of these anatomical features removes a useful signal for the registration algorithm and could result in worse alignment. Our results suggest that this is not the case, but rather that groupwise-average templates out perform individual templates, in agreement with other work on the human hippocampus from MRI (Avants et al., 2010), in ants (Arganda-Carreras et al., 2017), and *Drosophila* (Arganda-Carreras et al., 2018).

If an anatomical feature is blurred or lost in the process of template construction, then that feature must have been poorly aligned on average across the population, due perhaps to large anatomical variability. It could be that the presence of unreliable/highly variable anatomy is useless or detrimental on average for registration across a large population. For example, highly variable anatomy could result in over-warping, especially when using algorithms with very flexible transformation models, since they can "force" improvements to the similarity measure even for incompatible anatomy, analogous to overfitting in machine learning. This is another possible reason that average templates outperform individual templates.

4.4 Symmetry

The central brain of *Drosophila* has an asymmetry of note, but is largely left-right symmetric (Pascual et al., 2004). Any template created without enforcing symmetry would have small but widespread asymmetries caused by the particular specimens and images that contributed to the average, not

biologically meaningful asymmetries. We therefore created a set of left-right symmetric templates. Of course, this has the disadvantage of removing *real* asymmetries from the template brain. For researchers interested in analyzing asymmetries, they can be recovered by measuring left-right differences in the deformations to a symmetric template using deformation based morphometry (Ashburner et al., 1998). An advantage of symmetry is that the estimation of a transform mapping the left hemisphere to the right and vice-versa ("a mirroring transformation") is straightforward. Manton et al. (2014) and Schlegel et al. (2017), for example, describe how such mirroring transforms are useful in performing neuronal comparisons across hemispheres, since many neurons in one hemisphere correspond to a partner in the other.

4.5 Influence of number of individuals to build atlas

Our templates were built using many more individuals than other average templates. The FCWB template averaged 26 individuals, and the Tefor brain averaged 10 individuals, where we average 36 female individuals, and 26 male individuals for the sex-specific but consider twice as many images by left-right flipping each individual. As a result, we are more confident that our templates are near the "mean shape" of the central brain for each sex. Arganda-Carreras et al. (2018) explored how the number of individuals that comprised a template effects the registration quality to those templates. They found a plateau of performance for templates built using between seven and ten individuals. Yet, JRC 2018 generally outperforms Tefor. Next, we outline some of the potential reasons for this.

If the conclusion of Arganda-Carreras et al. (2018) is true, then whatever performance improvement JRC 2018 achieves over the Tefor brain is not due to the number of individuals comprising the templates. We note first that the mean distance measures for JRC 2018 and Tefor are very similar when using the best performing, but most costly registration algorithm (ANTs A). Using this algorithm, the average deformation energy (measured by Jacobian determinant) is smaller for JRC 2018 (0.17) than for Tefor (0.23) (see Figure 5), suggesting that it is "closer" to the mean of our test subjects than the Tefor brain. This could also explain why JRC 2018 achieves better performance than Tefor when using registration methods that are more highly regularized (e.g. ANTs B and CMTK C). It could be the case that the template shape does not converge after only seven to ten individuals have been averaged, but that this shape change is not reflected in registration performance measures. It seems unlikely that image acquisi-

tion would affect the average deformation when registering to a template. Given that, our results support the conclusion that using more individuals for a template yields a more representative shape which reduces deformations for a given level of performance, or enables better performance for a fixed (smaller) amount of deformation.

Finally, we note that one of the most widely used anatomical templates, the Allen Mouse Common Coordinate Framework, used many more individuals (1675) than we used in this work, and, as we did, also included left-right flips as well as the original images for a total of 3350 (Allen Institute for Brain Science, 2015).

4.6 Influence of tissue staining and preparation

Arganda-Carreras et al. (2018) compare their Tefor template to the FCWB template (Ostrovsky and Jefferis, 2014) and show that Tefor has improved performance, a conclusion that our results corroborate. They suggest that the difference between tissue staining protocols could be a contributing factor in the observed performance improvement. Nc82 images were used both to build the Tefor brain and for testing in Arganda-Carreras et al. (2018). In our work, we also use nc82 images for testing, but instead use brp-SNAP tag for images that contributed to our template. Still, evidence suggests that nc82 images are more reliably registered to our template than to Tefor, despite the fact that images contributing to our template underwent different sample preparation and imaging, and that similar methodology (groupwise registration) was used to construct our template and Tefor. The SNAP labeling results in more even contrast throughout the brain. Our results suggest that a template built with images having differing but improved contrast is a better registration target than a template of the same modality but worse contrast.

4.7 Influence of template resolution

The resolutions of a brain template could affect the ability of registration algorithms to produce an accurate alignment. It could be that templates rendered at isotropic resolution could outperform those with anisotropic voxels, even when the moving image is anisotropic, as is the case with our testing data that were acquired with a confocal microscope. One of the anisotropic templates we evaluated here performs well in the best case (Tefor), while the other (FCWB) performs worse than isotropic templates generally.

We also explored how varying the resolution of the two best templates (JRC 2018 and Tefor) affects registration performance, the results of which are shown in Appendix A.4. We conclude from those observations that it is possible for lower resolution templates to achieve similar performance to high resolution templates, and this can yield computational savings. However, it is worth exploring different choices of algorithms in this case, since any given algorithm may not have uniform performance across different resolutions.

4.8 Anatomical variability

In a previous study, Jefferis et al. (2007) measured biological variability and registration accuracy by measuring the branch point of a projection neuron (PN) after entering the lateral horn, and estimated spatial variability of 2.64, 1.80, and 2.81 µm, for the three axes. This yields a mean euclidean distance of about 4.3 µm. Separately, they found that the mean axon positions of PNs within the inner antennocerebral tract (iACT) were 3.4 µm apart. In another study Peng et al. (2011), developed a pointwise image registration method, "Brainaligner," and assessed its accuracy, as well as natural biological variability. They estimated the spatial variability of the axons in the iACT to 3.26 µm, quite similar to the 3.4 µm estimate in Jefferis et al. (2007). These estimates, taken together are consistent with our estimate of a mean skeleton distance of about 4.0 µm for the best registration algorithm and the best template. This figure is slightly less than the 4.3 µm distance of the lateral horn PN branch point from and slightly greater than the 3.4 µm estimate of the iACT from Jefferis et al. (2007). The 3.26 µm estimate of Peng et al. (2011) is lower still. We expect part of this difference has to do with the fact that their measure focuses on a single, perhaps easily localizable region, whereas we examine distances across the entire brain.

4.9 Accuracy/time tradeoff

The required level of accuracy of registration will vary from task to task. We recommend that researchers first experiment with the less computationally demanding algorithms/parameter sets, determine whether the results are adequate for their particular task, and if not, to try the potentially more accurate but more computationally demanding options. One major benefit of the JRC 2018 template presented here is its much better performance when using faster algorithms. For instance, of all the algorithm-template pairs under 10 CPU-hours, the best performing pair using the JRC 2018 template

achieved a mean distance under 4.1 µm (at about 4 CPU-hrs), whereas the next best performing template was the Tefor template at about 4.5 µm (at about 6 CPU-hrs). This pattern generally holds when using down-sampled template versions, see Appendix A.4.

5 Acknowledgements

The authors would like to thank Philipp Hanslovsky, Igor Pisarev, Alice Robie, Yoshi Aso, Greg Jefferis, and Michael Reiser for helpful discussions, Zhihao Zheng for help with EM-LM registration analysis, Arnim Jenett and Ignacio Arganda-Carreras for the Tefor brain template. This work was supported by the Howard Hughes Medical Institute.

References

Allen Institute for Brain Science. Techincal white paper: Allen mouse common coordinate framework. Technical Report v.1, 2015. URL http//:help.brain-map.org/download/attachments/2818171/MouseCCF.pdf.

I. Arganda-Carreras, D. G. Gordon, S. Arganda, M. Beaudoin, and J. F. Traniello. Group-wise 3D registration based templates to study the evolution of ant worker neuroanatomy. In *International Symposium on Biomedical Imaging*, pages 429–432, 2017.

I. Arganda-Carreras, T. Manoliu, N. Mazuras, F. Schulze, J. E. Iglesias, K. Bhler, A. Jenett, F. Rouyer, and P. Andrey. A statistically representative atlas for mapping neuronal circuits in the drosophila adult brain. *Frontiers in Neuroinformatics*, 12:13, 2018.

J. Ashburner, C. Hutton, R. Frackowiak, I. Johnsrude, C. Price, and K. Friston. Identifying global anatomical differences: Deformation-based morphometry. *Human Brain Mapping*, 6(5-6):348–357, 1998.

Y. Aso, D. Hattori, Y. Yu, R. M. Johnston, N. A. Iyer, T.-T. Ngo, H. Dionne, L. F. Abbott, R. Axel, H. Tanimoto, and G. M. Rubin. The neuronal architecture of the mushroom body provides a logic for associative learning. *eLife*, 3:e04577, 2014.

B. Avants and J. C. Gee. Geodesic estimation for large deformation anatomical shape averaging and interpolation. *NeuroImage*, 23:S139–150, 2004.

B. B. Avants, C. L. Epstein, M. Grossman, and J. C. Gee. Symmetric diffeomorphic image registration with cross-correlation: Evaluating automated labeling of elderly and neurodegenerative brain. *Med Image Anal*, 12(1):26–41, 2009.

B. B. Avants, P. Yushkevich, J. Pluta, D. Minkoff, M. Korczykowski, J. Detre, and J. C. Gee. The optimal template effect in hippocampus studies of diseased populations. *NeuroImage*, 49(3):2457–2466, 2010.

B. B. Avants, N. Tustison, G. Song, P. A. Cook, A. Klein, and J. C. Gee. A reproducible evaluation of ANTs similarity metric performance in brain image registration. *Neuroimage*, 54(3):2033–44, 2011.

J. A. Bogovic, P. Hanslovsky, A. Wong, and S. Saalfeld. Robust registration of calcium images by learned contrast synthesis. In *International Symposium on Biomedical Imaging*, pages 1123–1126, 2016.

J. Brner and C. Duch. Average shape standard atlas for the adult Drosophila ventral nerve cord. *J Comp Neur*, 518(13):2437–2455, 2010.

M. Cabezas, A. Oliver, X. Lladó, J. Freixenet, and M. Bach Cuadra. A review of atlas-based segmentation for magnetic resonance brain images. *Computer Methods and Programs in Biomedicine*, 104(3):e158–e177, dec 2011.

S. Cachero, A. D. Ostrovsky, J. Y. Yu, B. J. Dickson, and G. S. Jefferis. Sexual dimorphism in the fly brain. *Current biology*, 20(18):1589–601, 2010.

A. Cardona, S. Saalfeld, J. Schindelin, I. Arganda-Carreras, S. Preibisch, M. Longair, P. Tomančák, V. Hartenstein, and R. J. Douglas. Trakem2 software for neural circuit reconstruction. *PLoS ONE*, 7(6):e38011, 2012. doi: 10.1371/journal.pone.0038011.

A.-S. Chiang, C.-Y. Lin, C.-C. Chuang, H.-M. Chang, C.-H. Hsieh, C.-W. Yeh, C.-T. Shih, J.-J. Wu, G.-T. Wang, Y.-C. Chen, C.-C. Wu, G.-Y. Chen, Y.-T. Ching, P.-C. Lee, C.-Y. Lin, H.-H. Lin, C.-C. Wu, H.-W. Hsu, Y.-A. Huang, J.-Y. Chen, H.-J. Chiang, C.-F. Lu, R.-F. Ni, C.-Y. Yeh, and J.-K. Hwang. Three-Dimensional Reconstruction of Brain-wide Wiring Networks in Drosophila at Single-Cell Resolution. *Current Biology*, 21(1): 1–11, jan 2011.

M. Costa, J. D. Manton, A. D. Ostrovsky, S. Prohaska, and G. S. Jefferis. NBLAST: Rapid, Sensitive Comparison of Neuronal Structure and Construction of Neuron Family Databases. *Neuron*, 91(2):293–311, 2016.

R. C. Court, J. D. Armstrong, J. Borner, G. Card, M. Costa, M. Dickinson, C. Duch, W. Korff, R. Mann, D. Merritt, R. Murphey, S. Namiki, A. Seeds, D. Shepherd, T. Shirangi, J. Simpson, J. Truman, J. Tuthill, and D. Williams. A systematic nomenclature for the drosophila ventral nervous system. *bioRxiv*, 2017. doi: 10.1101/122952.

J. B. Grimm, T. A. Brown, B. P. English, T. Lionnet, and L. D. Lavis. Synthesis of Janelia Fluor HaloTag and SNAP-tag ligands and their use in cellular imaging experiments. In H. Erfle, editor, *Super-Resolution Microscopy: Methods and Protocols*, pages 179–188. Springer New York, New York, NY, 2017. ISBN 978-1-4939-7265-4. doi: 10.1007/978-1-4939-7265-4_15.

L. Heinrich, J. Funke, C. Pape, J. Nunez-Iglesias, and S. Saalfeld. Synaptic cleft segmentation in non-isotropic volume electron microscopy of the complete drosophila brain. *arXiv:1805.02718 [cs.CV]*, 2018.

J. D. Hunter. Matplotlib: A 2d graphics environment. *Computing In Science & Engineering*, 9(3):90–95, 2007. doi: 10.1109/MCSE.2007.55.

J. E. Iglesias and M. E. Sabuncu. Multi-Atlas Segmentation of Biomedical Images: A Survey. *Medical Image Analysis*, 24(1):205–19, 2015.

K. Ito, K. Shinomiya, M. Ito, J. Armstrong, G. Boyan, V. Hartenstein, S. Harzsch, M. Heisenberg, U. Homberg, A. Jenett, H. Keshishian, L. Restifo, W. Rssler, J. Simpson, N. Strausfeld, R. Strauss, L. B. Vosshall, and I. Brain Name Working Group. A Systematic Nomenclature for the Insect Brain. *Neuron*, 81(4):755–765, 2014.

G. S. Jefferis, C. J. Potter, A. M. Chan, E. C. Marin, T. Rohlfing, J. Maurer, Calvin R., and L. Luo. Comprehensive Maps of Drosophila Higher Olfactory Centers: Spatially Segregated Fruit and Pheromone Representation. *Cell*, 128(8):1187–1203, 2007.

A. Jenett, G. M. Rubin, T. T. B. Ngo, D. Sheperd, C. Murphy, H. Dionne, C. T. Zugates, and et al. A GAL4-Driver Line Resource for Drosophila Neurobiology. *Cell Reports*, 2(4):991–1001, 2012.

T. Kawase, S. S. Sugano, T. Shimada, and I. Hara-Nishimura. A direction-selective local-thresholding method, DSLT, in combination with a dye-based method for automated three-dimensional segmentation of cells and airspaces in developing leaves. *The Plant Journal*, 81(2):357–366, jan 2015.

V. Kaynig, B. Fischer, E. Müller, and J. M. Buhmann. Fully automatic stitching and distortion correction of transmission electron microscope images. *Journal of Structural Biology*, 171(2):163–173, 2010. doi: 10.1016/j.jsb.2010.04.012.

R. J. Kittel, C. Wichmann, T. M. Rasse, W. Fouquet, M. Schmidt, A. Schmid, D. A. Wagh, C. Pawlu, R. R. Kellner, K. I. Willig, S. W. Hell, E. Buchner, M. Heckmann, and S. J. Sigrist. Bruchpilot promotes active zone assembly, Ca^2+ channel clustering, and vesicle release. *Science*, 312(5776): 1051–1054, 2006.

J. Kohl, J. Ng, S. Cachero, E. Ciabatti, M.-J. Dolan, B. Sutcliffe, A. Tozer, S. Ruehle, D. Krueger, S. Frechter, T. Branco, M. Tripodi, and G. S. X. E. Jefferis. Ultrafast tissue staining with chemical tags. *PNAS*, 111:E3805–E3814, 2014.

H. Lacin and J. W. Truman. Lineage mapping identifies molecular and architectural similarities between the larval and adult Drosophila central nervous system. *eLife*, 5:e13399, mar 2016.

J. L. Lancaster, M. G. Wolodorff, L. M. Parsons, M. Liotti, C. S. Freitas, L. Rainey, P. V. Kochunov, D. Nickerson, S. A. Mikiten, and P. T. Fox. Automated talairach atlas labels for functional brain mapping. *Human Brain Mapping*, 10:120–131, 2000.

E. S. Lein, M. J. Hawrylycz, A. R. Jones, and et al. Genome-wide atlas of gene expression in the adult mouse brain. *Nature*, 445(7124):168–176, 2007.

F. Long, H. Peng, X. Liu, S. K. Kim, and E. Myers. A 3D digital atlas of C. elegans and its application to single-cell analyses. *Nature Methods*, 6: 667–672, 2009.

H. Luan, N. C. Peabody, C. Vinson, and B. H. White. Refined Spatial Manipulation of Neuronal Function by Combinatorial Restriction of Transgene Expression. *Neuron*, 52(3):425–436, 2006.

J. D. Manton, A. D. Ostrovsky, L. Goetz, M. Costa, and T. Rohlfing. Combining genome-scale Drosophila 3D neuroanatomical data by bridging template brains. *bioRxiv*, page 6353, 2014.

C. R. Maurer and J. M. Fitzpatrick. A review of medical image registration. In *Interactive imageguided neurosurgery*, volume 66(2), pages 17–44. 1993.

W. McKinney. Data Structures for Statistical Computing in Python. In S. van der Walt and J. Millman, editors, *Proceedings of the 9th Python in Science Conference*, pages 51–56, 2010.

I. A. Meinertzhagen. Of what use is connectomics? A personal perspective on the Drosophila connectome. *The Journal of experimental biology*, 221 (10), may 2018.

A. Nern, B. D. Pfeiffer, and G. M. Rubin. Optimized tools for multicolor stochastic labeling reveal diverse stereotyped cell arrangements in the fly visual system. *Proceedings of the National Academy of Sciences USA*, 112 (22):E2967–76, jun 2015.

A. D. Ostrovsky and G. S. X. E. Jefferis. FCWB template brain [data set], 2014.

K. Panser, L. Tirian, F. Schulze, S. Villalba, G. S. Jefferis, K. Bühler, and A. D. Straw. Automatic Segmentation of Drosophila Neural Compartments Using GAL4 Expression Data Reveals Novel Visual Pathways . *Current Biology*, 26(15):1943–1954, 2016.

A. Pascual, K.-L. Huang, J. Neveu, and T. Préat. Brain asymmetry and long-term memory. *Nature*, 427:605–606, 2004.

H. Peng, P. Chung, F. Long, L. Qu, A. Jenett, A. M. Seeds, E. W. Myers, and J. H. Simpson. BrainAligner: 3D registration atlases of Drosophila brains. *Nature Methods*, 8(6):493–498, 2011.

B. D. Pfeiffer, T.-T. B. Ngo, K. L. Hibbard, C. Murphy, A. Jenett, J. W. Truman, and G. M. Rubin. Refinement of Tools for Targeted Gene Expression in Drosophila. *Genetics*, 186(2):735–755, 2010.

T. Pietzsch, S. Preibisch, P. Tomančák, and S. Saalfeld. ImgLib2generic image processing in Java. *Bioinformatics*, 28(22):3009–3011, 2012.

S. Preibisch, S. Saalfeld, and P. Tomancak. Globally optimal stitching of tiled 3D microscopic image acquisitions. *Bioinformatics*, 25(11):1463–5, jun 2009.

A. Prokop and G. Technau. The origin of postembryonic neuroblasts in the ventral nerve cord of Drosophila melanogaster. *Development*, 111(1), 1991.

K. Rein, M. Zckler, M. T. Mader, C. Grbel, and M. Heisenberg. The Drosophila standard brain . *Curr Biol*, 12(3):227–231, 2002.

A. A. Robie, J. Hirokawa, A. W. Edwards, L. A. Umayam, A. Lee, M. L. Phillips, G. M. Card, W. Korff, G. M. Rubin, J. H. Simpson, M. B. Reiser, and K. Branson. Mapping the Neural Substrates of Behavior. *Cell*, 170(2): 393–406.e28, 2017.

T. Rohlfing. Image similarity and tissue overlaps as surrogates for image registration accuracy: widely used but unreliable. *IEEE TMI*, 31(2):153–63, 2012.

T. Rohlfing and C. R. Maurer. Nonrigid image registration in shared-memory multiprocessor environments with application to brains, breasts, and bees. *IEEE transactions on information technology in biomedicine*, 7(1):16–25, 2003.

J. Schindelin, I. Arganda-Carreras, E. Frise, V. Kaynig, M. Longair, T. Pietzsch, S. Preibisch, C. Rueden, S. Saalfeld, B. Schmid, J.-Y. Tinevez, D. J. White, V. Hartenstein, K. Eliceiri, P. Tomancak, and A. Cardona. Fiji: an open-source platform for biological-image analysis. *Nature methods*, 9(7): 676–82, jul 2012.

P. Schlegel, M. Costa, and G. S. Jefferis. Learning from connectomics on the fly. *Current Opinion in Insect Science*, 24:96–105, dec 2017.

A. Sotiras, C. Davatzikos, and N. Paragios. Deformable medical image registration: a survey. *IEEE transactions on medical imaging*, 32(7):1153–90, jul 2013.

P. Stockinger, D. Kvitsiani, S. Rotkopf, L. Tirián, and B. J. Dickson. Neural Circuitry that Governs Drosophila Male Courtship Behavior. *Cell*, 121(5): 795–807, jun 2005.

J. Talairach and P. Tournoux. *Co-planar stereotaxic atlas of the human brain*. Thieme, New York, 1988.

L. Tirian and B. Dickson. The VT GAL4, LexA, and split-GAL4 driver line collections for targeted expression in the Drosophila nervous system. *bioRxiv*, page 198648, 2017. doi: 10.1101/198648. URL https://www.biorxiv.org/content/early/2017/10/05/198648.

H.-H. Yu, T. Awasaki, M. Schroeder, F. Long, J. Yang, Y. He, P. Ding, J.-C. Kao, G.-Y. Wu, H. Peng, G. Myers, and T. Lee. Clonal Development and Organization of the Adult Drosophila Central Brain. *Current Biology*, 23 (8):633–643, apr 2013.

Z. Zheng, J. S. Lauritzen, E. Perlman, C. G. Robinson, M. Nichols, D. Milkie, O. Torrens, J. Price, C. B. Fisher, N. Sharifi, S. A. Calle-Schuler, L. Kmecova, I. J. Ali, B. Karsh, E. T. Trautman, J. Bogovic, P. Hanslovsky, G. S. X. E. Jefferis, M. Kazhdan, K. Khairy, S. Saalfeld, R. D. Fetter, and D. D. Bock. A complete electron microscopy volume of the brain of adult Drosophila melanogaster. *bioRxiv*, page 140905, 2017.

A Supplementary Notes

A.1 Reference image overlay

Figure 8 shows two examples of test images (randomly selected from the 20 test images) aligned to four different templates using the "best" algorithm (ANTs A above). Some differences are visible upon close inspection. For example, the right mushroom body is poorly aligned for Fly B using the FCWB template. Small misalignments near the mushroom body are evident for both flies after registration to JFRC 2013. Otherwise, alignment appears generally good.

A.2 Algorithm comparison

Table 5 shows skeleton distances averaged across driver lines and compartment labels for six different registration algorithms choices. The second column also averages across the five different brain templates tested. Two different parameter settings of ANTs performed best when averaging across templates, but ANTs A, CMTK A, and CMTK B performed similarly when evaluated on JRC 2018.

	Mean distance		Median
Algorithm	All templates	JRC 2018	All
ANTs A	4.19 µm	3.97 µm	3.24 µm
ANTs B	4.53 µm	4.34 µm	3.60 µm
CMTK A	4.64 µm	4.03 µm	3.54 µm
CMTK B	4.75 µm	4.04 µm	3.61 µm
ANTs C	4.89 µm	4.53 µm	3.81 µm
CMTK C	5.05 µm	4.13 µm	4.06 µm

Table 5: Mean skeleton distance by algorithm, sorted by mean performance across all templates.

A.3 Size and shape normalization for evaluation

Figure 9 shows the results of mean skeleton distance and Jacobian determinant standard deviation (JSD) after normalization by using only the affine part of the bridging transformation. This is in contrast to Figure 5, in which both the affine and deformable parts of the transformation contributed to

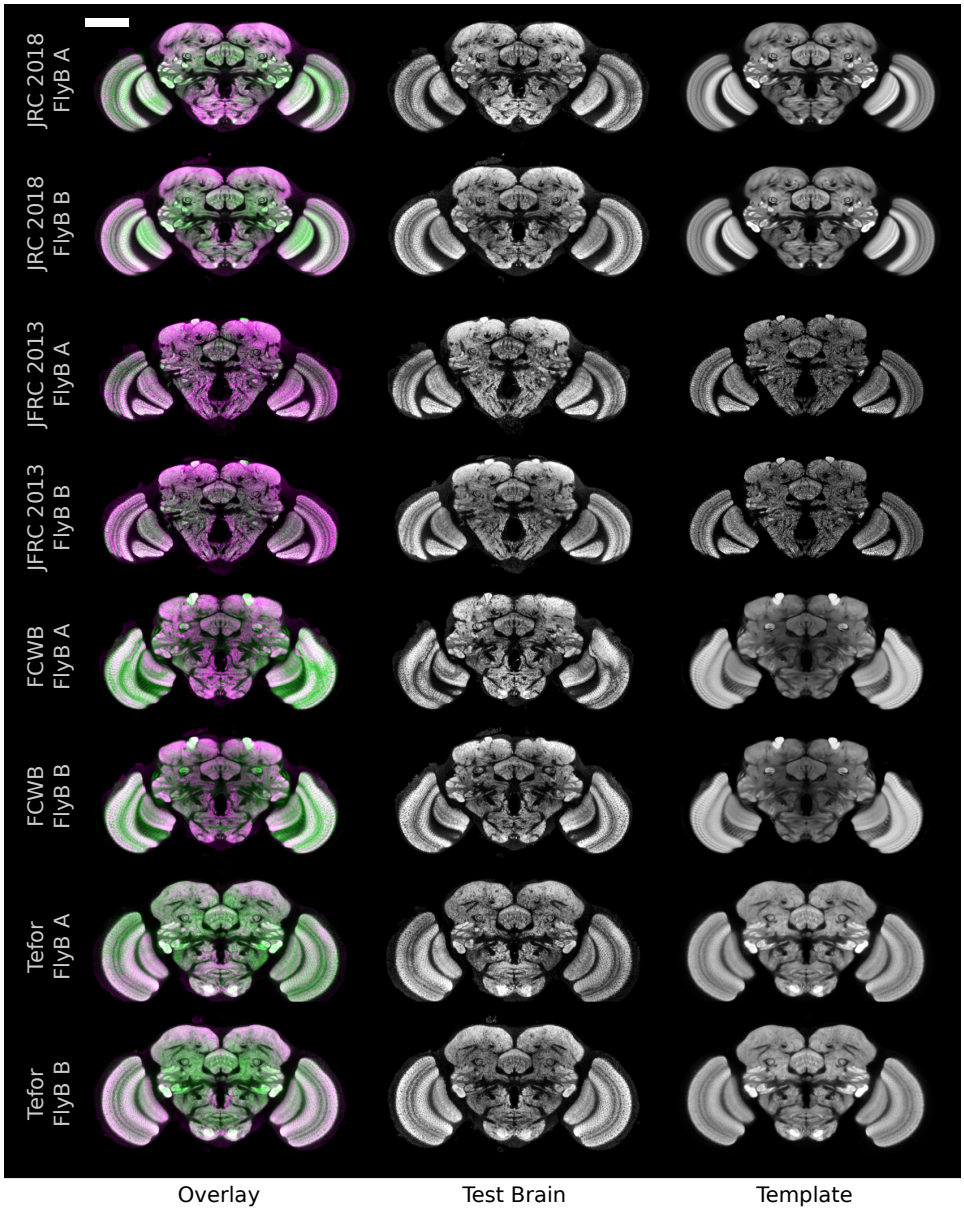

Figure 8: Overlays of the reference (nc82) channel. Scale bar 100 µm.

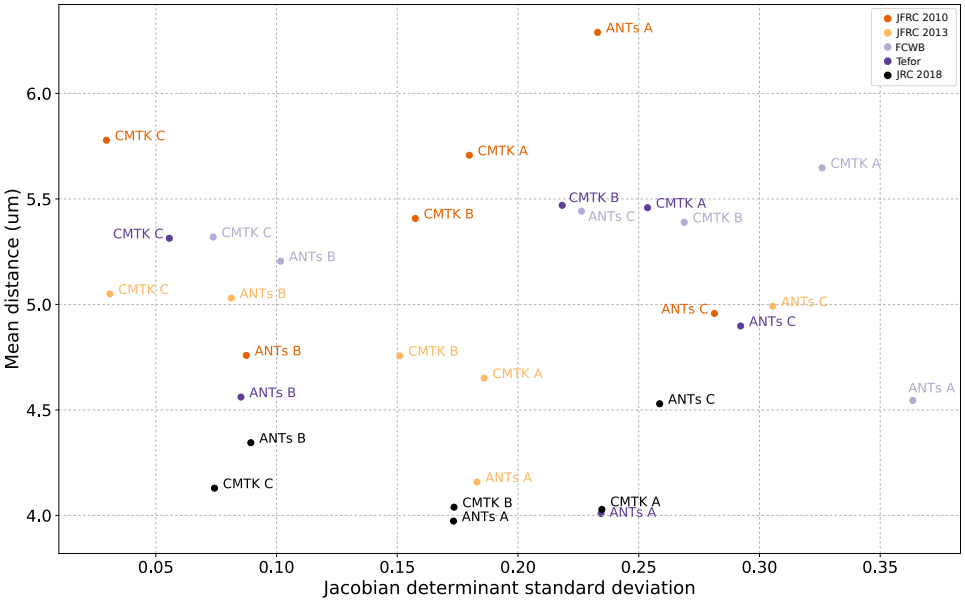

Figure 9: Scatterplot showing mean skeleton distance and standard deviation of Jacobian transform map for template-algorithm pairs using affine-only normalization.

normalization. We observed that results are generally very similar. The largest difference we observe is that the distance measures for the FCWB template are notably larger (worse performance) when using affine-only normalization.

A.4 Effect of resolution

We performed experiments to explore the effect that the resolution of a template has on the tradeoff between registration quality and computational cost. We repeated the evaluation described in section Section 3.2 using down-sampled versions of the two best performing templates: JRC 2018 and Tefor. We resampled each of these two templates from its native resolution to three lower, isotropic resolutions: 1.2, 2.4, and 3.6 µm. These resolutions correspond to downsampling in xy by factors of 2, 3, and 4 (approximately). Figure 10 shows a scatterplot of mean skeleton distance (our measure of registration accuracy) against mean CPU time for template-algorithm pairs at various resolutions. The same results are listed in Table 6.

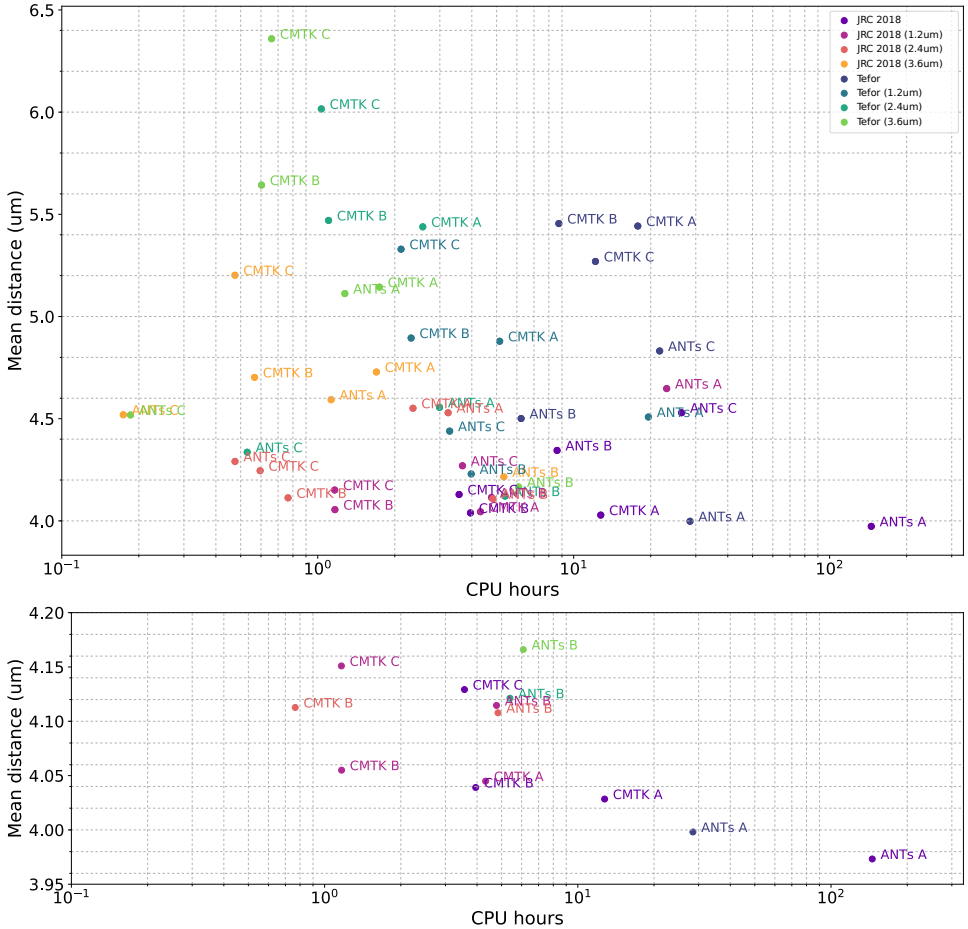

Figure 10: Scatterplot showing mean skeleton distance and the mean computation time in CPU-hours for the JRC 2018 and Tefor templates at various resolutions (above), and the best performing pairs (below).

We observed that some down-sampled templates perform as well or nearly as well as the full-resolution templates. For instance, JRC 2018, sampled at 1.2 µm performs competitively with the full-resolution template using CMTK A and CMTK B, though only the latter gives computational savings. Downsampled versions of Tefor seem to suffer somewhat more in terms of performance, though are competitive when using ANTs B, but without the speed-up observed for JRC 2018. Detailed exploration of algorithm parameters will influence the time-performance tradeoff, and may be worthwhile for some tasks. Here we give values for reasonable ranges of parameters from faster and more highly regularized to slower with potentially greater accuracy.

A.5 Deformation measure

Table 8 shows the mean and standard deviations of the distributions of the Jacobian determinants for all templates and algorithms. As expected, the means for all methods are generally close to 1.0, and the standard deviations are smaller for algorithms with stronger regularization (ANTs B and CMTK C). This is in line with our reasoning above, suggesting that the standard deviation of the Jacobian determinant maps is a more informative statistic than the mean.

The mean values of the Jacobian determinant for JFRC 2013 appear to be significantly different both from 1.0 and the other templates. This could be due to a difference in size of that individual template and the cohort of individuals that we tested with, though the affine part of the transformation should account for gross size differences, and this statistic is computed from the deformation only, making it difficult to reach a definitive conclusion.

A.6 Inter-modality registration

Zheng et al. (2017) present a complete electron microscopy (EM) volume of the *Drosophila* brain (FAFB), including a manual registration between the EM volume and a LM brain template. The transformation described therein used a Fiji (Schindelin et al., 2012) plugin called ELM (`https://github.com/saalfeldlab/elm`) based on BigWarp (Bogovic et al., 2016) to manually place landmark point correspondences between FAFB and JFRC 2013. While this approach can yield good results, it is limited in the following ways. Humans are limited to exploring the 3D EM data in one (arbitrary, i.e. not necessarily axis-aligned) 2D cross section at a time, and need to infer

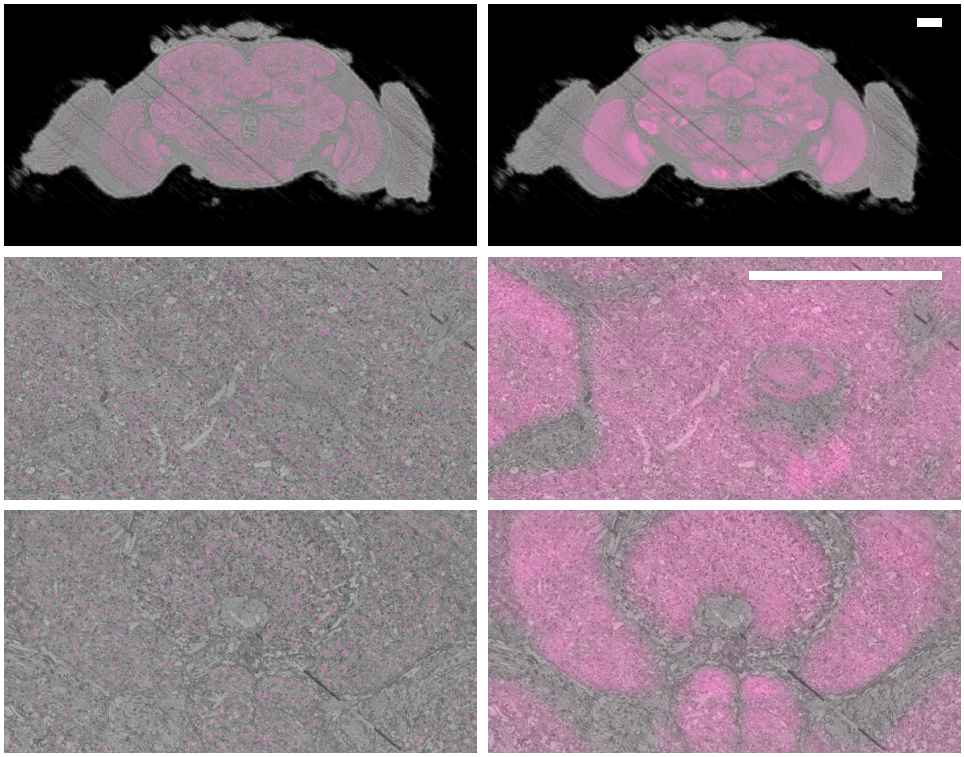

Figure 11: A visualization of the registration between JRC 2018 (magenta) and the FAFB electron microscopy volume (gray). The left column shows synaptic cleft predictions (magenta). The right column shows the resulting registration. Scale bar 50 µm.

3D structure from these views. Landmark placement can be difficult where the primary structures are not points, but rather planes, lines or curves. Furthermore, the EM volume is very large, and it is time consuming for a human to even look at the entire volume at a fine scale, and therefore accuracy of the transformation is likely to vary significantly over space. An automatically generated registration between these two modalities would improve upon some of these shortcomings.

In this work, we created a new, automatic alignment between that FAFB and the JRC 2018 brain template. The primary challenge is that the image contrast from EM and LM are at vastly different scales and measure different tissue properties. Typical approaches for inter-modality registration usually rely on choosing a similarity measure such as mutual information

that works well across modalities, but this is highly unlikely to produce adequate results given the differences of scale and contrast. Our approach is to use an image derived from the EM instead of the EM image directly. Since brp-SNAP tag produces contrast at synapses, we created an image of synapses resembling our chemical tag stains (or nc82 images) using the automated synapse predictions by Heinrich et al. (2018), applied to FAFB. The bottom row of Figure 3 shows that the image of synapses estimated from EM does indeed resemble an LM template brain.

We reproduce the analyses by Zheng et al. (2017) that lead to figures 5B, 5C, S7B, and S7C in that work in order to demonstrate that our proposed brain template and this EM to LM transformation will be useful in this domain. The conclusions drawn by Zheng et al. (2017) are that projection neurons (PNs) arising from the same glomerulus cluster more tightly in the calyx of the mushroom body than previous observed using light microscopy.

One set of neurons was manually traced in FAFB by Zheng et al. (2017), while the other set came from the Fly Circuit (Chiang et al., 2011) database of neurons from light microscopy, pooling over several individual fly brains that have been co-registered to the FCWB template, as described by Costa et al. (2016). The neurons traced from LM were transformed to the space of JFRC 2010 using bridging registrations from Manton et al. (2014). The neurons traced from EM went through two transformations: the first from FAFB to JFRC 2013 generated manually as described above. The second was the automatically estimated transformation between JFRC 2013 and FCWB (Manton et al., 2014).

The details of the analysis can be found in Zheng et al. (2017), but briefly, it consists of identifying projection neurons (PNs) in the calyx and grouping these by the glomerulus to which they project, then computing similarity/distance measures between pairs of PNs in the same group. Two related similarity scores between pairs of neurons were computed: the NBLAST score (Costa et al., 2016) and the mean Euclidean distance (NBLAST uses distance as part of its computation of score).

We repeated this analysis using our automatically generated transformation from FAFB to JRC 2018 followed by our bridging transformation from JRC 2018 to FCWB. This shows that our new automatic EM to LM transform can be used to draw the same conclusions. Figure 12 shows the results. Red and blue points and bars show the measurements of FAFB traced neurons and LM database neurons, respectively, exactly as in Zheng et al. (2017) with ELM. Black points and bars show the same results using our EM to LM transformation. Notice that the distributions of red and black

are very similar as they should be, given that they are measures of the same neurons transformed in different ways. Note that the LM neurons in this analysis were co-registered to the FCWB template by Costa et al. (2016); Jefferis et al. (2007), which we have shown to be a less reliable/accurate registration target than JRC 2018. Better results (more similar to the EM) could be possible by co-registering to an improved brain template.

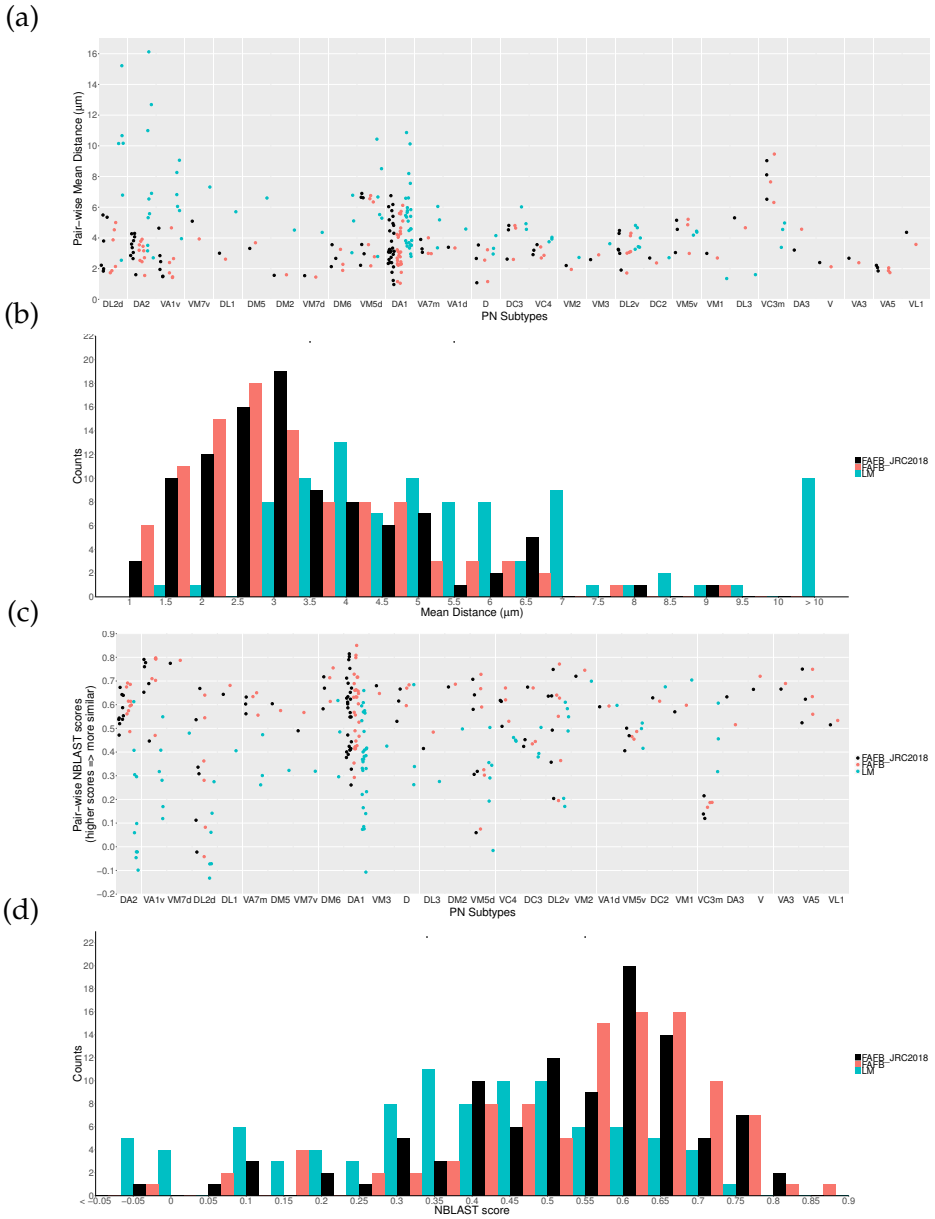

Figure 12: Scatterplots and histograms of (a)-(b) mean skeleton distance and (c)-(d) NBLAST scores for various projection neuron subtypes traced from electron microscopy.

Template	Algorithm	Mean distance (µm)	Mean CPU time (hrs)
JRC 2018	ANTs A	3.97	145.48
	ANTs B	4.34	8.61
	ANTs C	4.53	26.40
	CMTK A	4.03	12.76
	CMTK C	4.13	3.57
	CMTK B	4.04	3.95
JRC 2018 (1.2 µm)	ANTs A	4.65	23.09
	ANTs B	4.11	4.77
	ANTs C	4.27	3.68
	CMTK A	4.04	4.32
	CMTK C	4.15	1.17
	CMTK B	4.06	1.17
JRC 2018 (2.4 µm)	ANTs A	4.53	3.23
	ANTs B	4.11	4.84
	ANTs C	4.29	0.47
	CMTK A	4.55	2.36
	CMTK C	4.25	0.60
	CMTK B	4.11	0.77
JRC 2018 (3.6 µm)	ANTs A	4.59	1.13
	ANTs B	4.22	5.34
	ANTs C	4.52	0.17
	CMTK A	4.73	1.70
	CMTK C	5.20	0.47
	CMTK B	4.70	0.57
Tefor	ANTs A	4.00	28.48
	ANTs B	4.50	6.23
	ANTs C	4.83	21.68
	CMTK A	5.44	17.81
	CMTK C	5.27	12.16
	CMTK B	5.45	8.75
Tefor (1.2 µm)	ANTs A	4.51	19.58
	ANTs B	4.23	3.98
	ANTs C	4.44	3.28
	CMTK A	4.88	5.14
	CMTK C	5.33	2.12
	CMTK B	4.89	2.32
Tefor (2.4 µm)	ANTs A	4.56	2.99
	ANTs B	4.12	5.39
	ANTs C	4.34	0.53
	CMTK A	5.44	2.57
	CMTK C	6.02	1.03
	CMTK B	5.47	1.10
Tefor (3.6 µm)	ANTs A	5.11	1.28
	ANTs B	4.17	6.09
	ANTs C	4.52	0.19
	CMTK A	5.14	1.74
	CMTK C	6.36	0.66
	CMTK B	5.64	0.60

Table 6: Mean skeleton distances and mean CPU time by template and algorithm at different resolutions.

Template	Algorithm	Mean	Std dev	Median
JRC 2018	ANTs A	3.97	3.65	3.08
JRC 2018	CMTK A	4.03	3.70	3.16
JRC 2018	CMTK B	4.04	3.70	3.16
JFRC 2013	ANTs A	4.10	3.81	3.16
JRC 2018	CMTK C	4.13	3.74	3.24
FCWB	ANTs B	4.18	3.55	3.32
Tefor	ANTs A	4.19	3.91	3.24
FCWB	ANTs C	4.23	3.53	3.46
FCWB	ANTs A	4.34	4.09	3.24
JRC 2018	ANTs B	4.34	3.94	3.46
JRC 2018	ANTs C	4.53	4.07	3.61
JFRC 2013	CMTK A	4.64	4.61	3.54
JFRC 2010	ANTs B	4.69	4.23	3.67
Tefor	ANTs B	4.70	4.22	3.67
JFRC 2013	CMTK B	4.75	4.77	3.61
JFRC 2010	ANTs C	4.89	4.32	3.81
JFRC 2013	ANTs B	4.94	4.36	3.81
JFRC 2013	ANTs C	4.95	4.37	3.81
JFRC 2013	CMTK C	5.05	4.23	4.06
Tefor	ANTs C	5.05	4.54	3.87
JFRC 2010	CMTK B	5.33	5.12	3.87
Tefor	CMTK C	5.51	5.75	4.06
JFRC 2010	CMTK A	5.64	5.49	4.12
JFRC 2010	CMTK C	5.68	5.24	4.30
Tefor	CMTK A	5.70	6.10	3.87
Tefor	CMTK B	5.70	6.08	3.87
JFRC 2010	ANTs A	6.21	6.07	4.47
FCWB	CMTK A	8.92	8.22	6.52
FCWB	CMTK B	9.03	8.17	6.67
FCWB	CMTK C	9.03	7.45	6.86

Table 7: Skeleton distance statistics (in µm) for all algorithm/template pairs, sorted by mean distance.

Template	Algorithm	Mean (stdev)
JFRC 2010	ANTs A	1.0543 (0.2330)
JFRC 2010	ANTs B	0.9833 (0.0875)
JFRC 2010	ANTs C	0.9642 (0.2814)
JFRC 2010	CMTK A	1.0115 (0.1798)
JFRC 2010	CMTK B	1.0258 (0.1575)
JFRC 2010	CMTK C	0.9997 (0.0296)
JFRC 2013	ANTs A	0.9542 (0.1830)
JFRC 2013	ANTs B	0.9601 (0.0812)
JFRC 2013	ANTs C	0.9718 (0.3055)
JFRC 2013	CMTK A	0.9343 (0.1860)
JFRC 2013	CMTK B	0.9420 (0.1511)
JFRC 2013	CMTK C	0.9720 (0.0310)
Tefor	ANTs A	1.0401 (0.2344)
Tefor	ANTs B	0.9791 (0.0853)
Tefor	ANTs C	0.9717 (0.2922)
Tefor	CMTK A	1.0033 (0.2536)
Tefor	CMTK B	1.0175 (0.2183)
Tefor	CMTK C	1.0048 (0.0556)
JRC 2018	ANTs A	0.9935 (0.1733)
JRC 2018	ANTs B	0.9656 (0.0893)
JRC 2018	ANTs C	0.9579 (0.2587)
JRC 2018	CMTK A	0.9795 (0.2347)
JRC 2018	CMTK B	0.9857 (0.1735)
JRC 2018	CMTK C	0.9945 (0.0743)
FCWB	ANTs A	0.9710 (0.3635)
FCWB	ANTs B	0.9795 (0.1017)
FCWB	ANTs C	0.9681 (0.2263)
FCWB	CMTK A	1.0082 (0.3260)
FCWB	CMTK B	0.9986 (0.2688)
FCWB	CMTK C	0.9890 (0.0737)

Table 8: Mean (Standard deviation) of Jacobian determinant by template. Observe that all mean values are close to 1.0, whereas standard deviations vary much more across template/algorithm pairs. For instance, ANTs B and CMTK C have consistently smaller standard deviations because they are more regularized.

B Supplementary Tables

S1 CRE_R : crepine 47
S2 CAN_R : cantle 48
S3 AMMC_R : antennal mechanosensory and motor center . . 49
S4 ICL_R : inferior clamp 50
S5 VES_R : vest 51
S6 IB_R : inferior bridge 52
S7 ATL_R : antler 53
S8 CRE_R : crepine 54
S9 MB_PED_R : pedunculus of adult mushroom body 55
S10 MB_VL_R : vertical lobe of adult mushroom body 56
S11 MB_ML_R : medial lobe of adult mushroom body 57
S12 FLA_R : flange 58
S13 LOP_R : lobula plate 59
S14 EB : ellipsoid body 60
S15 AL_R : adult antennal lobe 61
S16 ME_R : medulla 62
S17 FB : fan-shaped body 63
S18 SLP_R : superior lateral protocerebrum 64
S19 SIP_R : superior intermediate protocerebrum 65
S20 SMP_R : superior medial protocerebrum 66
S21 AME_R : accessory medulla 67
S22 AVLP_R : anterior ventrolateral protocerebrum 68
S23 PVLP_R : posterior ventrolateral protocerebrum 69
S24 IVLP_R : wedge 70
S25 PLP_R : posterior lateral protocerebrum 71
S26 AOTU_R : anterior optic tubercle 72
S27 GOR_R : gorget 73
S28 MB_CA_R : calyx of adult mushroom body 74
S29 SPS_R : superior posterior slope 75
S30 IPS_R : inferior posterior slope 76
S31 SCL_R : superior clamp 77
S32 LO_R : lobula 78
S33 EPA_R : epaulette 79
S34 GNG : adult gnathal ganglion 80
S35 NO : nodulus 81
S36 PRW : prow 82
S37 GA_R : gall 83
S38 AME_L : accessory medulla 84

S39 LO_L : lobula 85
S40 BU_L : bulb 86
S41 LH_L : lateral horn 87
S42 LAL_L : lateral accessory lobe 88
S43 CAN_L : cantle 89
S44 AMMC_L : antennal mechanosensory and motor center . . 90
S45 ICL_L : inferior clamp 91
S46 BU_R : bulb 92
S47 VES_L : vest 93
S48 IB_L : inferior bridge 94
S49 ATL_L : antler 95
S50 CRE_L : crepine 96
S51 MB_PED_L : pedunculus of adult mushroom body 97
S52 MB_VL_L : vertical lobe of adult mushroom body 98
S53 MB_ML_L : medial lobe of adult mushroom body 99
S54 FLA_L : flange 100
S55 LOP_L : lobula plate 101
S56 PB : protocerebral bridge 102
S57 AL_L : adult antennal lobe 103
S58 ME_L : medulla 104
S59 SLP_L : superior lateral protocerebrum 105
S60 SIP_L : superior intermediate protocerebrum 106
S61 SMP_L : superior medial protocerebrum 107
S62 AVLP_L : anterior ventrolateral protocerebrum 108
S63 PVLP_L : posterior ventrolateral protocerebrum 109
S64 IVLP_L : wedge 110
S65 PLP_L : posterior lateral protocerebrum 111
S66 AOTU_L : anterior optic tubercle 112
S67 LH_R : lateral horn 113
S68 GOR_L : gorget 114
S69 MB_CA_L : calyx of adult mushroom body 115
S70 SPS_L : superior posterior slope 116
S71 IPS_L : inferior posterior slope 117
S72 SCL_L : superior clamp 118
S73 EPA_L : epaulette 119
S74 GA_L : gall 120
S75 LAL_R : lateral accessory lobe 121
S76 SAD : saddle 122

Template	Algorithm	Mean	Std dev	10th perc	median	90th perc	N
FCWB	ANTs A	5.50	4.76	1.00	4.00	12.12	128116
	ANTs B	8.15	5.52	2.12	7.04	16.09	103628
	ANTs C	7.90	5.37	2.00	6.82	15.33	113236
	CMTK A	7.26	5.37	1.58	5.87	15.18	105712
	CMTK C	6.67	4.87	1.58	5.43	13.66	125260
	CMTK B	6.85	5.31	1.58	5.34	14.92	109638
JFRC2013	ANTs A	4.57	3.73	1.00	3.61	9.25	138368
	ANTs B	6.72	4.94	1.58	5.52	13.67	128144
	ANTs C	6.56	5.08	1.58	5.20	13.53	133550
	CMTK A	5.41	4.35	1.22	4.18	11.18	130310
	CMTK C	6.11	4.70	1.41	5.00	12.49	141378
	CMTK B	5.51	4.34	1.22	4.36	11.38	135338
Tefor	ANTs A	4.64	3.84	1.00	3.61	9.54	141758
	ANTs B	4.82	3.72	1.22	3.81	9.75	143886
	ANTs C	5.03	3.60	1.41	4.18	9.85	165882
	CMTK A	7.43	5.16	1.58	6.36	14.93	140012
	CMTK C	5.21	4.22	1.00	4.00	11.09	205034
	CMTK B	6.94	4.93	1.58	5.87	13.95	136286
JRC2018	ANTs A	4.66	3.82	1.00	3.61	9.51	140804
	ANTs B	4.93	3.85	1.22	3.87	9.72	135624
	ANTs C	5.31	4.04	1.41	4.30	10.46	141770
	CMTK A	5.00	4.02	1.22	3.87	10.02	124912
	CMTK C	4.83	3.88	1.22	3.81	9.67	128432
	CMTK B	4.91	3.97	1.22	3.81	9.85	124664
JFRC2010	ANTs A	8.62	6.72	1.58	7.04	17.85	256308
	ANTs B	4.96	3.95	1.22	3.81	10.07	146800
	ANTs C	5.20	3.87	1.41	4.24	10.22	146628
	CMTK A	8.45	8.46	1.58	5.79	17.96	118112
	CMTK C	7.69	7.71	1.73	5.52	15.13	137414
	CMTK B	7.78	7.47	1.58	5.43	16.65	119994

Table S1: CRE_R : crepine

Template	Algorithm	Mean	Std dev	10th perc	median	90th perc	N
FCWB	ANTs A	3.75	2.67	1.00	3.08	7.25	22464
	ANTs B	3.84	2.34	1.22	3.54	6.75	26150
	ANTs C	3.76	2.27	1.22	3.46	6.71	22568
	CMTK A	3.81	2.65	1.00	3.24	7.28	46938
	CMTK C	4.07	2.85	1.00	3.54	7.91	33454
	CMTK B	3.87	2.70	1.00	3.24	7.38	31124
JFRC2013	ANTs A	3.93	2.80	1.00	3.24	7.65	21630
	ANTs B	3.35	2.28	1.00	2.92	6.32	47016
	ANTs C	3.15	2.23	0.71	2.65	6.00	44028
	CMTK A	3.53	2.67	1.00	2.92	6.86	24354
	CMTK C	4.10	2.59	1.22	3.61	7.58	34654
	CMTK B	3.56	2.69	1.00	2.92	6.96	24016
Tefor	ANTs A	4.26	2.99	1.22	3.61	8.19	19428
	ANTs B	4.27	2.67	1.41	3.81	7.65	24896
	ANTs C	4.94	2.94	1.58	4.53	8.63	30864
	CMTK A	4.76	3.17	1.41	4.12	9.27	23110
	CMTK C	4.49	3.09	1.41	3.81	8.54	21146
	CMTK B	4.86	3.10	1.41	4.24	9.34	23078
JRC2018	ANTs A	3.77	2.75	1.00	3.00	7.38	21558
	ANTs B	4.13	2.79	1.00	3.61	7.65	23310
	ANTs C	4.04	2.63	1.22	3.54	7.42	26778
	CMTK A	3.87	2.80	1.00	3.16	7.62	21388
	CMTK C	3.81	2.84	1.00	3.08	7.55	21214
	CMTK B	3.91	2.91	1.00	3.08	7.84	21008
JFRC2010	ANTs A	7.40	6.98	1.58	4.95	18.22	16290
	ANTs B	4.24	2.56	1.41	3.81	7.58	30124
	ANTs C	4.13	2.59	1.22	3.61	7.42	37836
	CMTK A	6.26	6.62	1.22	4.06	15.00	35436
	CMTK C	6.02	5.70	1.58	4.18	14.93	33842
	CMTK B	5.94	6.30	1.22	3.81	14.92	30950

Table S2: CAN_R : cantle

Template	Algorithm	Mean	Std dev	10th perc	median	90th perc	N
FCWB	ANTs A	4.77	4.22	1.41	3.87	8.28	198206
	ANTs B	5.61	5.45	1.58	4.47	9.54	118958
	ANTs C	5.23	4.52	1.58	4.18	9.25	129264
	CMTK A	5.30	4.59	1.58	4.36	9.30	189414
	CMTK C	5.17	4.63	1.58	4.24	8.75	153568
	CMTK B	5.28	4.67	1.58	4.30	9.22	187246
JFRC2013	ANTs A	4.67	4.55	1.22	3.67	7.91	194144
	ANTs B	6.25	6.12	1.58	4.74	11.18	163990
	ANTs C	6.09	6.20	1.58	4.53	11.27	159530
	CMTK A	5.04	4.73	1.58	4.06	8.63	178554
	CMTK C	5.76	4.96	1.58	4.53	10.44	139908
	CMTK B	5.07	4.72	1.41	4.06	8.66	172350
Tefor	ANTs A	4.63	4.46	1.22	3.67	7.81	195792
	ANTs B	4.94	4.87	1.41	3.81	8.54	206934
	ANTs C	5.29	5.41	1.58	4.18	8.72	221890
	CMTK A	5.10	4.74	1.41	3.87	9.03	198934
	CMTK C	5.16	5.23	1.58	4.12	8.51	201560
	CMTK B	4.90	4.53	1.41	3.87	8.51	203194
JRC2018	ANTs A	4.58	4.50	1.22	3.61	7.65	196510
	ANTs B	4.85	4.56	1.41	3.87	8.15	200496
	ANTs C	5.00	4.94	1.41	3.87	8.51	220340
	CMTK A	4.66	4.62	1.22	3.67	7.84	192616
	CMTK C	4.75	4.40	1.41	3.81	8.03	193484
	CMTK B	4.67	4.50	1.41	3.67	7.91	190402
JFRC2010	ANTs A	7.15	7.96	1.58	4.53	19.77	225304
	ANTs B	5.23	4.99	1.58	4.18	8.75	187944
	ANTs C	5.42	5.06	1.58	4.36	9.17	193640
	CMTK A	5.18	4.71	1.41	4.12	9.19	189018
	CMTK C	5.25	5.02	1.58	4.18	8.75	187834
	CMTK B	5.02	4.60	1.41	4.06	8.60	194876

Table S3: AMMC_R : antennal mechanosensory and motor center

Template	Algorithm	Mean	Std dev	10th perc	median	90th perc	N
FCWB	ANTs A	2.76	2.81	0.71	2.00	5.87	334680
	ANTs B	3.55	3.41	0.71	2.45	7.94	310126
	ANTs C	3.38	3.28	0.71	2.35	7.42	305450
	CMTK A	5.38	5.55	0.71	3.54	12.98	283240
	CMTK C	3.83	4.04	0.71	2.55	8.63	304944
	CMTK B	4.97	5.25	0.71	3.24	11.27	264802
JFRC2013	ANTs A	2.70	2.77	0.71	2.00	5.57	321788
	ANTs B	3.43	3.35	0.71	2.35	7.68	299558
	ANTs C	3.22	3.17	0.71	2.24	7.04	303386
	CMTK A	3.01	2.87	0.71	2.12	6.40	293092
	CMTK C	4.04	3.56	0.71	3.00	8.49	263762
	CMTK B	3.17	2.97	0.71	2.24	6.82	290932
Tefor	ANTs A	2.67	2.67	0.71	2.00	5.57	321736
	ANTs B	3.09	2.85	0.71	2.24	6.56	322866
	ANTs C	3.24	3.13	0.71	2.24	7.04	319676
	CMTK A	3.47	4.31	0.71	2.12	8.03	296402
	CMTK C	3.49	3.25	0.71	2.55	7.58	319366
	CMTK B	3.59	4.50	0.71	2.12	8.34	299568
JRC2018	ANTs A	2.67	2.70	0.71	2.00	5.57	319308
	ANTs B	2.86	2.66	0.71	2.12	5.74	326204
	ANTs C	2.90	2.82	0.71	2.12	6.00	329458
	CMTK A	2.68	2.80	0.71	2.00	5.57	298028
	CMTK C	2.72	2.68	0.71	2.00	5.57	303460
	CMTK B	2.66	2.77	0.71	1.73	5.57	296780
JFRC2010	ANTs A	8.84	7.21	1.41	6.75	19.51	501078
	ANTs B	3.17	2.99	0.71	2.24	6.67	316016
	ANTs C	3.31	3.20	0.71	2.35	7.11	307394
	CMTK A	4.21	5.41	0.71	2.24	11.20	293368
	CMTK C	4.18	4.48	0.71	2.83	9.22	331886
	CMTK B	4.16	5.57	0.71	2.24	9.54	289230

Table S4: ICL_R : inferior clamp

Template	Algorithm	Mean	Std dev	10th perc	median	90th perc	N
FCWB	ANTs A	4.79	3.99	1.00	3.67	9.59	112756
	ANTs B	4.88	3.64	1.41	4.06	9.51	221906
	ANTs C	4.97	3.86	1.41	4.06	9.85	184380
	CMTK A	7.35	5.92	1.58	5.43	16.34	189818
	CMTK C	6.27	4.81	1.58	4.95	13.29	153026
	CMTK B	6.95	5.47	1.58	5.29	14.87	139980
JFRC2013	ANTs A	4.54	3.63	1.00	3.61	9.06	113054
	ANTs B	4.51	3.46	1.22	3.61	8.86	279266
	ANTs C	4.57	3.67	1.00	3.61	9.25	244618
	CMTK A	4.72	3.65	1.22	3.81	9.54	98662
	CMTK C	4.88	3.86	1.22	3.81	10.02	182464
	CMTK B	4.76	3.66	1.22	3.81	9.51	99628
Tefor	ANTs A	4.44	3.50	1.00	3.61	8.75	120918
	ANTs B	4.47	3.39	1.22	3.61	8.66	201810
	ANTs C	5.26	3.79	1.41	4.36	10.27	194238
	CMTK A	7.31	5.61	1.58	5.79	16.02	156436
	CMTK C	6.88	5.23	1.58	5.29	14.85	165862
	CMTK B	7.40	5.64	1.58	5.87	16.02	160204
JRC2018	ANTs A	4.46	3.63	1.00	3.61	8.97	111894
	ANTs B	4.93	3.72	1.22	4.06	9.82	136380
	ANTs C	4.97	3.60	1.41	4.06	9.92	135970
	CMTK A	4.53	3.62	1.00	3.61	9.00	95754
	CMTK C	4.59	3.67	1.00	3.67	9.22	100094
	CMTK B	4.54	3.63	1.00	3.61	9.06	92400
JFRC2010	ANTs A	8.27	6.72	1.73	6.20	18.12	124266
	ANTs B	4.62	3.63	1.22	3.81	8.97	171134
	ANTs C	4.85	4.00	1.00	3.81	9.92	176908
	CMTK A	7.38	6.75	1.41	5.00	17.28	162750
	CMTK C	6.43	6.08	1.41	4.30	15.20	184334
	CMTK B	7.22	6.80	1.41	4.74	17.13	139584

Table S5: VES_R : vest

Template	Algorithm	Mean	Std dev	10th perc	median	90th perc	N
FCWB	ANTs A	3.34	2.86	0.71	2.55	6.86	208368
	ANTs B	4.80	3.68	1.00	3.81	10.15	295074
	ANTs C	3.92	2.90	1.00	3.16	7.91	345268
	CMTK A	6.35	5.29	1.22	4.74	13.96	204434
	CMTK C	4.28	3.73	1.00	3.08	9.51	246048
	CMTK B	5.75	4.96	1.00	4.12	12.92	198092
JFRC2013	ANTs A	3.16	2.77	0.71	2.35	6.56	210128
	ANTs B	4.26	3.37	1.00	3.32	8.77	324356
	ANTs C	4.21	3.29	1.00	3.32	8.77	325204
	CMTK A	3.37	2.87	0.71	2.55	6.96	181380
	CMTK C	4.82	3.92	1.00	3.61	11.07	207494
	CMTK B	3.51	2.88	0.71	2.65	7.28	178796
Tefor	ANTs A	3.11	2.66	0.71	2.35	6.36	212832
	ANTs B	3.85	3.21	1.00	2.92	8.03	239752
	ANTs C	4.00	3.25	1.00	3.08	8.51	275152
	CMTK A	4.51	4.17	0.71	3.00	10.86	206740
	CMTK C	4.51	3.87	1.00	3.24	10.22	206512
	CMTK B	4.50	4.22	0.71	3.00	10.98	208652
JRC2018	ANTs A	3.10	2.67	0.71	2.35	6.40	216404
	ANTs B	3.41	2.89	0.71	2.65	7.07	226268
	ANTs C	3.21	2.67	0.71	2.55	6.56	227828
	CMTK A	3.32	3.02	0.71	2.45	7.11	183046
	CMTK C	3.13	2.74	0.71	2.35	6.44	195562
	CMTK B	3.19	2.84	0.71	2.35	6.67	181056
JFRC2010	ANTs A	5.84	5.36	1.00	3.87	13.42	212072
	ANTs B	4.07	3.36	1.00	3.08	8.66	255490
	ANTs C	4.10	3.19	1.00	3.24	8.43	364138
	CMTK A	4.72	4.54	1.00	3.24	10.63	247624
	CMTK C	4.42	4.45	1.00	3.08	9.22	370982
	CMTK B	4.46	4.37	1.00	3.08	9.64	257816

Table S6: IB_R : inferior bridge

Template	Algorithm	Mean	Std dev	10th perc	median	90th perc	N
FCWB	ANTs A	3.67	2.49	1.00	3.16	6.86	95158
	ANTs B	4.52	2.95	1.22	3.81	8.75	107846
	ANTs C	4.26	2.85	1.22	3.61	8.37	118618
	CMTK A	5.78	5.22	1.41	4.36	11.36	72358
	CMTK C	4.26	3.00	1.22	3.61	8.09	88152
	CMTK B	5.52	5.18	1.41	4.06	11.18	76574
JFRC2013	ANTs A	3.49	2.50	1.00	2.92	6.56	102024
	ANTs B	4.52	3.08	1.22	3.81	8.89	113776
	ANTs C	4.54	3.20	1.00	3.81	9.11	110298
	CMTK A	3.45	2.29	1.00	2.92	6.48	93474
	CMTK C	4.57	2.98	1.41	3.87	8.72	90024
	CMTK B	3.57	2.34	1.00	3.08	6.67	90208
Tefor	ANTs A	3.24	2.25	1.00	2.83	6.08	104392
	ANTs B	4.07	2.64	1.22	3.61	7.62	99864
	ANTs C	4.38	3.00	1.22	3.67	8.54	108260
	CMTK A	3.88	2.72	1.00	3.24	7.58	112418
	CMTK C	4.28	2.71	1.22	3.81	8.00	98510
	CMTK B	3.82	2.62	1.00	3.24	7.35	114492
JRC2018	ANTs A	3.24	2.28	1.00	2.65	6.08	105940
	ANTs B	3.61	2.45	1.00	3.08	6.71	101916
	ANTs C	3.55	2.44	1.00	3.00	6.67	101848
	CMTK A	3.38	2.44	1.00	2.92	6.48	100240
	CMTK C	3.41	2.29	1.00	2.92	6.36	97688
	CMTK B	3.37	2.37	1.00	2.92	6.44	99604
JFRC2010	ANTs A	4.34	3.45	1.00	3.54	8.49	125792
	ANTs B	4.23	2.71	1.22	3.67	8.03	99154
	ANTs C	4.47	3.16	1.00	3.67	9.00	116250
	CMTK A	4.91	3.65	1.00	4.00	10.00	100040
	CMTK C	4.18	3.05	1.00	3.54	8.28	124706
	CMTK B	4.74	3.42	1.00	3.87	9.54	100534

Table S7: ATL_R : antler

Template	Algorithm	Mean	Std dev	10th perc	median	90th perc	N
FCWB	ANTs A	5.50	4.76	1.00	4.00	12.12	128116
	ANTs B	8.15	5.52	2.12	7.04	16.09	103628
	ANTs C	7.90	5.37	2.00	6.82	15.33	113236
	CMTK A	7.26	5.37	1.58	5.87	15.18	105712
	CMTK C	6.67	4.87	1.58	5.43	13.66	125260
	CMTK B	6.85	5.31	1.58	5.34	14.92	109638
JFRC2013	ANTs A	4.57	3.73	1.00	3.61	9.25	138368
	ANTs B	6.72	4.94	1.58	5.52	13.67	128144
	ANTs C	6.56	5.08	1.58	5.20	13.53	133550
	CMTK A	5.41	4.35	1.22	4.18	11.18	130310
	CMTK C	6.11	4.70	1.41	5.00	12.49	141378
	CMTK B	5.51	4.34	1.22	4.36	11.38	135338
Tefor	ANTs A	4.64	3.84	1.00	3.61	9.54	141758
	ANTs B	4.82	3.72	1.22	3.81	9.75	143886
	ANTs C	5.03	3.60	1.41	4.18	9.85	165882
	CMTK A	7.43	5.16	1.58	6.36	14.93	140012
	CMTK C	5.21	4.22	1.00	4.00	11.09	205034
	CMTK B	6.94	4.93	1.58	5.87	13.95	136286
JRC2018	ANTs A	4.66	3.82	1.00	3.61	9.51	140804
	ANTs B	4.93	3.85	1.22	3.87	9.72	135624
	ANTs C	5.31	4.04	1.41	4.30	10.46	141770
	CMTK A	5.00	4.02	1.22	3.87	10.02	124912
	CMTK C	4.83	3.88	1.22	3.81	9.67	128432
	CMTK B	4.91	3.97	1.22	3.81	9.85	124664
JFRC2010	ANTs A	8.62	6.72	1.58	7.04	17.85	256308
	ANTs B	4.96	3.95	1.22	3.81	10.07	146800
	ANTs C	5.20	3.87	1.41	4.24	10.22	146628
	CMTK A	8.45	8.46	1.58	5.79	17.96	118112
	CMTK C	7.69	7.71	1.73	5.52	15.13	137414
	CMTK B	7.78	7.47	1.58	5.43	16.65	119994

Table S8: CRE_R : crepine

Template	Algorithm	Mean	Std dev	10th perc	median	90th perc	N
FCWB	ANTs A	4.94	4.18	1.00	3.81	10.44	74328
	ANTs B	4.66	3.93	1.00	3.54	10.15	60650
	ANTs C	5.30	4.42	1.22	4.06	11.20	61662
	CMTK A	5.70	4.15	1.58	4.53	11.62	48344
	CMTK C	4.72	3.80	1.00	3.61	10.39	63940
	CMTK B	5.69	4.27	1.58	4.53	11.73	49326
JFRC2013	ANTs A	4.84	3.79	1.00	3.81	10.27	73940
	ANTs B	5.86	4.43	1.41	4.69	12.00	63096
	ANTs C	5.79	4.42	1.41	4.58	11.94	59998
	CMTK A	5.17	4.03	1.22	4.12	10.72	72824
	CMTK C	5.71	4.19	1.41	4.58	11.94	63138
	CMTK B	5.40	4.08	1.22	4.36	11.18	70880
Tefor	ANTs A	4.90	3.80	1.00	3.81	10.46	76484
	ANTs B	4.95	3.77	1.22	3.87	10.51	70062
	ANTs C	5.14	3.86	1.22	4.12	10.79	74764
	CMTK A	5.83	5.58	1.00	4.00	13.30	69062
	CMTK C	5.10	4.30	1.00	3.81	11.02	71454
	CMTK B	5.86	5.85	1.00	3.81	13.68	66370
JRC2018	ANTs A	4.85	3.80	1.00	3.81	10.40	75608
	ANTs B	4.79	3.77	1.00	3.67	10.30	76030
	ANTs C	4.96	3.86	1.22	3.81	10.54	73184
	CMTK A	4.83	3.83	1.00	3.67	10.46	74458
	CMTK C	4.80	3.81	1.00	3.61	10.39	74460
	CMTK B	4.77	3.79	1.00	3.61	10.34	74242
JFRC2010	ANTs A	7.21	7.13	1.58	5.20	14.18	74380
	ANTs B	5.17	3.88	1.22	4.12	10.63	70674
	ANTs C	5.38	4.17	1.22	4.18	11.49	68636
	CMTK A	5.75	4.34	1.00	4.53	12.19	64380
	CMTK C	6.03	5.01	1.41	4.53	12.67	59820
	CMTK B	6.01	5.35	1.00	4.30	13.51	61530

Table S9: MB_PED_R : pedunculus of adult mushroom body

Template	Algorithm	Mean	Std dev	10th perc	median	90th perc	N
FCWB	ANTs A	5.57	4.40	1.41	4.47	11.20	94886
	ANTs B	5.30	3.94	1.58	4.36	9.85	71238
	ANTs C	6.00	4.19	1.73	5.00	11.68	72886
	CMTK A	4.88	3.62	1.41	4.06	9.46	103216
	CMTK C	4.73	3.31	1.41	4.06	8.86	72578
	CMTK B	4.96	3.76	1.58	4.00	9.75	95366
JFRC2013	ANTs A	5.09	3.74	1.41	4.30	9.72	116878
	ANTs B	5.69	4.37	1.58	4.53	11.18	100764
	ANTs C	5.70	4.11	1.58	4.74	11.16	97684
	CMTK A	4.82	3.67	1.22	4.06	9.33	118996
	CMTK C	6.15	4.09	1.73	5.20	11.58	71658
	CMTK B	5.14	3.70	1.58	4.36	9.72	112736
Tefor	ANTs A	4.20	3.54	1.00	3.46	7.91	128050
	ANTs B	4.67	3.62	1.41	3.81	8.75	110182
	ANTs C	4.63	3.54	1.22	3.81	8.77	123050
	CMTK A	6.94	8.52	1.00	3.81	18.65	111368
	CMTK C	5.44	4.41	1.58	4.30	10.70	96924
	CMTK B	7.28	9.25	1.22	3.87	19.03	106430
JRC2018	ANTs A	4.20	3.52	1.00	3.32	7.81	128470
	ANTs B	4.91	3.81	1.41	3.87	9.64	116984
	ANTs C	4.87	3.84	1.22	3.87	9.54	124096
	CMTK A	4.17	3.54	1.00	3.24	7.91	125576
	CMTK C	4.47	3.66	1.00	3.61	8.72	120790
	CMTK B	4.29	3.64	1.00	3.46	8.31	121318
JFRC2010	ANTs A	6.25	5.40	1.41	4.58	13.87	148586
	ANTs B	5.02	3.99	1.41	4.06	9.51	104580
	ANTs C	5.00	3.82	1.41	4.12	9.62	120192
	CMTK A	5.03	4.51	1.00	3.67	11.00	118312
	CMTK C	6.40	6.22	1.58	4.36	14.66	93648
	CMTK B	6.13	7.28	1.00	3.81	14.25	114094

Table S10: MB_VL_R : vertical lobe of adult mushroom body

Template	Algorithm	Mean	Std dev	10th perc	median	90th perc	N
FCWB	ANTs A	4.44	4.30	1.00	3.16	9.30	220032
	ANTs B	5.19	4.42	1.22	4.06	10.46	142946
	ANTs C	5.80	4.83	1.41	4.53	12.17	131222
	CMTK A	5.24	4.26	1.22	4.06	10.72	211104
	CMTK C	4.45	3.88	1.00	3.32	9.22	196264
	CMTK B	4.98	4.10	1.22	3.81	10.22	219434
JFRC2013	ANTs A	4.01	3.82	1.00	2.92	8.09	255556
	ANTs B	4.96	4.39	1.00	3.67	10.44	202548
	ANTs C	5.38	4.81	1.22	3.87	11.60	176168
	CMTK A	4.72	4.17	1.00	3.54	9.92	221616
	CMTK C	5.40	4.58	1.22	4.06	11.36	150036
	CMTK B	4.73	4.19	1.00	3.54	10.02	214090
Tefor	ANTs A	4.08	3.84	1.00	3.00	8.19	254684
	ANTs B	3.87	3.61	0.71	2.92	7.84	267642
	ANTs C	4.38	3.77	1.00	3.24	8.77	255450
	CMTK A	4.78	3.95	1.00	3.67	9.72	245312
	CMTK C	4.67	4.18	1.00	3.54	9.92	279808
	CMTK B	4.81	4.05	1.00	3.67	9.90	239164
JRC2018	ANTs A	4.03	3.84	1.00	2.92	8.03	258948
	ANTs B	3.99	3.76	0.71	2.92	8.09	257518
	ANTs C	4.23	3.83	1.00	3.16	8.40	249260
	CMTK A	4.17	3.92	1.00	3.08	8.40	249050
	CMTK C	4.09	3.77	1.00	3.00	8.31	245308
	CMTK B	4.16	3.87	1.00	3.08	8.40	244526
JFRC2010	ANTs A	6.15	5.54	1.00	4.06	14.93	234816
	ANTs B	3.86	3.65	0.71	2.92	8.03	274290
	ANTs C	4.29	3.78	1.00	3.24	8.66	243720
	CMTK A	6.74	8.62	1.00	3.67	17.01	217274
	CMTK C	5.71	7.19	0.71	3.46	13.51	273894
	CMTK B	5.74	6.69	0.71	3.54	13.44	227764

Table S11: MB_ML_R : medial lobe of adult mushroom body

Template	Algorithm	Mean	Std dev	10th perc	median	90th perc	N
FCWB	ANTs A	2.52	2.46	0.71	2.12	5.00	422600
	ANTs B	3.85	3.36	1.00	3.08	7.25	303022
	ANTs C	3.84	3.39	1.00	3.00	7.35	316062
	CMTK A	3.22	2.74	0.71	2.65	6.32	393608
	CMTK C	3.13	2.66	0.71	2.55	6.12	336788
	CMTK B	3.22	2.93	0.71	2.65	6.12	391004
JFRC2013	ANTs A	2.68	2.26	0.71	2.12	5.34	399670
	ANTs B	4.49	3.95	1.00	3.61	8.63	262524
	ANTs C	4.07	3.67	1.00	3.24	7.68	272910
	CMTK A	2.64	2.23	0.71	2.12	5.20	424002
	CMTK C	3.38	2.73	0.71	2.92	6.40	303820
	CMTK B	2.63	2.20	0.71	2.12	5.20	410600
Tefor	ANTs A	2.50	2.34	0.71	2.12	5.00	426156
	ANTs B	3.40	2.94	0.71	2.83	6.56	366804
	ANTs C	3.48	3.21	0.71	2.65	6.75	414964
	CMTK A	3.08	2.68	0.71	2.45	6.36	379488
	CMTK C	3.70	3.88	0.71	2.65	6.96	363462
	CMTK B	3.32	3.01	0.71	2.55	6.96	363494
JRC2018	ANTs A	2.42	2.11	0.71	2.00	4.74	408766
	ANTs B	3.13	2.71	0.71	2.55	6.20	384048
	ANTs C	3.45	3.07	0.71	2.65	6.82	379300
	CMTK A	2.46	2.19	0.71	2.12	4.90	449412
	CMTK C	2.47	2.17	0.71	2.12	4.95	402876
	CMTK B	2.46	2.23	0.71	2.12	4.80	421730
JFRC2010	ANTs A	5.47	8.07	0.71	2.92	11.60	354210
	ANTs B	3.32	2.69	0.71	2.83	6.36	377092
	ANTs C	3.27	2.79	0.71	2.65	6.44	419414
	CMTK A	3.68	4.16	0.71	2.55	7.38	352410
	CMTK C	3.64	3.61	0.71	2.65	7.42	348282
	CMTK B	3.64	4.14	0.71	2.55	7.28	361674

Table S12: FLA_R : flange

Template	Algorithm	Mean	Std dev	10th perc	median	90th perc	N
FCWB	ANTs A	6.77	5.50	1.73	5.43	13.15	411806
	ANTs B	6.73	4.92	2.00	5.57	12.75	359238
	ANTs C	6.79	4.89	2.12	5.70	12.77	392490
	CMTK A	7.54	5.49	2.12	6.24	14.39	416848
	CMTK C	7.69	5.41	2.24	6.36	14.87	404082
	CMTK B	7.40	5.46	2.12	6.08	14.16	391324
JFRC2013	ANTs A	6.05	5.29	1.58	4.74	11.94	442126
	ANTs B	6.66	5.18	1.73	5.39	13.00	445352
	ANTs C	7.05	5.20	2.00	5.87	13.53	444334
	CMTK A	7.23	6.54	1.58	5.20	15.18	426364
	CMTK C	6.76	4.71	2.12	5.70	12.77	449680
	CMTK B	7.26	6.49	1.73	5.34	14.87	424412
Tefor	ANTs A	5.81	5.07	1.58	4.53	11.36	436920
	ANTs B	6.26	4.86	1.73	5.15	11.79	378356
	ANTs C	6.95	5.09	2.00	5.83	13.30	416008
	CMTK A	7.14	5.66	1.73	5.70	14.23	471104
	CMTK C	6.55	5.36	1.73	5.20	12.43	409754
	CMTK B	7.12	5.63	1.73	5.70	13.95	455220
JRC2018	ANTs A	5.65	4.93	1.58	4.36	11.07	439706
	ANTs B	5.68	4.80	1.58	4.53	11.00	435238
	ANTs C	6.01	4.98	1.58	4.74	11.83	457370
	CMTK A	5.61	4.93	1.41	4.36	11.05	468788
	CMTK C	5.76	5.06	1.58	4.53	11.07	448426
	CMTK B	5.60	4.91	1.58	4.36	10.91	458608
JFRC2010	ANTs A	8.66	6.73	2.35	6.93	17.13	475654
	ANTs B	6.80	4.84	2.12	5.74	12.77	388000
	ANTs C	7.30	4.93	2.12	6.32	13.58	458102
	CMTK A	8.49	5.92	2.24	7.11	16.63	509662
	CMTK C	7.21	4.91	2.12	6.08	13.95	497312
	CMTK B	7.64	5.09	2.12	6.52	14.83	460728

Table S13: LOP_R : lobula plate

Template	Algorithm	Mean	Std dev	10th perc	median	90th perc	N
FCWB	ANTs A	3.47	1.98	1.22	3.16	6.04	265968
	ANTs B	3.53	2.41	1.00	3.00	6.86	373646
	ANTs C	3.64	2.40	1.00	3.08	6.96	345156
	CMTK A	5.69	4.23	1.58	4.53	11.68	302648
	CMTK C	3.88	2.68	1.00	3.24	7.58	330860
	CMTK B	5.22	3.96	1.41	4.12	10.82	302658
JFRC2013	ANTs A	3.49	1.99	1.22	3.24	6.08	269494
	ANTs B	3.91	2.30	1.41	3.61	6.96	287216
	ANTs C	3.83	2.24	1.22	3.54	6.82	279940
	CMTK A	3.63	2.07	1.22	3.32	6.36	263754
	CMTK C	3.37	2.12	1.00	2.92	6.20	355066
	CMTK B	3.72	2.14	1.22	3.46	6.56	271152
Tefor	ANTs A	3.47	1.98	1.00	3.16	6.08	267228
	ANTs B	3.59	2.02	1.22	3.32	6.20	258562
	ANTs C	3.60	2.06	1.22	3.32	6.36	272178
	CMTK A	4.52	2.94	1.41	3.87	8.40	240954
	CMTK C	4.12	2.56	1.41	3.61	7.55	302688
	CMTK B	4.45	2.87	1.41	3.81	8.31	242188
JRC2018	ANTs A	3.48	1.98	1.22	3.16	6.08	269700
	ANTs B	3.55	1.99	1.22	3.24	6.16	266400
	ANTs C	3.60	2.02	1.22	3.32	6.24	266182
	CMTK A	3.60	2.11	1.22	3.24	6.40	242150
	CMTK C	3.58	2.02	1.22	3.24	6.20	256428
	CMTK B	3.60	2.09	1.22	3.24	6.36	243970
JFRC2010	ANTs A	5.63	5.64	1.41	3.81	13.67	239966
	ANTs B	3.59	2.02	1.22	3.24	6.24	267694
	ANTs C	3.70	2.10	1.22	3.46	6.48	259974
	CMTK A	6.33	7.02	1.58	4.36	11.34	246854
	CMTK C	5.34	4.64	1.58	4.18	9.72	246128
	CMTK B	5.28	4.70	1.58	4.06	9.85	244064

Table S14: EB : ellipsoid body

Template	Algorithm	Mean	Std dev	10th perc	median	90th perc	N
FCWB	ANTs A	3.47	2.34	1.00	3.08	6.04	1524310
	ANTs B	3.96	3.02	1.22	3.24	7.28	1045354
	ANTs C	4.37	3.84	1.22	3.46	8.25	1108210
	CMTK A	3.57	2.36	1.22	3.16	6.20	1536540
	CMTK C	3.72	2.56	1.22	3.24	6.56	1328746
	CMTK B	3.58	2.46	1.22	3.16	6.20	1510018
JFRC2013	ANTs A	3.22	2.01	1.00	2.92	5.57	1517212
	ANTs B	4.30	3.66	1.22	3.32	8.25	1094568
	ANTs C	4.45	4.03	1.22	3.32	8.75	1157590
	CMTK A	3.51	2.53	1.00	3.00	6.08	1436332
	CMTK C	3.78	2.78	1.22	3.16	6.96	1085438
	CMTK B	3.55	2.52	1.00	3.08	6.20	1403924
Tefor	ANTs A	3.18	2.01	1.00	2.92	5.52	1543712
	ANTs B	3.39	2.26	1.00	3.00	5.87	1526548
	ANTs C	3.70	3.15	1.22	3.16	6.20	1584950
	CMTK A	3.72	2.59	1.22	3.24	6.71	1540136
	CMTK C	3.88	3.08	1.22	3.24	6.96	1531560
	CMTK B	3.70	2.57	1.22	3.24	6.67	1554432
JRC2018	ANTs A	3.14	1.98	1.00	2.92	5.43	1549380
	ANTs B	3.34	2.08	1.00	3.00	5.74	1520126
	ANTs C	3.47	2.14	1.22	3.16	6.08	1530696
	CMTK A	3.15	1.99	1.00	2.92	5.43	1545220
	CMTK C	3.21	2.01	1.00	2.92	5.52	1561296
	CMTK B	3.16	1.99	1.00	2.92	5.43	1555946
JFRC2010	ANTs A	5.26	6.24	1.22	3.46	10.82	1405498
	ANTs B	3.44	2.36	1.00	3.00	6.00	1443546
	ANTs C	3.53	2.49	1.22	3.08	6.08	1542696
	CMTK A	4.33	4.24	1.22	3.24	7.65	1383128
	CMTK C	4.98	5.73	1.22	3.46	9.11	1307010
	CMTK B	4.42	4.63	1.22	3.24	7.75	1366692

Table S15: AL_R : adult antennal lobe

Template	Algorithm	Mean	Std dev	10th perc	median	90th perc	N
FCWB	ANTs A	4.79	4.18	1.58	4.12	8.43	3302824
	ANTs B	5.48	4.65	1.58	4.69	9.64	3156232
	ANTs C	6.41	5.01	2.00	5.52	11.45	3176428
	CMTK A	6.06	5.19	1.73	5.00	11.07	3333848
	CMTK C	6.02	4.84	1.73	5.20	10.77	3069468
	CMTK B	5.86	5.09	1.73	4.80	10.58	3310852
JFRC2013	ANTs A	4.81	4.25	1.58	4.12	8.54	3210516
	ANTs B	5.41	4.88	1.58	4.53	9.72	3020702
	ANTs C	5.80	4.70	1.73	5.00	10.34	3127004
	CMTK A	5.78	5.39	1.58	4.69	10.02	2897718
	CMTK C	6.24	5.05	2.12	5.39	10.63	2760140
	CMTK B	6.03	5.70	1.73	4.80	10.42	2829810
Tefor	ANTs A	4.63	4.20	1.41	4.00	8.19	3254842
	ANTs B	5.10	4.66	1.58	4.18	9.06	2995846
	ANTs C	5.81	4.84	1.58	4.95	10.39	3193460
	CMTK A	6.93	7.53	1.58	4.74	14.37	2953692
	CMTK C	6.88	8.35	1.58	4.74	12.12	2878476
	CMTK B	6.90	7.43	1.58	4.74	14.18	2969518
JRC2018	ANTs A	4.60	4.07	1.41	4.00	8.09	3275738
	ANTs B	5.02	4.68	1.58	4.18	8.77	3215812
	ANTs C	5.49	5.04	1.58	4.53	9.90	3275980
	CMTK A	4.63	4.19	1.41	4.06	8.09	3215146
	CMTK C	4.83	4.26	1.58	4.18	8.51	3271916
	CMTK B	4.67	4.14	1.58	4.06	8.15	3236520
JFRC2010	ANTs A	6.37	6.84	1.58	4.74	11.40	3492090
	ANTs B	5.04	4.52	1.58	4.24	8.86	2962300
	ANTs C	5.36	4.47	1.58	4.53	9.51	3300890
	CMTK A	5.50	4.50	1.58	4.64	10.05	3257940
	CMTK C	5.77	4.47	1.73	5.00	10.27	3006892
	CMTK B	5.20	4.36	1.58	4.53	9.22	3184846

Table S16: ME_R : medulla

Template	Algorithm	Mean	Std dev	10th perc	median	90th perc	N
FCWB	ANTs A	2.88	2.19	0.71	2.35	5.70	1171342
	ANTs B	3.57	2.72	1.00	2.92	7.42	1313512
	ANTs C	3.66	2.67	1.00	3.00	7.35	1167140
	CMTK A	4.42	3.63	1.00	3.32	9.46	1075760
	CMTK C	3.78	2.95	1.00	3.00	7.81	1222786
	CMTK B	4.06	3.45	1.00	3.00	8.72	1131062
JFRC2013	ANTs A	2.87	2.16	0.71	2.35	5.57	1182032
	ANTs B	3.69	2.67	1.00	3.00	7.31	1066842
	ANTs C	3.59	2.57	1.00	2.92	7.11	1061936
	CMTK A	3.06	2.33	0.71	2.55	6.04	1038332
	CMTK C	3.09	2.40	0.71	2.55	6.20	1491892
	CMTK B	3.17	2.38	0.71	2.55	6.20	1104670
Tefor	ANTs A	2.85	2.17	0.71	2.24	5.57	1183568
	ANTs B	3.24	2.31	1.00	2.65	6.20	1104308
	ANTs C	3.46	2.50	1.00	2.92	6.67	1056266
	CMTK A	4.15	3.54	1.00	3.08	8.72	959660
	CMTK C	3.71	2.73	1.00	3.00	7.21	1116838
	CMTK B	4.12	3.58	1.00	3.00	8.63	959546
JRC2018	ANTs A	2.85	2.16	0.71	2.24	5.57	1186334
	ANTs B	2.89	2.18	0.71	2.35	5.70	1202048
	ANTs C	3.01	2.26	0.71	2.45	5.87	1109464
	CMTK A	3.09	2.39	0.71	2.55	6.08	981638
	CMTK C	2.91	2.22	0.71	2.35	5.70	1130808
	CMTK B	3.04	2.37	0.71	2.45	6.04	986594
JFRC2010	ANTs A	5.05	5.47	1.00	3.00	12.41	1232930
	ANTs B	3.31	2.41	1.00	2.65	6.48	1139068
	ANTs C	3.80	2.62	1.00	3.16	7.42	978550
	CMTK A	5.80	6.42	1.00	3.61	13.08	980474
	CMTK C	5.59	5.96	1.00	3.81	11.68	899172
	CMTK B	5.22	5.67	1.00	3.24	11.60	1010442

Table S17: FB : fan-shaped body

Template	Algorithm	Mean	Std dev	10th perc	median	90th perc	N
FCWB	ANTs A	4.16	4.48	0.71	2.65	9.54	556460
	ANTs B	5.17	4.66	1.00	3.81	11.20	508568
	ANTs C	5.23	4.59	1.00	3.87	11.25	580398
	CMTK A	4.88	4.20	1.00	3.81	10.00	531436
	CMTK C	4.69	4.88	0.71	3.00	10.77	519088
	CMTK B	4.96	4.26	1.00	3.87	10.22	537216
JFRC2013	ANTs A	3.92	4.22	0.71	2.35	9.19	572468
	ANTs B	4.50	4.42	0.71	3.00	10.39	544380
	ANTs C	4.40	4.20	0.71	3.00	9.92	600090
	CMTK A	4.71	4.47	0.71	3.32	10.32	488296
	CMTK C	5.57	4.33	1.22	4.53	11.45	476410
	CMTK B	4.84	4.41	1.00	3.61	10.39	496718
Tefor	ANTs A	3.65	4.03	0.71	2.24	8.40	581644
	ANTs B	4.27	4.03	0.71	3.00	9.25	596168
	ANTs C	4.29	4.14	0.71	3.00	9.46	685590
	CMTK A	4.83	6.29	0.71	2.24	12.92	560746
	CMTK C	4.65	4.78	0.71	3.08	10.42	608104
	CMTK B	4.88	6.28	0.71	2.45	12.53	564910
JRC2018	ANTs A	3.67	4.10	0.71	2.24	8.40	567250
	ANTs B	4.11	4.20	0.71	2.83	9.22	537770
	ANTs C	4.13	4.17	0.71	2.92	9.30	605432
	CMTK A	3.77	4.17	0.71	2.35	8.63	566692
	CMTK C	3.73	4.00	0.71	2.35	8.43	570396
	CMTK B	3.67	4.09	0.71	2.24	8.37	559170
JFRC2010	ANTs A	6.08	5.90	1.00	4.36	13.06	554674
	ANTs B	4.29	4.28	0.71	2.92	9.85	527882
	ANTs C	4.40	4.36	0.71	3.00	9.87	607662
	CMTK A	4.39	5.11	0.71	2.45	10.70	533858
	CMTK C	4.62	5.46	0.71	2.65	11.00	488598
	CMTK B	4.23	4.93	0.71	2.45	10.02	538746

Table S18: SLP_R : superior lateral protocerebrum

Template	Algorithm	Mean	Std dev	10th perc	median	90th perc	N
FCWB	ANTs A	6.01	5.20	1.22	4.47	12.83	93454
	ANTs B	5.78	5.02	1.22	4.24	12.77	87372
	ANTs C	5.80	4.80	1.22	4.47	12.29	99798
	CMTK A	5.87	4.72	1.58	4.58	12.10	102856
	CMTK C	4.84	4.43	1.00	3.54	10.39	118616
	CMTK B	5.89	4.75	1.58	4.53	12.29	102774
JFRC2013	ANTs A	4.97	3.98	1.00	3.87	9.95	108890
	ANTs B	5.61	4.82	1.22	4.24	11.75	93530
	ANTs C	5.41	4.53	1.22	4.12	11.38	102344
	CMTK A	5.62	4.34	1.22	4.58	11.27	118528
	CMTK C	5.77	4.40	1.41	4.64	11.79	104072
	CMTK B	5.76	4.40	1.41	4.69	11.77	117768
Tefor	ANTs A	4.87	3.96	1.00	3.81	9.87	115056
	ANTs B	4.94	3.86	1.22	3.87	9.90	115340
	ANTs C	5.05	4.02	1.22	4.06	10.39	128406
	CMTK A	6.84	6.89	1.22	4.53	15.81	108018
	CMTK C	5.41	4.47	1.22	4.18	11.02	141996
	CMTK B	6.72	6.26	1.22	4.53	15.72	108284
JRC2018	ANTs A	4.81	3.95	1.00	3.81	9.62	111998
	ANTs B	5.01	4.12	1.00	3.87	10.22	108210
	ANTs C	5.26	4.13	1.22	4.24	10.63	109810
	CMTK A	4.78	4.02	1.00	3.67	9.62	111720
	CMTK C	4.89	4.12	1.00	3.81	9.85	106268
	CMTK B	4.79	4.08	1.00	3.67	9.62	107786
JFRC2010	ANTs A	7.57	5.73	1.58	6.24	15.20	204222
	ANTs B	5.24	4.16	1.22	4.18	10.42	102366
	ANTs C	5.39	4.29	1.22	4.30	10.89	116736
	CMTK A	5.94	5.11	1.22	4.53	12.77	105298
	CMTK C	6.20	5.49	1.41	4.53	13.53	98082
	CMTK B	5.47	4.55	1.22	4.24	10.91	101264

Table S19: SIP_R : superior intermediate protocerebrum

Template	Algorithm	Mean	Std dev	10th perc	median	90th perc	N
FCWB	ANTs A	2.69	2.59	0.71	2.00	5.74	1984280
	ANTs B	3.21	2.84	0.71	2.45	6.71	1554920
	ANTs C	3.34	3.08	0.71	2.55	7.07	1532000
	CMTK A	3.12	2.79	0.71	2.35	6.56	1858790
	CMTK C	3.27	2.85	0.71	2.45	7.04	1688338
	CMTK B	3.05	2.74	0.71	2.24	6.44	1759028
JFRC2013	ANTs A	2.49	2.35	0.71	1.73	5.29	1971190
	ANTs B	2.80	2.58	0.71	2.12	5.92	1889764
	ANTs C	2.80	2.63	0.71	2.12	6.04	1873850
	CMTK A	2.74	2.59	0.71	2.00	5.87	1856670
	CMTK C	3.40	2.85	0.71	2.65	7.14	1670644
	CMTK B	2.86	2.64	0.71	2.12	6.16	1832456
Tefor	ANTs A	2.52	2.44	0.71	1.73	5.39	1968522
	ANTs B	2.65	2.42	0.71	2.00	5.70	2000184
	ANTs C	2.68	2.41	0.71	2.12	5.70	2215018
	CMTK A	3.43	4.03	0.71	2.24	7.38	1750938
	CMTK C	3.12	3.00	0.71	2.24	6.71	1928770
	CMTK B	3.38	3.97	0.71	2.24	7.11	1758512
JRC2018	ANTs A	2.53	2.45	0.71	1.73	5.43	1976502
	ANTs B	2.57	2.46	0.71	2.00	5.43	1908536
	ANTs C	2.58	2.50	0.71	1.73	5.52	1983574
	CMTK A	2.52	2.36	0.71	2.00	5.20	1963182
	CMTK C	2.60	2.43	0.71	2.00	5.39	1856570
	CMTK B	2.55	2.38	0.71	2.00	5.20	1884060
JFRC2010	ANTs A	4.34	4.45	0.71	2.92	10.15	2145362
	ANTs B	2.68	2.44	0.71	2.12	5.70	2003074
	ANTs C	2.73	2.48	0.71	2.12	5.79	2169630
	CMTK A	4.00	5.30	0.71	2.35	8.54	1631608
	CMTK C	3.89	5.26	0.71	2.24	8.40	1886180
	CMTK B	3.73	4.46	0.71	2.24	8.34	1653970

Table S20: SMP_R : superior medial protocerebrum

Template	Algorithm	Mean	Std dev	10th perc	median	90th perc	N
FCWB	ANTs A	3.98	2.15	1.41	3.67	7.00	22106
	ANTs B	4.86	2.70	1.58	4.47	8.66	15848
	ANTs C	5.27	3.08	1.58	4.90	9.72	21440
	CMTK A	4.84	3.36	1.58	4.12	9.08	20416
	CMTK C	4.76	2.54	1.58	4.53	8.34	18488
	CMTK B	4.63	2.96	1.58	4.12	8.31	21260
JFRC2013	ANTs A	3.97	2.25	1.22	3.61	7.11	22506
	ANTs B	4.51	2.46	1.58	4.18	7.91	20674
	ANTs C	4.46	2.58	1.41	4.18	8.03	22488
	CMTK A	4.90	4.01	1.58	3.87	8.75	23436
	CMTK C	4.57	3.36	1.41	4.06	7.81	22442
	CMTK B	4.73	3.63	1.58	4.00	8.19	23594
Tefor	ANTs A	4.22	2.36	1.41	3.87	7.52	20588
	ANTs B	4.44	2.53	1.40	4.18	7.91	23460
	ANTs C	4.77	2.90	1.41	4.36	8.89	36240
	CMTK A	5.38	4.03	1.58	4.53	9.41	20008
	CMTK C	4.59	3.00	1.22	4.12	8.51	22322
	CMTK B	5.08	3.48	1.58	4.53	8.94	19784
JRC2018	ANTs A	3.98	2.26	1.22	3.67	7.11	22296
	ANTs B	4.10	2.35	1.22	3.81	7.25	23672
	ANTs C	4.19	2.41	1.22	3.87	7.52	25636
	CMTK A	4.13	2.24	1.41	3.81	7.28	22846
	CMTK C	4.11	2.27	1.41	3.81	7.14	23220
	CMTK B	4.11	2.24	1.41	3.81	7.21	22464
JFRC2010	ANTs A	5.33	4.56	1.58	4.36	9.54	21022
	ANTs B	4.72	2.71	1.58	4.47	8.31	22324
	ANTs C	4.85	2.79	1.58	4.53	8.54	21462
	CMTK A	4.92	2.65	1.58	4.58	8.60	19230
	CMTK C	5.48	3.22	1.73	5.00	9.67	19076
	CMTK B	4.78	2.70	1.58	4.47	8.51	19312

Table S21: AME_R : accessory medulla

Template	Algorithm	Mean	Std dev	10th perc	median	90th perc	N
FCWB	ANTs A	5.47	4.04	1.41	4.53	10.68	661724
	ANTs B	6.11	4.27	1.58	5.20	11.79	519096
	ANTs C	6.49	4.68	1.58	5.43	12.75	542078
	CMTK A	6.17	4.30	1.58	5.20	11.96	642618
	CMTK C	6.08	4.25	1.58	5.15	11.85	534082
	CMTK B	6.00	4.26	1.58	5.05	11.66	618072
JFRC2013	ANTs A	4.93	3.49	1.41	4.18	9.30	682792
	ANTs B	6.24	4.37	1.58	5.20	12.12	610754
	ANTs C	6.26	4.59	1.58	5.20	12.51	631998
	CMTK A	5.67	4.00	1.58	4.74	10.84	639244
	CMTK C	6.60	4.40	2.00	5.70	12.43	491772
	CMTK B	5.79	4.10	1.58	4.95	11.14	616978
Tefor	ANTs A	4.94	3.49	1.41	4.18	9.30	707608
	ANTs B	5.28	3.60	1.58	4.53	9.85	654438
	ANTs C	5.50	3.86	1.58	4.69	10.46	698276
	CMTK A	6.07	5.11	1.41	4.74	12.21	751188
	CMTK C	5.73	4.57	1.58	4.64	11.02	686572
	CMTK B	6.11	5.21	1.41	4.74	12.43	731016
JRC2018	ANTs A	4.91	3.47	1.41	4.18	9.30	690704
	ANTs B	5.11	3.60	1.41	4.36	9.64	665526
	ANTs C	5.29	3.73	1.41	4.53	10.10	701290
	CMTK A	4.88	3.42	1.41	4.18	9.17	680930
	CMTK C	4.99	3.54	1.41	4.24	9.43	655926
	CMTK B	4.90	3.46	1.41	4.18	9.22	670036
JFRC2010	ANTs A	7.65	6.82	1.73	5.57	16.26	636130
	ANTs B	5.62	4.00	1.58	4.74	10.89	609838
	ANTs C	5.74	4.16	1.58	4.74	11.25	675888
	CMTK A	6.12	4.52	1.58	5.05	12.10	690236
	CMTK C	6.49	5.25	1.58	5.20	12.77	577554
	CMTK B	6.01	4.52	1.58	4.95	12.00	669340

Table S22: AVLP_R : anterior ventrolateral protocerebrum

Template	Algorithm	Mean	Std dev	10th perc	median	90th perc	N
FCWB	ANTs A	5.11	3.83	1.22	4.18	10.05	258754
	ANTs B	6.45	4.36	1.73	5.57	12.19	225392
	ANTs C	6.81	4.57	1.73	5.87	12.77	222422
	CMTK A	6.41	4.59	1.58	5.43	12.23	241870
	CMTK C	6.43	4.56	1.58	5.43	12.51	223584
	CMTK B	6.23	4.47	1.58	5.20	12.12	247198
JFRC2013	ANTs A	4.92	3.73	1.22	4.06	9.62	259998
	ANTs B	6.16	4.27	1.58	5.29	11.85	241008
	ANTs C	5.93	4.12	1.58	5.10	11.16	238628
	CMTK A	5.52	4.24	1.41	4.53	10.82	261984
	CMTK C	6.06	4.15	1.58	5.20	11.49	257662
	CMTK B	5.56	4.23	1.41	4.53	10.98	261318
Tefor	ANTs A	4.97	3.77	1.22	4.06	9.64	265258
	ANTs B	5.57	3.96	1.58	4.74	10.63	258156
	ANTs C	5.74	4.03	1.58	4.95	10.91	255876
	CMTK A	7.15	6.75	1.41	5.00	16.37	257948
	CMTK C	6.32	5.19	1.58	4.95	13.06	264876
	CMTK B	7.29	7.20	1.41	4.95	17.00	253230
JRC2018	ANTs A	4.95	3.76	1.22	4.06	9.64	261926
	ANTs B	5.11	3.79	1.22	4.24	9.92	260726
	ANTs C	5.14	3.81	1.22	4.30	9.95	255404
	CMTK A	5.00	3.72	1.22	4.12	9.72	249954
	CMTK C	5.02	3.78	1.22	4.12	9.75	252970
	CMTK B	5.00	3.75	1.22	4.12	9.82	250250
JFRC2010	ANTs A	8.85	8.17	1.73	6.08	21.22	258570
	ANTs B	5.80	4.04	1.58	5.00	10.98	234778
	ANTs C	6.25	4.32	1.58	5.43	11.85	238116
	CMTK A	7.74	6.96	1.58	5.74	16.46	248546
	CMTK C	7.12	5.55	1.73	5.70	14.47	236602
	CMTK B	7.14	6.37	1.58	5.29	15.02	238766

Table S23: PVLP_R : posterior ventrolateral protocerebrum

Template	Algorithm	Mean	Std dev	10th perc	median	90th perc	N
FCWB	ANTs A	4.80	2.97	1.58	4.36	8.19	185122
	ANTs B	5.37	3.34	1.73	4.74	9.49	177740
	ANTs C	5.37	3.39	1.73	4.74	9.33	180198
	CMTK A	5.58	3.67	1.73	4.95	9.85	197506
	CMTK C	5.29	3.30	1.73	4.74	9.22	188836
	CMTK B	5.32	3.37	1.73	4.74	9.22	191900
JFRC2013	ANTs A	4.65	3.06	1.58	4.18	7.91	170612
	ANTs B	5.31	3.34	1.73	4.74	9.25	189622
	ANTs C	5.13	3.29	1.73	4.58	8.80	194948
	CMTK A	4.81	3.19	1.58	4.24	8.34	177804
	CMTK C	5.53	3.65	1.73	4.74	10.00	181296
	CMTK B	4.94	3.33	1.58	4.36	8.63	175958
Tefor	ANTs A	4.70	3.04	1.58	4.24	7.91	178492
	ANTs B	5.11	3.19	1.73	4.58	8.63	183638
	ANTs C	5.15	3.20	1.73	4.64	8.75	191264
	CMTK A	5.57	3.79	1.58	4.80	10.15	202582
	CMTK C	5.39	3.54	1.73	4.74	9.41	201050
	CMTK B	5.61	3.90	1.58	4.80	10.44	198986
JRC2018	ANTs A	4.61	3.00	1.58	4.18	7.81	173092
	ANTs B	4.91	3.12	1.58	4.47	8.31	172192
	ANTs C	4.94	3.03	1.58	4.53	8.37	180874
	CMTK A	4.70	3.03	1.58	4.24	8.03	170442
	CMTK C	4.77	3.11	1.58	4.30	8.09	166222
	CMTK B	4.73	3.05	1.58	4.24	8.03	166110
JFRC2010	ANTs A	6.47	5.09	1.73	5.00	13.67	201136
	ANTs B	5.09	3.31	1.73	4.53	8.72	175108
	ANTs C	5.11	3.28	1.73	4.53	8.94	186916
	CMTK A	5.68	4.14	1.73	4.74	10.61	180800
	CMTK C	5.69	3.81	1.73	5.00	10.42	174120
	CMTK B	5.39	3.62	1.58	4.69	9.72	176222

Table S24: IVLP_R : wedge

Template	Algorithm	Mean	Std dev	10th perc	median	90th perc	N
FCWB	ANTs A	3.64	4.55	0.71	2.12	9.00	471818
	ANTs B	4.23	4.37	0.71	2.65	9.85	425034
	ANTs C	4.16	4.30	0.71	2.65	9.46	428146
	CMTK A	6.29	6.21	1.00	4.06	15.07	357542
	CMTK C	4.42	5.06	0.71	2.65	10.70	408458
	CMTK B	5.84	5.67	1.00	3.87	13.34	326860
JFRC2013	ANTs A	3.49	4.43	0.71	2.00	8.63	426466
	ANTs B	4.01	4.12	0.71	2.65	9.22	436614
	ANTs C	3.94	4.19	0.71	2.55	9.22	446714
	CMTK A	4.10	4.46	0.71	2.55	9.92	394782
	CMTK C	4.60	4.55	0.71	3.00	10.72	417880
	CMTK B	4.23	4.55	0.71	2.65	9.92	396906
Tefor	ANTs A	3.44	4.40	0.71	1.73	8.63	443520
	ANTs B	3.82	4.13	0.71	2.35	9.03	435004
	ANTs C	3.97	4.28	0.71	2.45	9.46	434722
	CMTK A	4.14	5.69	0.71	2.12	10.61	405412
	CMTK C	4.37	5.01	0.71	2.55	10.61	418774
	CMTK B	4.29	5.88	0.71	2.12	11.07	406718
JRC2018	ANTs A	3.42	4.38	0.71	1.73	8.57	433598
	ANTs B	3.58	4.30	0.71	2.12	8.54	421340
	ANTs C	3.55	4.28	0.71	2.12	8.54	437168
	CMTK A	3.43	4.49	0.71	1.73	8.49	412332
	CMTK C	3.42	4.31	0.71	2.00	8.25	406596
	CMTK B	3.39	4.42	0.71	1.73	8.28	408696
JFRC2010	ANTs A	8.14	7.83	1.00	5.29	20.01	436308
	ANTs B	3.87	4.33	0.71	2.35	9.30	431512
	ANTs C	4.29	4.36	0.71	2.83	9.95	405618
	CMTK A	4.17	5.67	0.71	2.12	11.00	408410
	CMTK C	4.76	5.43	0.71	2.92	11.62	392684
	CMTK B	4.09	5.28	0.71	2.12	10.46	408162

Table S25: PLP_R : posterior lateral protocerebrum

Template	Algorithm	Mean	Std dev	10th perc	median	90th perc	N
FCWB	ANTs A	7.66	7.97	1.00	4.47	19.46	16620
	ANTs B	7.11	8.12	1.00	4.36	17.97	10226
	ANTs C	8.18	8.49	1.22	5.00	22.68	13788
	CMTK A	9.58	8.35	1.58	6.71	22.16	15260
	CMTK C	7.06	8.32	1.00	3.46	20.85	17600
	CMTK B	9.16	8.11	1.58	6.24	21.69	15174
JFRC2013	ANTs A	7.03	7.09	1.00	4.30	17.48	17460
	ANTs B	6.47	7.14	1.00	3.61	16.70	14228
	ANTs C	6.38	7.36	1.00	3.24	17.94	13420
	CMTK A	10.65	9.17	1.41	7.58	24.21	19620
	CMTK C	10.03	8.35	2.00	7.28	22.37	18320
	CMTK B	10.42	8.96	1.41	7.68	23.63	19254
Tefor	ANTs A	7.08	6.97	1.00	4.36	17.58	17286
	ANTs B	7.91	7.03	1.58	5.70	18.15	13698
	ANTs C	6.94	6.83	1.00	4.47	17.36	17156
	CMTK A	10.06	8.43	1.41	7.42	22.86	19664
	CMTK C	7.79	7.48	1.22	4.58	19.52	23164
	CMTK B	9.89	8.23	1.41	7.28	22.75	19914
JRC2018	ANTs A	7.16	7.20	1.00	4.30	17.78	17150
	ANTs B	7.45	7.59	1.00	4.30	19.21	16210
	ANTs C	7.85	7.67	1.22	4.69	20.26	15504
	CMTK A	7.12	6.91	1.00	4.47	17.33	17054
	CMTK C	7.32	7.22	1.00	4.53	18.37	15946
	CMTK B	7.11	7.05	1.00	4.36	17.82	17370
JFRC2010	ANTs A	13.33	10.28	2.12	10.86	28.33	17992
	ANTs B	7.81	8.32	1.00	4.06	21.33	14808
	ANTs C	8.09	7.94	1.22	5.00	20.92	14984
	CMTK A	8.70	8.21	1.22	5.34	21.95	16612
	CMTK C	9.81	9.48	1.58	5.70	25.06	13412
	CMTK B	9.65	9.37	1.22	5.39	25.16	16454

Table S26: AOTU_R : anterior optic tubercle

Template	Algorithm	Mean	Std dev	10th perc	median	90th perc	N
FCWB	ANTs A	3.22	2.56	0.71	2.55	6.67	97924
	ANTs B	3.97	2.74	1.00	3.32	7.65	94372
	ANTs C	3.71	2.65	1.00	3.08	7.25	94252
	CMTK A	6.95	7.08	1.00	4.30	18.35	67048
	CMTK C	3.88	3.41	0.71	2.92	8.03	102780
	CMTK B	6.22	6.15	1.00	4.06	15.23	80174
JFRC2013	ANTs A	3.24	2.49	0.71	2.65	6.67	101422
	ANTs B	4.39	3.45	1.00	3.54	9.22	99430
	ANTs C	4.34	3.43	1.00	3.46	9.22	97998
	CMTK A	3.36	2.71	0.71	2.65	7.07	84030
	CMTK C	4.23	3.31	1.00	3.54	8.00	99184
	CMTK B	3.42	2.79	0.71	2.65	7.11	86578
Tefor	ANTs A	3.17	2.43	0.71	2.55	6.48	98684
	ANTs B	3.80	3.09	0.71	2.92	8.03	107810
	ANTs C	4.03	3.14	0.71	3.24	8.31	101590
	CMTK A	4.01	4.60	0.71	2.65	8.19	82046
	CMTK C	3.85	3.42	1.00	3.00	7.52	106304
	CMTK B	3.91	4.40	0.71	2.65	8.03	82136
JRC2018	ANTs A	3.21	2.47	0.71	2.65	6.56	99712
	ANTs B	3.61	2.88	0.71	2.92	7.62	103552
	ANTs C	3.36	2.58	0.71	2.65	6.86	97756
	CMTK A	3.38	2.69	0.71	2.65	7.14	81058
	CMTK C	3.22	2.43	0.71	2.65	6.48	96996
	CMTK B	3.36	2.64	0.71	2.65	7.07	82722
JFRC2010	ANTs A	7.79	8.29	1.22	5.00	19.96	113000
	ANTs B	3.84	3.17	0.71	2.92	8.19	105928
	ANTs C	4.13	3.29	0.71	3.24	8.77	103418
	CMTK A	5.09	6.90	0.71	2.92	11.27	84104
	CMTK C	5.24	6.33	1.00	3.16	11.77	98656
	CMTK B	5.05	6.51	0.71	2.92	11.07	85226

Table S27: GOR_R : gorget

Template	Algorithm	Mean	Std dev	10th perc	median	90th perc	N
FCWB	ANTs A	4.13	3.03	1.00	3.46	8.09	315408
	ANTs B	5.56	4.44	1.41	4.36	11.42	262056
	ANTs C	5.03	3.93	1.22	4.06	10.22	304860
	CMTK A	5.06	4.06	1.00	3.87	10.51	375234
	CMTK C	5.34	4.10	1.22	4.30	10.82	240104
	CMTK B	4.83	3.78	1.00	3.81	9.67	370578
JFRC2013	ANTs A	5.16	3.95	1.22	4.12	10.61	309960
	ANTs B	5.49	4.21	1.41	4.36	11.07	312332
	ANTs C	5.55	4.33	1.41	4.36	11.42	305446
	CMTK A	3.90	2.55	1.00	3.32	7.42	238400
	CMTK C	5.28	3.73	1.41	4.47	10.27	184862
	CMTK B	4.20	2.85	1.22	3.61	8.09	228912
Tefor	ANTs A	3.44	2.38	1.00	2.92	6.71	414600
	ANTs B	5.30	4.15	1.22	4.12	11.00	262940
	ANTs C	5.30	4.20	1.22	4.12	11.27	316732
	CMTK A	4.97	5.00	1.00	3.46	10.70	338350
	CMTK C	5.52	4.72	1.22	4.18	11.34	242994
	CMTK B	5.12	5.22	1.00	3.54	10.82	320050
JRC2018	ANTs A	3.55	2.45	1.00	2.92	7.00	421666
	ANTs B	4.48	3.10	1.22	3.81	8.66	400478
	ANTs C	4.32	2.93	1.22	3.67	8.28	417118
	CMTK A	3.65	2.52	1.00	3.00	7.11	423462
	CMTK C	3.97	2.56	1.00	3.54	7.52	390700
	CMTK B	3.77	2.53	1.00	3.16	7.28	407944
JFRC2010	ANTs A	4.84	3.58	1.22	4.00	9.64	449372
	ANTs B	5.48	4.27	1.41	4.36	11.09	284214
	ANTs C	4.77	3.40	1.22	4.06	9.30	374730
	CMTK A	5.12	4.59	1.00	3.81	10.72	364534
	CMTK C	5.81	5.69	1.22	4.18	11.60	292448
	CMTK B	4.71	3.85	1.00	3.67	9.30	360984

Table S28: MB_CA_R : calyx of adult mushroom body

Template	Algorithm	Mean	Std dev	10th perc	median	90th perc	N
FCWB	ANTs A	5.11	3.89	1.22	4.12	10.27	392366
	ANTs B	5.40	4.06	1.41	4.36	10.98	426566
	ANTs C	5.24	3.85	1.41	4.30	10.51	415894
	CMTK A	6.27	5.71	1.41	4.69	13.00	314618
	CMTK C	5.69	4.89	1.41	4.30	12.10	368580
	CMTK B	6.00	5.60	1.41	4.36	12.53	331114
JFRC2013	ANTs A	4.78	3.82	1.00	3.81	9.64	365592
	ANTs B	5.87	4.31	1.58	4.80	11.85	354298
	ANTs C	5.65	4.08	1.58	4.69	11.14	379870
	CMTK A	4.89	3.88	1.22	3.81	10.00	309642
	CMTK C	5.41	4.22	1.41	4.30	11.05	394108
	CMTK B	4.89	3.85	1.22	3.81	9.92	319706
Tefor	ANTs A	4.69	3.64	1.00	3.81	9.54	388030
	ANTs B	5.10	3.89	1.22	4.12	10.25	446012
	ANTs C	5.55	4.06	1.41	4.53	10.98	415622
	CMTK A	5.51	4.93	1.22	4.12	11.60	323322
	CMTK C	5.34	4.14	1.41	4.24	10.72	438296
	CMTK B	5.49	4.77	1.22	4.12	11.42	327944
JRC2018	ANTs A	4.61	3.64	1.00	3.61	9.46	365344
	ANTs B	5.14	3.90	1.22	4.12	10.39	368634
	ANTs C	5.14	3.83	1.41	4.18	10.12	366652
	CMTK A	5.00	3.88	1.22	4.06	10.12	313232
	CMTK C	5.00	3.84	1.22	4.06	9.92	329436
	CMTK B	4.95	3.88	1.22	4.00	10.00	311026
JFRC2010	ANTs A	7.06	5.82	1.58	5.43	15.02	416104
	ANTs B	5.34	4.03	1.41	4.30	10.82	403054
	ANTs C	5.70	4.10	1.41	4.74	11.40	430918
	CMTK A	7.13	6.98	1.41	4.74	16.28	309582
	CMTK C	6.35	6.00	1.41	4.47	13.91	423128
	CMTK B	6.27	5.80	1.41	4.53	13.45	318590

Table S29: SPS_R : superior posterior slope

Template	Algorithm	Mean	Std dev	10th perc	median	90th perc	N
FCWB	ANTs A	5.66	4.18	1.41	4.58	11.42	323078
	ANTs B	6.48	4.42	1.73	5.43	12.73	261148
	ANTs C	6.93	4.62	2.12	5.92	13.23	225102
	CMTK A	7.54	5.22	2.00	6.24	15.25	304856
	CMTK C	6.95	4.66	2.00	5.87	13.67	254194
	CMTK B	6.91	4.94	1.73	5.70	14.05	299012
JFRC2013	ANTs A	5.75	4.48	1.41	4.53	12.17	301130
	ANTs B	7.40	4.88	2.24	6.20	14.58	219492
	ANTs C	7.20	4.72	2.12	6.12	13.95	230954
	CMTK A	5.63	4.32	1.41	4.53	11.58	282136
	CMTK C	6.51	4.55	1.73	5.34	13.13	293938
	CMTK B	5.79	4.33	1.58	4.69	11.70	277218
Tefor	ANTs A	5.07	4.00	1.22	4.06	10.54	320492
	ANTs B	6.73	4.52	2.00	5.70	13.17	265242
	ANTs C	7.19	4.68	2.12	6.12	13.73	240284
	CMTK A	7.27	6.90	1.41	4.80	17.00	316638
	CMTK C	6.58	5.48	1.58	5.00	14.04	346162
	CMTK B	7.32	6.93	1.58	4.95	17.01	312412
JRC2018	ANTs A	4.87	3.89	1.22	3.81	10.02	313820
	ANTs B	6.14	4.56	1.58	5.00	12.55	273266
	ANTs C	6.02	4.27	1.58	5.00	11.83	268456
	CMTK A	5.26	4.01	1.41	4.24	10.51	290294
	CMTK C	5.73	4.27	1.58	4.58	11.49	249432
	CMTK B	5.35	4.09	1.41	4.30	10.72	271122
JFRC2010	ANTs A	8.13	5.73	2.12	6.67	16.40	342866
	ANTs B	6.74	4.69	1.73	5.70	13.34	245712
	ANTs C	7.95	5.08	2.45	6.86	15.18	201122
	CMTK A	7.65	5.36	2.00	6.20	15.67	229274
	CMTK C	7.37	4.97	2.00	6.20	14.71	222776
	CMTK B	7.25	5.12	1.73	5.83	14.98	231834

Table S30: IPS_R : inferior posterior slope

Template	Algorithm	Mean	Std dev	10th perc	median	90th perc	N
FCWB	ANTs A	3.28	3.56	0.71	2.12	7.52	301648
	ANTs B	3.63	3.92	0.71	2.24	8.63	288116
	ANTs C	3.55	3.73	0.71	2.24	8.28	304246
	CMTK A	4.28	4.83	0.71	2.55	10.65	244114
	CMTK C	3.32	3.99	0.71	2.00	7.42	317350
	CMTK B	4.02	4.34	0.71	2.55	9.43	250492
JFRC2013	ANTs A	2.53	2.98	0.71	1.58	5.74	345434
	ANTs B	3.09	3.51	0.71	1.73	7.31	316090
	ANTs C	3.09	3.44	0.71	2.00	7.21	326860
	CMTK A	2.85	3.23	0.71	1.73	6.16	343224
	CMTK C	3.71	3.54	0.71	2.65	7.94	299000
	CMTK B	3.02	3.28	0.71	2.12	6.52	338554
Tefor	ANTs A	2.50	2.88	0.71	1.58	5.52	349796
	ANTs B	2.75	3.01	0.71	1.73	6.12	334934
	ANTs C	2.85	3.17	0.71	1.73	6.44	345290
	CMTK A	3.19	4.76	0.71	1.58	7.04	336610
	CMTK C	3.16	4.00	0.71	2.00	6.71	339266
	CMTK B	3.21	4.69	0.71	1.58	7.52	331342
JRC2018	ANTs A	2.45	2.86	0.71	1.58	5.43	347798
	ANTs B	2.72	2.90	0.71	1.73	5.87	345134
	ANTs C	2.76	2.92	0.71	1.73	6.08	351358
	CMTK A	2.46	2.94	0.71	1.58	5.43	346020
	CMTK C	2.51	3.02	0.71	1.58	5.57	343496
	CMTK B	2.47	2.98	0.71	1.58	5.43	346934
JFRC2010	ANTs A	6.05	5.92	0.71	3.87	14.49	315090
	ANTs B	2.96	3.35	0.71	1.73	6.86	335148
	ANTs C	3.03	3.28	0.71	2.00	6.96	312856
	CMTK A	3.55	5.02	0.71	1.58	9.90	333098
	CMTK C	3.76	4.90	0.71	2.00	9.46	325342
	CMTK B	3.49	4.91	0.71	1.58	9.11	333226

Table S31: SCL_R : superior clamp

Template	Algorithm	Mean	Std dev	10th perc	median	90th perc	N
FCWB	ANTs A	4.66	4.05	1.22	3.61	8.63	629916
	ANTs B	5.37	4.12	1.58	4.36	10.02	738100
	ANTs C	6.04	4.51	1.73	4.95	11.60	704222
	CMTK A	8.84	7.56	1.73	6.16	20.41	621926
	CMTK C	6.57	5.15	1.73	5.10	13.62	739520
	CMTK B	7.67	6.65	1.73	5.34	17.69	579792
JFRC2013	ANTs A	4.59	4.04	1.22	3.61	8.51	630492
	ANTs B	5.34	4.53	1.58	4.12	10.51	625254
	ANTs C	5.22	4.46	1.41	4.12	10.02	601610
	CMTK A	6.06	5.75	1.58	4.24	13.30	689216
	CMTK C	5.83	4.45	1.58	4.58	11.79	660042
	CMTK B	6.34	6.12	1.58	4.36	14.46	681688
Tefor	ANTs A	4.39	3.67	1.22	3.61	8.03	639674
	ANTs B	4.93	4.06	1.41	3.87	9.22	612498
	ANTs C	5.10	4.33	1.41	4.06	9.64	582010
	CMTK A	7.18	6.63	1.58	4.80	16.69	722676
	CMTK C	6.57	5.88	1.58	4.69	14.58	613750
	CMTK B	7.20	6.65	1.58	4.95	16.58	714756
JRC2018	ANTs A	4.37	3.70	1.22	3.61	7.91	633808
	ANTs B	4.54	3.82	1.41	3.61	8.31	649512
	ANTs C	4.66	3.91	1.41	3.81	8.54	633012
	CMTK A	4.36	3.62	1.22	3.61	7.91	650942
	CMTK C	4.44	3.66	1.22	3.61	8.06	623624
	CMTK B	4.36	3.59	1.22	3.61	7.91	628218
JFRC2010	ANTs A	8.08	8.07	1.58	5.20	19.30	765240
	ANTs B	5.24	4.28	1.58	4.18	9.95	635108
	ANTs C	5.89	4.74	1.58	4.58	11.94	612046
	CMTK A	8.76	7.82	1.73	5.87	20.86	674518
	CMTK C	7.78	6.61	1.73	5.74	16.52	709042
	CMTK B	7.28	6.56	1.58	5.15	16.20	633590

Table S32: LO_R : lobula

Template	Algorithm	Mean	Std dev	10th perc	median	90th perc	N
FCWB	ANTs A	4.43	3.64	1.00	3.24	9.41	18974
	ANTs B	5.64	4.77	1.41	4.18	12.27	20592
	ANTs C	5.45	4.97	1.00	3.87	12.21	20774
	CMTK A	5.64	5.75	1.00	3.81	12.83	11616
	CMTK C	5.66	5.59	1.00	3.54	13.60	20246
	CMTK B	6.46	5.19	1.41	5.05	12.98	14828
JFRC2013	ANTs A	3.90	3.01	1.00	3.00	8.28	20466
	ANTs B	7.99	6.65	1.73	5.57	19.16	10842
	ANTs C	8.40	6.70	1.58	5.70	18.72	12826
	CMTK A	3.62	2.71	1.00	2.92	7.65	16792
	CMTK C	5.97	5.27	1.22	4.36	12.59	16420
	CMTK B	3.69	2.84	1.00	2.92	7.68	17748
Tefor	ANTs A	3.76	2.80	1.00	3.00	7.91	20450
	ANTs B	6.68	6.13	1.00	4.30	15.91	15576
	ANTs C	6.19	5.22	1.41	4.61	13.37	14578
	CMTK A	5.61	8.65	0.71	2.65	10.79	15534
	CMTK C	5.28	4.43	1.00	4.00	11.18	20264
	CMTK B	5.58	8.52	0.71	2.65	10.61	16134
JRC2018	ANTs A	3.88	2.88	1.00	3.08	8.03	20550
	ANTs B	4.84	4.51	1.00	3.24	11.02	19126
	ANTs C	4.77	4.33	1.00	3.54	10.00	16668
	CMTK A	3.48	2.66	0.71	2.92	7.04	17250
	CMTK C	3.71	2.81	1.00	2.92	7.91	18484
	CMTK B	3.40	2.57	0.71	2.65	7.04	17552
JFRC2010	ANTs A	10.11	9.19	1.58	7.00	24.87	20032
	ANTs B	5.44	5.16	1.00	3.61	13.23	15862
	ANTs C	7.15	6.93	1.00	4.12	18.51	13508
	CMTK A	6.94	9.15	1.00	3.24	18.18	12426
	CMTK C	6.02	6.59	1.00	3.54	15.38	10854
	CMTK B	6.43	8.06	1.00	3.24	15.72	12974

Table S33: EPA_R : epaulette

Template	Algorithm	Mean	Std dev	10th perc	median	90th perc	N
FCWB	ANTs A	5.72	4.39	1.58	4.58	11.18	1668296
	ANTs B	6.50	4.47	2.12	5.52	12.17	1722224
	ANTs C	6.65	4.62	2.12	5.57	12.51	1752242
	CMTK A	6.77	4.82	2.00	5.70	13.00	1771876
	CMTK C	6.55	4.53	2.00	5.52	12.59	1636296
	CMTK B	6.64	4.79	2.00	5.52	12.69	1691152
JFRC2013	ANTs A	5.92	4.64	1.58	4.74	11.85	1676118
	ANTs B	7.17	5.03	2.12	6.00	13.60	1611632
	ANTs C	7.25	5.10	2.12	6.08	13.80	1658494
	CMTK A	5.86	4.32	1.58	4.80	11.34	1614130
	CMTK C	6.91	4.69	2.12	5.83	13.06	1507918
	CMTK B	5.93	4.32	1.58	4.95	11.40	1613038
Tefor	ANTs A	5.61	4.47	1.58	4.47	11.16	1660500
	ANTs B	7.06	4.85	2.12	6.00	13.30	1680796
	ANTs C	7.44	5.24	2.12	6.20	14.21	1731516
	CMTK A	6.50	5.09	1.58	5.15	13.21	1815200
	CMTK C	7.22	5.56	2.12	5.83	13.89	1738810
	CMTK B	6.56	5.12	1.58	5.15	13.29	1809270
JRC2018	ANTs A	5.42	4.43	1.41	4.24	10.89	1645444
	ANTs B	6.77	4.65	2.00	5.70	12.83	1637668
	ANTs C	6.91	4.80	2.12	5.79	13.11	1688056
	CMTK A	5.42	4.40	1.41	4.24	10.82	1654410
	CMTK C	5.72	4.44	1.58	4.53	11.14	1595976
	CMTK B	5.45	4.42	1.58	4.30	10.82	1601386
JFRC2010	ANTs A	7.02	5.61	1.73	5.57	13.80	1889608
	ANTs B	6.82	4.63	2.12	5.79	12.75	1696632
	ANTs C	6.95	4.77	2.12	5.87	13.08	1812676
	CMTK A	6.57	4.73	1.73	5.43	12.77	1859654
	CMTK C	6.92	4.71	2.12	5.87	13.00	1711540
	CMTK B	6.41	4.68	1.73	5.29	12.37	1736788

Table S34: GNG : adult gnathal ganglion

Template	Algorithm	Mean	Std dev	10th perc	median	90th perc	N
FCWB	ANTs A	3.74	3.33	0.71	2.92	7.31	41796
	ANTs B	3.96	2.29	1.41	3.61	7.11	63002
	ANTs C	4.19	2.39	1.41	3.81	7.52	59292
	CMTK A	5.90	4.18	1.58	5.34	10.27	67418
	CMTK C	4.47	2.81	1.41	4.06	8.06	55758
	CMTK B	5.30	3.81	1.41	4.53	9.92	48736
JFRC2013	ANTs A	3.58	3.00	1.00	2.92	6.96	43970
	ANTs B	4.21	2.73	1.41	3.81	7.55	60532
	ANTs C	4.32	2.59	1.41	4.00	7.78	59536
	CMTK A	3.94	3.28	1.00	3.16	7.62	38334
	CMTK C	4.00	2.61	1.22	3.61	7.14	57542
	CMTK B	3.97	3.22	1.00	3.24	7.62	39398
Tefor	ANTs A	3.48	2.94	0.71	2.92	6.75	44098
	ANTs B	4.10	3.04	1.00	3.54	7.91	50334
	ANTs C	4.23	3.22	1.00	3.54	8.28	45398
	CMTK A	4.59	3.42	1.22	3.81	8.87	42418
	CMTK C	4.58	3.17	1.22	3.87	8.75	58062
	CMTK B	4.75	3.48	1.22	4.06	9.11	44458
JRC2018	ANTs A	3.54	3.00	0.71	2.92	6.93	44366
	ANTs B	3.94	3.02	1.00	3.24	7.62	47364
	ANTs C	4.02	3.12	1.00	3.32	7.65	43868
	CMTK A	4.20	3.51	1.00	3.54	7.94	33850
	CMTK C	3.83	3.22	1.00	3.08	7.38	39328
	CMTK B	4.14	3.53	1.00	3.32	7.91	34784
JFRC2010	ANTs A	5.22	4.25	1.00	4.06	10.98	43164
	ANTs B	4.06	3.02	1.00	3.46	7.91	51038
	ANTs C	4.32	3.02	1.22	3.67	8.09	51848
	CMTK A	5.21	3.99	1.41	4.18	10.27	53416
	CMTK C	4.95	3.58	1.41	4.12	9.30	56954
	CMTK B	4.75	3.43	1.22	4.06	9.03	52090

Table S35: NO : nodulus

Template	Algorithm	Mean	Std dev	10th perc	median	90th perc	N
FCWB	ANTs A	4.26	3.61	1.00	3.81	7.31	460912
	ANTs B	6.58	5.22	1.73	5.10	13.67	280454
	ANTs C	7.17	6.48	1.58	5.00	16.76	341950
	CMTK A	4.27	3.65	1.00	3.67	7.65	463556
	CMTK C	4.52	3.68	1.00	3.81	8.25	373002
	CMTK B	4.28	3.74	1.00	3.81	7.55	449328
JFRC2013	ANTs A	5.29	4.57	1.41	4.12	10.58	368712
	ANTs B	7.39	5.89	2.00	5.52	16.02	197600
	ANTs C	6.67	5.30	1.73	5.10	14.04	215962
	CMTK A	4.31	3.51	1.00	3.67	7.55	425532
	CMTK C	5.60	4.14	1.58	4.58	10.82	245386
	CMTK B	4.41	3.52	1.22	3.81	7.75	402130
Tefor	ANTs A	3.86	3.15	1.00	3.54	6.56	446818
	ANTs B	5.08	4.00	1.58	4.30	8.94	387362
	ANTs C	5.22	4.46	1.58	4.24	9.22	421106
	CMTK A	4.09	3.32	1.00	3.61	7.11	457468
	CMTK C	5.45	5.67	1.58	4.18	8.63	389430
	CMTK B	4.40	3.67	1.22	3.67	7.68	445144
JRC2018	ANTs A	3.77	3.10	1.00	3.32	6.40	452490
	ANTs B	5.12	4.00	1.58	4.30	9.38	385182
	ANTs C	5.49	4.30	1.58	4.53	10.25	403048
	CMTK A	3.69	3.09	1.00	3.24	6.24	467804
	CMTK C	3.86	3.12	1.00	3.54	6.52	443426
	CMTK B	3.75	3.14	1.00	3.32	6.36	458750
JFRC2010	ANTs A	5.45	6.31	1.41	3.87	8.66	410994
	ANTs B	4.95	3.78	1.58	4.30	8.54	390412
	ANTs C	4.84	3.71	1.58	4.24	8.34	452552
	CMTK A	4.47	4.13	1.22	3.67	7.52	417922
	CMTK C	4.61	3.52	1.41	4.06	7.91	383418
	CMTK B	4.31	3.55	1.41	3.81	7.28	410878

Table S36: PRW : prow

Template	Algorithm	Mean	Std dev	10th perc	median	90th perc	N
FCWB	ANTs A	6.30	3.42	2.00	5.92	11.14	5590
	ANTs B	8.13	4.05	2.55	8.03	13.61	3196
	ANTs C	8.33	4.08	2.92	8.12	13.95	4078
	CMTK A	7.03	4.28	2.35	6.12	12.77	6136
	CMTK C	7.61	3.59	3.00	7.55	12.35	4046
	CMTK B	6.83	4.08	2.24	6.08	12.12	5632
JFRC2013	ANTs A	6.48	3.93	1.73	5.74	11.94	6140
	ANTs B	7.39	3.94	2.64	6.86	13.06	5440
	ANTs C	7.71	3.67	3.08	7.28	12.86	5362
	CMTK A	7.08	3.79	2.55	6.56	12.19	6426
	CMTK C	8.87	3.82	3.61	8.89	13.67	4532
	CMTK B	7.12	4.03	2.45	6.52	12.53	6260
Tefor	ANTs A	6.67	4.17	1.73	5.83	12.10	6206
	ANTs B	6.99	4.03	2.00	6.44	12.08	6332
	ANTs C	7.07	3.99	2.24	6.56	12.59	7242
	CMTK A	7.25	3.74	2.45	7.00	12.17	7508
	CMTK C	7.64	3.92	2.83	7.11	12.75	5630
	CMTK B	7.15	3.94	2.55	6.56	12.41	6372
JRC2018	ANTs A	6.54	4.02	1.73	5.74	12.10	6208
	ANTs B	6.65	4.03	1.73	5.89	12.17	6202
	ANTs C	6.86	4.02	2.12	6.08	12.37	6582
	CMTK A	6.83	4.19	2.12	6.08	12.25	5732
	CMTK C	6.75	4.09	2.12	6.08	12.19	5888
	CMTK B	6.76	4.15	2.00	5.92	12.43	6162
JFRC2010	ANTs A	8.65	6.58	3.24	7.28	13.06	12776
	ANTs B	6.73	3.63	2.12	6.32	11.85	5332
	ANTs C	6.92	3.74	2.24	6.44	12.12	5164
	CMTK A	8.27	4.08	3.24	7.92	13.67	4902
	CMTK C	8.12	4.04	3.08	7.65	13.80	4300
	CMTK B	8.35	4.73	2.83	7.65	15.10	5636

Table S37: GA_R : gall

Template	Algorithm	Mean	Std dev	10th perc	median	90th perc	N
FCWB	ANTs A	3.98	2.20	1.22	3.81	6.96	30514
	ANTs B	4.69	2.76	1.58	4.24	8.31	18914
	ANTs C	4.56	2.92	1.22	4.06	8.54	20840
	CMTK A	4.18	2.36	1.41	3.81	7.38	31992
	CMTK C	5.68	4.94	1.58	4.36	10.54	18984
	CMTK B	4.04	2.34	1.41	3.61	7.25	31278
JFRC2013	ANTs A	3.77	2.25	1.22	3.54	6.82	31780
	ANTs B	4.48	2.63	1.58	4.12	7.81	20492
	ANTs C	4.49	2.56	1.58	4.12	8.02	24386
	CMTK A	4.15	2.88	1.22	3.61	7.38	33056
	CMTK C	4.47	2.79	1.58	4.06	7.55	24506
	CMTK B	4.43	2.99	1.41	3.81	8.03	31064
Tefor	ANTs A	3.94	2.30	1.22	3.61	7.11	31502
	ANTs B	4.13	2.45	1.22	3.81	7.52	30136
	ANTs C	4.17	2.52	1.22	3.81	7.62	31770
	CMTK A	4.90	3.87	1.41	3.87	9.49	33304
	CMTK C	4.50	3.31	1.22	3.61	8.99	27266
	CMTK B	4.97	3.79	1.41	4.06	9.75	33040
JRC2018	ANTs A	3.79	2.25	1.00	3.54	6.96	34898
	ANTs B	3.87	2.35	1.00	3.54	7.11	32926
	ANTs C	4.06	2.52	1.00	3.61	7.42	32226
	CMTK A	3.73	2.18	1.22	3.46	6.67	35186
	CMTK C	3.78	2.23	1.00	3.54	6.86	35504
	CMTK B	3.77	2.19	1.22	3.46	6.75	35516
JFRC2010	ANTs A	6.33	6.59	1.41	4.18	15.56	30288
	ANTs B	4.39	2.40	1.58	4.12	7.65	26644
	ANTs C	4.46	2.50	1.58	4.18	7.78	27714
	CMTK A	5.38	4.69	1.41	4.12	10.10	29566
	CMTK C	6.25	5.08	2.00	4.95	11.96	23192
	CMTK B	5.20	4.79	1.41	4.00	9.38	32256

Table S38: AME_L : accessory medulla

Template	Algorithm	Mean	Std dev	10th perc	median	90th perc	N
FCWB	ANTs A	5.16	4.38	1.41	4.12	9.87	623178
	ANTs B	5.58	4.11	1.58	4.64	10.39	712332
	ANTs C	5.87	4.36	1.58	4.95	10.98	704666
	CMTK A	8.59	7.03	2.00	6.36	18.97	632218
	CMTK C	7.31	6.01	2.00	5.52	15.33	701258
	CMTK B	7.65	6.50	1.73	5.57	16.82	590680
JFRC2013	ANTs A	4.98	4.25	1.41	4.00	9.43	641886
	ANTs B	5.42	4.31	1.58	4.36	10.39	642512
	ANTs C	5.49	4.56	1.58	4.36	10.54	632428
	CMTK A	6.47	7.07	1.58	4.47	13.30	662426
	CMTK C	5.81	4.27	1.58	4.74	11.27	670968
	CMTK B	6.59	7.13	1.58	4.53	13.62	653836
Tefor	ANTs A	4.86	4.03	1.41	3.87	9.06	634782
	ANTs B	5.21	4.29	1.58	4.18	9.72	610874
	ANTs C	5.61	4.76	1.58	4.47	10.72	594648
	CMTK A	7.05	6.69	1.58	4.90	16.05	686944
	CMTK C	6.70	6.13	1.58	4.95	14.30	606444
	CMTK B	7.03	6.67	1.58	4.90	16.14	677718
JRC2018	ANTs A	4.85	4.07	1.41	3.87	9.00	634598
	ANTs B	4.94	4.08	1.41	4.06	9.19	642236
	ANTs C	5.28	4.35	1.58	4.30	9.85	638966
	CMTK A	4.78	4.03	1.41	3.81	8.77	627192
	CMTK C	4.86	4.03	1.41	4.00	8.97	616346
	CMTK B	4.77	3.96	1.41	3.87	8.75	613616
JFRC2010	ANTs A	8.73	7.64	1.73	6.08	20.10	622814
	ANTs B	5.58	4.27	1.58	4.58	10.51	661486
	ANTs C	5.92	4.65	1.58	4.74	11.53	681546
	CMTK A	8.66	7.35	1.73	6.12	19.74	686186
	CMTK C	7.34	5.86	1.73	5.70	15.26	772914
	CMTK B	7.79	6.78	1.58	5.52	18.03	664092

Table S39: LO_L : lobula

Template	Algorithm	Mean	Std dev	10th perc	median	90th perc	N
FCWB	ANTs A	5.04	3.13	1.58	4.53	9.22	10884
	ANTs B	6.54	4.05	1.73	5.87	12.27	9206
	ANTs C	6.17	3.63	2.00	5.74	10.46	8972
	CMTK A	7.47	5.15	1.73	6.56	15.38	9084
	CMTK C	5.56	3.97	1.41	4.47	11.15	15624
	CMTK B	7.05	5.13	1.58	5.87	14.78	11732
JFRC2013	ANTs A	4.80	3.12	1.41	4.18	9.17	13144
	ANTs B	5.84	3.59	1.73	5.15	10.67	14382
	ANTs C	5.23	2.96	1.73	4.74	9.11	14040
	CMTK A	4.61	3.11	1.41	4.00	8.75	14896
	CMTK C	4.62	3.18	1.41	3.87	8.66	21730
	CMTK B	4.47	3.07	1.22	3.67	8.73	16488
Tefor	ANTs A	4.98	3.09	1.58	4.36	9.49	11456
	ANTs B	5.66	3.35	1.73	5.15	10.07	10102
	ANTs C	5.95	3.29	2.12	5.52	10.54	10986
	CMTK A	7.10	6.07	1.58	5.20	15.36	11576
	CMTK C	6.30	3.81	1.73	5.57	11.85	12474
	CMTK B	7.16	5.58	1.58	5.57	15.52	11120
JRC2018	ANTs A	4.88	3.06	1.41	4.30	9.19	11708
	ANTs B	4.88	3.14	1.41	4.30	9.11	13174
	ANTs C	5.20	3.24	1.58	4.53	9.49	11572
	CMTK A	4.66	3.10	1.41	4.06	8.80	15284
	CMTK C	4.64	3.05	1.41	4.06	8.80	15242
	CMTK B	4.67	3.14	1.41	4.06	8.97	15040
JFRC2010	ANTs A	7.69	7.34	2.00	5.70	12.85	20148
	ANTs B	5.51	3.22	1.73	5.15	9.75	10686
	ANTs C	6.08	3.45	1.73	5.74	10.70	9926
	CMTK A	8.69	6.94	1.73	6.40	19.85	8478
	CMTK C	9.89	6.31	3.61	8.03	20.29	4994
	CMTK B	8.11	6.01	2.12	6.36	17.73	9118

Table S40: BU_L : bulb

Template	Algorithm	Mean	Std dev	10th perc	median	90th perc	N
FCWB	ANTs A	5.30	3.61	1.41	4.58	10.05	333478
	ANTs B	6.69	5.23	1.73	5.43	12.59	251700
	ANTs C	6.77	5.06	1.73	5.57	13.23	280818
	CMTK A	6.28	5.51	1.58	5.00	11.49	283790
	CMTK C	6.16	4.33	1.73	5.20	11.62	272040
	CMTK B	5.71	4.79	1.58	4.74	10.22	292828
JFRC2013	ANTs A	4.91	3.56	1.22	4.18	9.33	305420
	ANTs B	6.76	5.44	1.73	5.43	13.08	268188
	ANTs C	6.40	5.54	1.58	5.00	12.53	295292
	CMTK A	5.22	3.81	1.41	4.36	10.12	329340
	CMTK C	5.66	4.46	1.22	4.53	11.51	344122
	CMTK B	5.05	3.59	1.41	4.24	9.67	321452
Tefor	ANTs A	4.79	3.47	1.22	4.12	9.03	318946
	ANTs B	5.73	4.66	1.41	4.58	11.09	292186
	ANTs C	6.16	5.29	1.58	4.80	11.85	323302
	CMTK A	7.81	9.07	1.41	4.69	19.81	270274
	CMTK C	6.96	7.78	1.41	4.74	13.67	283214
	CMTK B	8.03	9.26	1.41	4.74	21.08	266200
JRC2018	ANTs A	4.79	3.41	1.22	4.12	9.03	320566
	ANTs B	5.58	4.40	1.41	4.53	10.79	297424
	ANTs C	5.67	4.24	1.58	4.69	11.07	326468
	CMTK A	4.85	3.35	1.41	4.18	9.00	322432
	CMTK C	5.11	3.58	1.41	4.36	9.62	297512
	CMTK B	4.85	3.36	1.41	4.18	9.03	309956
JFRC2010	ANTs A	6.13	4.69	1.58	5.00	12.10	273626
	ANTs B	5.76	4.97	1.41	4.53	11.40	271974
	ANTs C	6.34	5.18	1.58	5.00	12.43	282188
	CMTK A	6.44	4.69	1.58	5.34	12.83	438598
	CMTK C	7.00	4.97	1.73	5.79	13.95	397448
	CMTK B	6.35	4.62	1.58	5.20	12.53	401034

Table S41: LH_L : lateral horn

Template	Algorithm	Mean	Std dev	10th perc	median	90th perc	N
FCWB	ANTs A	6.46	4.88	1.58	5.15	13.51	51556
	ANTs B	6.12	4.14	1.58	5.15	12.02	120738
	ANTs C	6.83	4.37	2.12	5.92	12.92	100878
	CMTK A	10.56	6.07	3.24	9.75	19.09	112532
	CMTK C	7.61	5.18	2.12	6.36	15.20	65444
	CMTK B	9.70	6.01	2.65	8.72	17.96	53776
JFRC2013	ANTs A	5.21	5.12	1.00	3.61	11.70	54360
	ANTs B	7.38	4.93	2.12	6.20	14.58	91644
	ANTs C	6.90	4.50	2.00	5.87	13.34	72940
	CMTK A	6.47	5.64	1.58	4.58	14.58	43294
	CMTK C	5.98	4.45	1.58	4.80	12.21	89800
	CMTK B	7.08	5.56	1.58	5.43	14.88	47452
Tefor	ANTs A	5.19	5.03	1.22	3.61	11.58	52200
	ANTs B	6.19	4.87	1.58	4.74	13.06	46310
	ANTs C	7.95	5.61	2.00	6.44	16.19	60762
	CMTK A	9.46	6.19	2.12	8.54	18.00	67854
	CMTK C	11.13	6.97	2.92	10.00	21.19	60618
	CMTK B	9.42	6.09	2.24	8.34	18.18	69588
JRC2018	ANTs A	5.20	5.15	1.00	3.61	11.85	53098
	ANTs B	5.45	4.80	1.41	4.12	11.53	56144
	ANTs C	5.27	4.18	1.58	4.24	9.89	71594
	CMTK A	5.44	5.28	1.22	3.81	12.37	39660
	CMTK C	5.67	5.39	1.22	4.06	12.53	37522
	CMTK B	5.47	5.25	1.22	3.87	12.19	39286
JFRC2010	ANTs A	10.24	6.32	2.35	9.72	19.12	121430
	ANTs B	5.45	4.41	1.58	4.30	10.91	73844
	ANTs C	5.31	3.82	1.58	4.47	10.25	74074
	CMTK A	8.58	5.99	2.12	7.00	17.46	100410
	CMTK C	7.02	5.58	1.58	5.15	15.31	135452
	CMTK B	8.91	5.98	2.24	7.62	17.52	86462

Table S42: LAL_L : lateral accessory lobe

Template	Algorithm	Mean	Std dev	10th perc	median	90th perc	N
FCWB	ANTs A	4.29	2.90	1.22	3.61	8.19	24878
	ANTs B	4.21	3.01	1.00	3.54	8.19	27174
	ANTs C	3.90	2.76	1.00	3.32	7.38	28356
	CMTK A	4.30	2.86	1.00	3.81	8.06	73796
	CMTK C	4.20	2.89	1.00	3.61	8.09	45984
	CMTK B	4.52	3.13	1.22	3.87	8.37	39270
JFRC2013	ANTs A	4.55	3.08	1.22	3.87	8.63	23450
	ANTs B	3.66	2.60	1.00	3.08	7.07	43696
	ANTs C	3.62	2.66	1.00	3.00	7.28	42390
	CMTK A	4.54	3.05	1.41	3.87	8.74	24904
	CMTK C	4.44	2.77	1.41	3.87	8.06	40470
	CMTK B	4.47	3.08	1.22	3.81	8.57	25474
Tefor	ANTs A	4.60	3.06	1.41	3.87	8.66	23362
	ANTs B	4.36	2.94	1.41	3.67	8.28	22966
	ANTs C	4.42	2.99	1.00	3.81	8.43	34566
	CMTK A	4.50	2.81	1.41	4.06	8.15	30862
	CMTK C	5.17	3.15	1.58	4.74	9.51	20416
	CMTK B	4.40	2.80	1.41	3.87	8.09	30122
JRC2018	ANTs A	4.38	3.04	1.22	3.67	8.49	24512
	ANTs B	4.51	3.04	1.22	3.81	8.51	24614
	ANTs C	4.32	2.85	1.00	3.81	8.09	28654
	CMTK A	4.71	3.13	1.41	4.06	8.89	26174
	CMTK C	4.54	3.11	1.22	3.81	8.75	25846
	CMTK B	4.58	3.06	1.22	3.87	8.75	25826
JFRC2010	ANTs A	9.18	8.03	1.73	6.52	22.47	19372
	ANTs B	4.41	2.86	1.22	3.87	8.28	29064
	ANTs C	4.15	3.04	1.00	3.46	8.31	47732
	CMTK A	6.17	4.92	1.41	4.95	12.77	55044
	CMTK C	5.45	3.46	1.58	4.97	9.82	40106
	CMTK B	5.43	3.65	1.41	4.69	10.44	48774

Table S43: CAN_L : cantle

Template	Algorithm	Mean	Std dev	10th perc	median	90th perc	N
FCWB	ANTs A	5.02	5.21	1.22	3.81	8.75	191558
	ANTs B	5.99	6.27	1.58	4.53	10.61	145952
	ANTs C	6.04	6.38	1.58	4.53	10.61	155918
	CMTK A	5.36	4.79	1.58	4.36	9.25	192852
	CMTK C	5.59	5.49	1.58	4.24	9.95	173954
	CMTK B	5.44	4.99	1.58	4.36	9.43	193322
JFRC2013	ANTs A	4.99	5.45	1.22	3.81	8.60	178108
	ANTs B	6.12	6.46	1.58	4.53	10.61	144664
	ANTs C	5.97	6.28	1.58	4.36	10.44	150050
	CMTK A	5.53	5.62	1.58	4.24	9.64	173606
	CMTK C	6.09	5.81	1.58	4.64	10.77	145314
	CMTK B	5.68	5.88	1.58	4.36	9.95	164712
Tefor	ANTs A	4.74	5.09	1.22	3.67	7.94	199464
	ANTs B	5.56	6.03	1.58	4.18	9.43	174346
	ANTs C	5.98	6.43	1.58	4.47	10.51	183560
	CMTK A	5.15	5.13	1.22	4.00	9.43	218888
	CMTK C	5.24	5.10	1.58	4.18	8.97	207136
	CMTK B	5.09	5.11	1.22	4.06	9.00	219208
JRC2018	ANTs A	4.73	5.17	1.00	3.67	7.94	197440
	ANTs B	5.37	5.74	1.41	4.12	9.30	181890
	ANTs C	5.68	5.74	1.58	4.36	10.05	192824
	CMTK A	4.84	5.36	1.00	3.67	8.19	197642
	CMTK C	4.98	5.31	1.22	3.81	8.51	193026
	CMTK B	4.87	5.36	1.00	3.67	8.31	194334
JFRC2010	ANTs A	5.70	5.27	1.58	4.47	10.82	199226
	ANTs B	5.71	6.22	1.58	4.30	9.62	165386
	ANTs C	5.75	5.99	1.58	4.53	9.62	187140
	CMTK A	5.13	5.15	1.41	4.06	8.80	218338
	CMTK C	5.46	5.77	1.58	4.18	9.41	200846
	CMTK B	5.00	4.85	1.41	4.06	8.63	218734

Table S44: AMMC_L : antennal mechanosensory and motor center

Template	Algorithm	Mean	Std dev	10th perc	median	90th perc	N
FCWB	ANTs A	3.20	2.94	0.71	2.24	7.11	285442
	ANTs B	3.88	3.60	0.71	2.65	8.66	266108
	ANTs C	3.83	3.37	0.71	2.83	8.57	261238
	CMTK A	5.66	5.29	1.00	3.81	12.92	244344
	CMTK C	4.13	4.12	0.71	2.65	9.67	249120
	CMTK B	5.22	5.14	1.00	3.61	11.42	228770
JFRC2013	ANTs A	2.96	2.74	0.71	2.12	6.52	274140
	ANTs B	3.96	3.56	0.71	2.92	8.77	273296
	ANTs C	3.62	3.40	0.71	2.55	8.09	272964
	CMTK A	3.40	3.01	0.71	2.55	7.21	251372
	CMTK C	4.38	3.39	1.00	3.54	9.00	252590
	CMTK B	3.55	3.14	0.71	2.65	7.52	250490
Tefor	ANTs A	2.93	2.68	0.71	2.12	6.36	274682
	ANTs B	3.53	3.18	0.71	2.55	7.81	263076
	ANTs C	3.69	3.35	0.71	2.65	8.28	259718
	CMTK A	4.03	4.99	0.71	2.24	9.72	250548
	CMTK C	3.85	3.78	0.71	2.65	8.63	251828
	CMTK B	4.13	5.00	0.71	2.24	10.39	254716
JRC2018	ANTs A	2.94	2.70	0.71	2.12	6.44	277906
	ANTs B	3.11	2.86	0.71	2.24	6.86	275250
	ANTs C	3.13	2.86	0.71	2.24	6.86	270738
	CMTK A	2.92	2.79	0.71	2.12	6.44	247334
	CMTK C	2.94	2.76	0.71	2.12	6.44	256194
	CMTK B	2.90	2.78	0.71	2.12	6.36	250582
JFRC2010	ANTs A	4.63	5.27	0.71	3.00	9.87	320720
	ANTs B	3.82	3.56	0.71	2.65	8.57	258504
	ANTs C	4.28	3.80	0.71	3.16	9.46	250196
	CMTK A	5.17	6.01	0.71	2.65	14.58	265902
	CMTK C	5.19	5.25	0.71	3.24	12.61	266652
	CMTK B	5.00	5.50	0.71	2.83	13.13	270070

Table S45: ICL_L : inferior clamp

Template	Algorithm	Mean	Std dev	10th perc	median	90th perc	N
FCWB	ANTs A	3.99	2.92	1.00	3.16	8.09	11384
	ANTs B	5.02	3.67	1.00	4.24	10.15	6992
	ANTs C	4.93	3.36	1.00	4.24	9.85	7812
	CMTK A	4.93	4.05	1.00	3.61	10.89	10626
	CMTK C	4.24	3.16	1.00	3.46	8.94	12936
	CMTK B	5.38	4.32	1.00	4.18	11.73	12736
JFRC2013	ANTs A	3.84	2.84	1.00	3.00	7.94	11872
	ANTs B	5.09	3.29	1.22	4.53	9.67	8524
	ANTs C	4.72	3.32	1.00	3.87	9.62	9558
	CMTK A	3.95	2.87	1.00	3.24	7.91	13272
	CMTK C	4.15	2.84	1.00	3.54	8.09	14454
	CMTK B	4.21	2.92	1.00	3.61	8.28	13264
Tefor	ANTs A	3.80	2.74	1.00	3.00	7.81	12254
	ANTs B	4.17	2.81	1.00	3.54	8.25	10092
	ANTs C	4.12	2.67	1.00	3.54	8.09	12988
	CMTK A	5.52	5.63	0.71	4.03	10.89	12094
	CMTK C	4.59	2.86	1.41	4.06	8.86	14446
	CMTK B	5.52	5.54	0.71	3.81	11.02	11236
JRC2018	ANTs A	3.78	2.80	1.00	3.00	7.78	11756
	ANTs B	3.73	2.85	0.71	2.92	7.91	11878
	ANTs C	3.87	2.87	1.00	3.00	8.09	10400
	CMTK A	3.58	2.69	0.71	2.92	7.25	13240
	CMTK C	3.54	2.77	0.71	2.65	7.65	13292
	CMTK B	3.52	2.68	0.71	2.83	7.38	13728
JFRC2010	ANTs A	6.84	6.26	1.58	5.10	13.38	22424
	ANTs B	4.09	2.93	1.00	3.24	8.31	11390
	ANTs C	4.51	3.03	1.22	3.81	8.94	10434
	CMTK A	6.86	6.41	0.71	4.64	17.12	8222
	CMTK C	8.12	5.61	2.45	7.00	16.51	5620
	CMTK B	7.24	7.92	1.00	4.74	17.64	7780

Table S46: BU_R : bulb

Template	Algorithm	Mean	Std dev	10th perc	median	90th perc	N
FCWB	ANTs A	4.40	3.63	1.00	3.46	8.86	116374
	ANTs B	4.55	3.28	1.41	3.81	8.63	230142
	ANTs C	4.72	3.34	1.41	4.06	8.97	212550
	CMTK A	7.13	5.52	1.58	5.70	15.07	201758
	CMTK C	6.45	5.04	1.58	5.00	13.67	164182
	CMTK B	7.04	5.44	1.58	5.57	14.87	151708
JFRC2013	ANTs A	4.25	3.41	1.00	3.46	8.43	115754
	ANTs B	4.41	3.30	1.22	3.61	8.63	279706
	ANTs C	4.62	3.38	1.22	3.81	9.19	254522
	CMTK A	4.82	3.87	1.00	3.81	9.85	104886
	CMTK C	4.82	3.44	1.41	4.06	9.43	194618
	CMTK B	4.86	3.76	1.22	3.81	9.85	109968
Tefor	ANTs A	4.27	3.44	1.00	3.46	8.49	120644
	ANTs B	4.49	3.30	1.22	3.67	8.80	210210
	ANTs C	5.06	3.69	1.41	4.12	10.07	177482
	CMTK A	7.09	5.77	1.41	5.34	15.91	165070
	CMTK C	6.85	5.35	1.58	5.29	14.73	164558
	CMTK B	7.40	6.05	1.58	5.52	16.64	161920
JRC2018	ANTs A	4.27	3.46	1.00	3.46	8.54	114502
	ANTs B	4.62	3.49	1.22	3.81	9.08	141690
	ANTs C	4.59	3.38	1.22	3.81	9.19	145422
	CMTK A	4.50	3.55	1.00	3.61	9.00	106820
	CMTK C	4.55	3.67	1.00	3.61	8.97	103616
	CMTK B	4.47	3.55	1.00	3.61	8.94	101196
JFRC2010	ANTs A	8.55	6.91	1.58	6.36	18.72	127354
	ANTs B	4.52	3.28	1.22	3.67	8.89	247654
	ANTs C	4.86	3.57	1.22	4.06	9.75	276772
	CMTK A	6.36	5.11	1.41	4.95	13.66	181760
	CMTK C	5.85	4.72	1.41	4.53	12.23	258396
	CMTK B	6.46	5.21	1.41	4.95	14.16	161820

Table S47: VES_L : vest

Template	Algorithm	Mean	Std dev	10th perc	median	90th perc	N
FCWB	ANTs A	3.39	3.02	0.71	2.55	7.28	226180
	ANTs B	4.59	3.57	1.00	3.61	9.62	298536
	ANTs C	3.78	2.92	1.00	3.00	7.75	366938
	CMTK A	6.49	5.47	1.41	4.80	14.11	190292
	CMTK C	4.27	3.89	0.71	3.00	9.54	250136
	CMTK B	5.71	5.13	1.00	4.06	12.77	195356
JFRC2013	ANTs A	3.05	2.71	0.71	2.24	6.44	223036
	ANTs B	4.11	3.31	1.00	3.24	8.40	358766
	ANTs C	4.16	3.33	1.00	3.24	8.94	370482
	CMTK A	3.20	2.74	0.71	2.55	6.44	190126
	CMTK C	4.75	3.77	1.00	3.61	10.44	230108
	CMTK B	3.24	2.74	0.71	2.55	6.56	188414
Tefor	ANTs A	3.05	2.74	0.71	2.24	6.36	224680
	ANTs B	3.92	3.50	0.71	2.92	8.54	228986
	ANTs C	3.95	3.50	0.71	2.92	8.86	252914
	CMTK A	4.38	3.96	0.71	3.00	10.30	206084
	CMTK C	4.33	3.82	0.71	3.16	9.54	203452
	CMTK B	4.34	3.95	0.71	3.00	10.12	208340
JRC2018	ANTs A	2.93	2.66	0.71	2.24	6.04	223680
	ANTs B	3.32	3.02	0.71	2.35	7.21	224980
	ANTs C	3.24	2.91	0.71	2.35	7.04	228840
	CMTK A	3.19	2.96	0.71	2.35	6.71	195902
	CMTK C	3.04	2.70	0.71	2.24	6.36	197050
	CMTK B	3.11	2.84	0.71	2.24	6.56	190138
JFRC2010	ANTs A	4.88	4.21	1.00	3.61	10.58	232736
	ANTs B	4.08	3.54	0.71	3.00	8.72	256620
	ANTs C	4.10	3.17	1.00	3.24	8.54	390228
	CMTK A	4.73	4.69	0.71	3.16	10.58	242754
	CMTK C	4.62	4.98	1.00	3.00	10.51	338184
	CMTK B	4.88	5.42	0.71	3.08	11.27	254096

Table S48: IB_L : inferior bridge

Template	Algorithm	Mean	Std dev	10th perc	median	90th perc	N
FCWB	ANTs A	3.39	2.41	1.00	2.92	6.24	77720
	ANTs B	4.20	2.90	1.22	3.54	8.51	85288
	ANTs C	4.05	2.62	1.22	3.54	7.65	95052
	CMTK A	5.63	5.16	1.41	4.12	11.60	63522
	CMTK C	3.87	2.63	1.00	3.32	7.21	66826
	CMTK B	5.41	5.39	1.22	3.67	11.79	63758
JFRC2013	ANTs A	3.11	2.13	1.00	2.65	5.83	79242
	ANTs B	4.12	2.87	1.00	3.54	8.06	96460
	ANTs C	4.27	3.11	1.00	3.54	8.97	84404
	CMTK A	3.23	2.19	1.00	2.83	6.08	74162
	CMTK C	4.37	2.93	1.22	3.81	8.34	67292
	CMTK B	3.45	2.31	1.00	3.00	6.52	70046
Tefor	ANTs A	3.01	2.07	0.71	2.55	5.70	80992
	ANTs B	3.66	2.40	1.00	3.16	6.71	77408
	ANTs C	3.98	2.65	1.00	3.54	7.55	72348
	CMTK A	3.68	2.53	1.00	3.08	7.21	90296
	CMTK C	3.98	2.61	1.00	3.54	7.38	81148
	CMTK B	3.72	2.55	1.00	3.16	7.31	92468
JRC2018	ANTs A	3.01	2.07	0.71	2.55	5.70	80720
	ANTs B	3.13	2.14	1.00	2.65	5.79	74448
	ANTs C	3.30	2.19	1.00	2.92	6.08	74372
	CMTK A	3.21	2.18	1.00	2.83	6.08	79102
	CMTK C	3.16	2.13	1.00	2.65	5.87	77660
	CMTK B	3.17	2.14	1.00	2.65	6.04	78520
JFRC2010	ANTs A	3.93	2.88	1.00	3.24	7.55	81610
	ANTs B	3.92	2.70	1.00	3.32	7.58	80346
	ANTs C	4.33	2.83	1.22	3.81	8.28	87234
	CMTK A	5.17	5.09	1.00	3.81	9.85	76872
	CMTK C	4.63	3.99	1.00	3.67	8.37	81250
	CMTK B	4.92	4.71	1.00	3.61	9.43	77040

Table S49: ATL_L : antler

Template	Algorithm	Mean	Std dev	10th perc	median	90th perc	N
FCWB	ANTs A	5.44	5.40	1.00	3.54	12.81	154238
	ANTs B	8.57	5.63	2.24	7.42	16.54	96860
	ANTs C	7.82	5.85	1.73	6.52	15.59	124264
	CMTK A	6.76	5.42	1.58	5.10	14.83	115928
	CMTK C	6.24	5.03	1.41	4.64	13.67	142558
	CMTK B	6.12	5.02	1.41	4.53	13.53	124330
JFRC2013	ANTs A	4.34	3.99	1.00	3.08	9.30	156584
	ANTs B	6.90	5.20	1.58	5.52	14.25	130784
	ANTs C	5.65	4.97	1.22	4.12	12.27	149384
	CMTK A	5.37	4.35	1.22	4.12	11.25	139624
	CMTK C	5.42	4.64	1.22	4.12	11.18	178982
	CMTK B	5.43	4.39	1.22	4.18	11.36	142824
Tefor	ANTs A	4.26	3.87	1.00	3.00	9.19	153390
	ANTs B	4.72	4.14	1.00	3.46	10.22	161208
	ANTs C	4.98	4.02	1.00	3.81	10.61	169534
	CMTK A	7.31	5.38	1.58	6.00	15.38	129854
	CMTK C	5.18	4.48	1.00	3.81	11.34	209880
	CMTK B	6.96	5.27	1.58	5.57	14.78	122228
JRC2018	ANTs A	4.43	3.96	1.00	3.16	9.49	150742
	ANTs B	4.93	4.29	1.00	3.61	10.70	145352
	ANTs C	5.01	4.23	1.00	3.81	10.58	144126
	CMTK A	4.68	4.01	1.00	3.54	9.85	128454
	CMTK C	4.66	3.98	1.00	3.54	9.71	135654
	CMTK B	4.58	3.99	1.00	3.46	9.64	127400
JFRC2010	ANTs A	7.84	6.12	1.41	6.36	16.31	239816
	ANTs B	4.88	4.25	1.00	3.61	10.54	169636
	ANTs C	5.23	4.29	1.22	4.06	10.82	145186
	CMTK A	7.48	6.08	1.58	5.74	16.09	112646
	CMTK C	6.94	5.33	1.73	5.57	13.67	145274
	CMTK B	6.83	5.51	1.41	5.34	14.44	115154

Table S50: CRE_L : crepine

Template	Algorithm	Mean	Std dev	10th perc	median	90th perc	N
FCWB	ANTs A	5.69	4.37	1.41	4.53	11.77	56720
	ANTs B	5.22	4.13	1.00	4.06	11.07	55698
	ANTs C	5.15	3.93	1.00	4.12	10.46	59852
	CMTK A	6.47	4.99	1.41	5.10	13.47	51692
	CMTK C	5.15	4.14	1.00	3.87	11.07	63016
	CMTK B	6.40	4.77	1.58	5.20	13.15	52692
JFRC2013	ANTs A	5.12	3.96	1.22	3.87	10.82	67314
	ANTs B	6.59	4.53	1.73	5.57	12.81	54366
	ANTs C	5.77	4.19	1.58	4.74	11.49	54350
	CMTK A	5.55	4.14	1.41	4.36	11.51	68540
	CMTK C	5.63	4.18	1.41	4.58	11.42	58542
	CMTK B	5.65	4.23	1.41	4.53	11.60	69752
Tefor	ANTs A	5.09	3.90	1.22	4.00	10.61	71160
	ANTs B	5.44	4.00	1.41	4.36	11.07	62306
	ANTs C	5.74	4.04	1.58	4.74	11.38	67984
	CMTK A	6.10	5.02	1.41	4.47	13.42	67056
	CMTK C	5.67	4.40	1.41	4.36	12.04	67684
	CMTK B	6.05	4.97	1.41	4.30	13.47	64964
JRC2018	ANTs A	5.16	3.96	1.22	4.06	10.72	69302
	ANTs B	5.29	4.01	1.22	4.18	10.91	68308
	ANTs C	5.25	3.99	1.41	4.12	10.82	66266
	CMTK A	5.16	4.01	1.22	3.87	10.89	67844
	CMTK C	5.21	4.01	1.41	4.06	10.98	67636
	CMTK B	5.15	3.99	1.22	3.87	10.86	67512
JFRC2010	ANTs A	7.15	8.01	1.58	4.74	13.96	91380
	ANTs B	6.23	4.28	1.58	5.29	12.41	60494
	ANTs C	6.42	4.30	1.58	5.52	12.59	58210
	CMTK A	6.66	5.24	1.41	5.05	14.39	60120
	CMTK C	6.46	4.58	1.58	5.34	13.29	74938
	CMTK B	6.41	4.97	1.58	5.00	13.58	81492

Table S51: MB_PED_L : pedunculus of adult mushroom body

Template	Algorithm	Mean	Std dev	10th perc	median	90th perc	N
FCWB	ANTs A	5.52	4.32	1.58	4.47	10.72	111644
	ANTs B	5.28	3.92	1.58	4.36	10.12	79092
	ANTs C	5.35	3.99	1.58	4.47	9.95	89654
	CMTK A	5.57	4.27	1.58	4.53	10.72	102496
	CMTK C	5.27	3.81	1.58	4.36	9.90	80306
	CMTK B	5.52	4.20	1.58	4.47	10.65	97158
JFRC2013	ANTs A	5.30	4.15	1.58	4.36	9.72	111872
	ANTs B	6.16	4.33	1.73	5.20	11.55	93068
	ANTs C	5.94	4.30	1.58	5.00	10.98	101550
	CMTK A	5.69	4.51	1.58	4.53	11.07	115624
	CMTK C	6.10	4.25	1.73	5.20	11.20	95824
	CMTK B	5.78	4.45	1.58	4.74	10.86	108634
Tefor	ANTs A	4.68	3.99	1.22	3.61	9.06	133834
	ANTs B	5.44	4.21	1.58	4.36	10.22	98620
	ANTs C	5.42	4.10	1.58	4.47	10.39	106004
	CMTK A	6.81	6.93	1.41	4.36	17.04	138644
	CMTK C	6.19	4.42	1.73	5.15	11.85	98746
	CMTK B	6.37	5.81	1.58	4.53	14.76	129842
JRC2018	ANTs A	4.68	4.02	1.22	3.61	9.00	131582
	ANTs B	5.28	4.16	1.58	4.24	10.00	115318
	ANTs C	5.38	4.24	1.58	4.36	10.46	122964
	CMTK A	4.72	4.15	1.22	3.61	9.25	128888
	CMTK C	5.32	4.16	1.58	4.30	9.95	119020
	CMTK B	4.94	4.14	1.41	3.81	9.43	126064
JFRC2010	ANTs A	5.89	5.05	1.58	4.53	11.60	135494
	ANTs B	5.65	4.23	1.58	4.58	10.79	93942
	ANTs C	6.06	4.52	1.58	5.00	11.62	98208
	CMTK A	5.18	3.90	1.58	4.30	9.62	124950
	CMTK C	5.96	4.32	1.73	5.05	10.98	88886
	CMTK B	5.24	4.13	1.58	4.24	9.85	121466

Table S52: MB_VL_L : vertical lobe of adult mushroom body

Template	Algorithm	Mean	Std dev	10th perc	median	90th perc	N
FCWB	ANTs A	4.68	4.37	1.00	3.32	10.02	194636
	ANTs B	5.36	4.39	1.41	4.12	11.16	155400
	ANTs C	5.27	4.51	1.22	3.87	10.98	184730
	CMTK A	5.60	4.75	1.41	4.18	11.79	193610
	CMTK C	5.02	4.18	1.22	3.81	10.61	178880
	CMTK B	5.41	4.57	1.41	4.06	11.49	192134
JFRC2013	ANTs A	4.09	3.70	1.00	3.00	8.28	229810
	ANTs B	5.87	4.82	1.58	4.53	12.02	161752
	ANTs C	5.25	4.78	1.00	3.81	10.79	168914
	CMTK A	5.09	4.26	1.22	3.81	10.63	207446
	CMTK C	4.82	4.39	1.00	3.54	10.10	182974
	CMTK B	5.16	4.28	1.22	3.87	10.68	206382
Tefor	ANTs A	4.10	3.68	1.00	3.08	8.19	238708
	ANTs B	4.27	3.74	1.00	3.24	8.75	229654
	ANTs C	4.69	4.24	1.00	3.54	9.62	222946
	CMTK A	5.67	4.65	1.41	4.36	11.94	218430
	CMTK C	5.21	4.51	1.22	3.81	11.18	226658
	CMTK B	5.61	4.57	1.41	4.36	11.60	218734
JRC2018	ANTs A	4.04	3.70	1.00	3.00	8.09	239818
	ANTs B	4.31	3.80	1.00	3.24	8.75	224826
	ANTs C	4.36	3.82	1.00	3.32	8.57	224532
	CMTK A	4.35	3.78	1.00	3.32	8.57	223708
	CMTK C	4.44	3.79	1.00	3.46	8.77	217188
	CMTK B	4.32	3.74	1.00	3.32	8.51	219828
JFRC2010	ANTs A	6.26	6.06	1.22	4.18	14.04	219070
	ANTs B	4.23	3.85	1.00	3.16	8.63	246608
	ANTs C	4.54	3.96	1.00	3.46	9.33	226850
	CMTK A	6.60	6.36	1.41	4.47	15.56	201488
	CMTK C	5.73	5.51	1.22	4.00	12.41	235838
	CMTK B	5.41	4.84	1.00	3.87	11.77	209146

Table S53: MB_ML_L : medial lobe of adult mushroom body

Template	Algorithm	Mean	Std dev	10th perc	median	90th perc	N
FCWB	ANTs A	2.88	2.54	0.71	2.24	5.70	408720
	ANTs B	3.69	2.86	1.00	3.00	7.07	325596
	ANTs C	3.55	3.06	0.71	2.92	6.93	361668
	CMTK A	3.41	2.97	0.71	2.92	6.56	379116
	CMTK C	3.34	2.69	0.71	2.65	6.52	341304
	CMTK B	3.28	3.08	0.71	2.65	6.24	397938
JFRC2013	ANTs A	2.87	2.45	0.71	2.24	5.70	392302
	ANTs B	4.25	3.38	1.00	3.54	8.00	277230
	ANTs C	3.78	3.16	1.00	3.00	7.21	295372
	CMTK A	2.94	2.38	0.71	2.35	5.79	420952
	CMTK C	3.43	2.58	1.00	2.92	6.56	335392
	CMTK B	2.95	2.41	0.71	2.35	5.79	412536
Tefor	ANTs A	2.86	2.48	0.71	2.24	5.70	403824
	ANTs B	3.58	2.96	0.71	2.92	6.86	346276
	ANTs C	3.52	2.99	0.71	2.92	6.71	395204
	CMTK A	3.30	2.76	0.71	2.65	6.67	431620
	CMTK C	3.74	3.06	1.00	3.00	7.11	375272
	CMTK B	3.43	2.85	0.71	2.83	6.86	402012
JRC2018	ANTs A	2.81	2.40	0.71	2.24	5.57	397460
	ANTs B	3.25	2.70	0.71	2.65	6.36	381326
	ANTs C	3.36	2.78	0.71	2.65	6.56	385464
	CMTK A	2.84	2.38	0.71	2.24	5.57	441218
	CMTK C	2.87	2.41	0.71	2.35	5.70	403114
	CMTK B	2.82	2.37	0.71	2.24	5.57	421384
JFRC2010	ANTs A	5.63	6.45	0.71	3.24	15.64	336696
	ANTs B	3.76	3.13	0.71	3.00	7.31	351018
	ANTs C	3.55	3.08	0.71	2.92	7.07	401822
	CMTK A	3.70	3.28	0.71	2.92	7.28	369328
	CMTK C	4.29	3.85	1.00	3.24	8.54	336458
	CMTK B	3.69	3.45	0.71	2.92	7.11	373918

Table S54: FLA_L : flange

Template	Algorithm	Mean	Std dev	10th perc	median	90th perc	N
FCWB	ANTs A	6.24	5.72	1.58	4.69	12.27	398870
	ANTs B	6.45	5.34	1.73	5.00	12.67	336656
	ANTs C	6.78	5.60	1.73	5.34	13.06	359718
	CMTK A	8.02	6.59	2.12	6.36	15.67	388196
	CMTK C	8.46	6.90	2.12	6.44	17.48	344492
	CMTK B	7.79	6.42	2.12	6.08	15.39	365136
JFRC2013	ANTs A	5.92	5.50	1.58	4.53	11.62	398430
	ANTs B	6.59	5.39	1.73	5.20	12.85	388774
	ANTs C	6.85	5.83	1.58	5.29	13.71	393766
	CMTK A	7.14	7.56	1.58	5.00	14.39	424038
	CMTK C	6.93	5.24	2.00	5.70	13.29	434874
	CMTK B	7.35	7.94	1.58	5.10	14.21	422190
Tefor	ANTs A	5.69	5.25	1.41	4.30	11.36	403146
	ANTs B	6.16	5.41	1.58	4.80	11.87	354400
	ANTs C	6.98	5.50	2.00	5.70	13.38	360948
	CMTK A	7.75	6.90	1.58	5.57	16.64	400468
	CMTK C	7.05	5.80	1.73	5.52	14.05	371694
	CMTK B	7.79	6.80	1.58	5.70	16.52	388860
JRC2018	ANTs A	5.66	5.19	1.41	4.24	11.34	405342
	ANTs B	5.86	5.18	1.58	4.53	11.40	389376
	ANTs C	6.16	5.30	1.58	4.74	12.17	399826
	CMTK A	5.60	5.11	1.41	4.24	11.07	426888
	CMTK C	5.79	5.17	1.58	4.47	11.34	401586
	CMTK B	5.64	5.21	1.41	4.24	11.18	414846
JFRC2010	ANTs A	8.63	6.87	2.24	6.86	16.78	362688
	ANTs B	6.77	5.48	2.00	5.52	12.59	338210
	ANTs C	7.04	5.55	2.00	5.70	13.29	401672
	CMTK A	8.76	6.66	2.24	6.96	17.96	409008
	CMTK C	7.38	5.53	2.12	5.92	14.53	433212
	CMTK B	7.88	5.87	2.12	6.36	15.91	383972

Table S55: LOP_L : lobula plate

Template	Algorithm	Mean	Std dev	10th perc	median	90th perc	N
FCWB	ANTs A	4.42	3.39	1.00	3.54	9.22	189324
	ANTs B	5.08	3.41	1.22	4.36	9.85	186316
	ANTs C	5.08	3.43	1.22	4.36	9.87	205584
	CMTK A	5.81	5.12	1.22	4.53	11.36	135822
	CMTK C	4.99	3.76	1.00	4.06	10.54	147642
	CMTK B	5.48	5.00	1.00	4.24	10.72	167728
JFRC2013	ANTs A	3.84	3.07	0.71	3.00	8.19	219702
	ANTs B	4.39	3.10	1.00	3.67	8.75	226656
	ANTs C	4.61	3.18	1.00	3.87	9.11	228424
	CMTK A	3.38	2.53	0.71	2.65	6.96	180538
	CMTK C	4.73	3.30	1.00	4.06	9.46	136042
	CMTK B	3.58	2.65	1.00	2.92	7.25	166454
Tefor	ANTs A	3.34	2.61	0.71	2.65	6.71	228940
	ANTs B	4.52	3.26	1.00	3.81	9.17	176804
	ANTs C	5.21	3.79	1.22	4.30	10.58	195598
	CMTK A	4.03	3.05	1.00	3.24	8.43	215812
	CMTK C	4.65	3.36	1.00	3.81	9.30	169744
	CMTK B	4.16	3.21	1.00	3.32	8.75	207496
JRC2018	ANTs A	3.38	2.64	0.71	2.65	6.86	233940
	ANTs B	3.68	2.89	0.71	2.92	7.42	234506
	ANTs C	3.98	3.24	1.00	3.08	8.15	247940
	CMTK A	3.58	2.78	0.71	2.92	7.42	231020
	CMTK C	3.53	2.74	0.71	2.92	7.25	228440
	CMTK B	3.52	2.73	0.71	2.92	7.25	229874
JFRC2010	ANTs A	5.08	4.23	1.00	3.81	10.98	272138
	ANTs B	4.44	3.25	1.00	3.61	9.08	193424
	ANTs C	4.76	3.30	1.00	4.06	9.54	229120
	CMTK A	5.42	4.94	1.00	3.67	12.77	215634
	CMTK C	4.40	3.62	1.00	3.24	9.59	220518
	CMTK B	4.55	4.22	1.00	3.24	9.87	236674

Table S56: PB : protocerebral bridge

Template	Algorithm	Mean	Std dev	10th perc	median	90th perc	N
FCWB	ANTs A	3.61	2.50	1.00	3.08	6.40	1499740
	ANTs B	4.07	3.26	1.22	3.24	7.52	1022826
	ANTs C	4.35	3.77	1.22	3.32	8.31	1150918
	CMTK A	3.71	2.59	1.22	3.24	6.56	1546656
	CMTK C	3.76	2.62	1.22	3.24	6.67	1414018
	CMTK B	3.73	2.66	1.22	3.24	6.56	1535038
JFRC2013	ANTs A	3.26	1.97	1.00	3.00	5.74	1545570
	ANTs B	4.38	3.87	1.22	3.32	8.40	1084472
	ANTs C	4.13	3.49	1.22	3.24	7.65	1202770
	CMTK A	3.51	2.32	1.00	3.08	6.20	1462514
	CMTK C	3.78	2.74	1.22	3.16	6.86	1126876
	CMTK B	3.56	2.36	1.00	3.08	6.36	1412544
Tefor	ANTs A	3.22	1.91	1.00	2.92	5.66	1573310
	ANTs B	3.53	2.35	1.00	3.08	6.16	1479424
	ANTs C	3.86	3.12	1.22	3.24	6.71	1554168
	CMTK A	3.79	2.63	1.00	3.24	6.86	1546958
	CMTK C	4.05	3.22	1.22	3.24	7.42	1560302
	CMTK B	3.75	2.60	1.00	3.24	6.71	1583232
JRC2018	ANTs A	3.18	1.88	1.00	2.92	5.57	1575740
	ANTs B	3.55	2.33	1.00	3.16	6.20	1454164
	ANTs C	3.70	2.46	1.22	3.24	6.56	1474432
	CMTK A	3.19	1.88	1.00	2.92	5.57	1604044
	CMTK C	3.28	1.96	1.00	3.00	5.74	1577672
	CMTK B	3.20	1.87	1.00	2.92	5.57	1605078
JFRC2010	ANTs A	5.08	5.52	1.22	3.54	10.32	1320934
	ANTs B	3.63	2.49	1.22	3.16	6.36	1378504
	ANTs C	3.69	2.55	1.22	3.24	6.44	1538688
	CMTK A	4.10	3.52	1.22	3.24	7.28	1392898
	CMTK C	4.13	3.23	1.22	3.46	7.55	1351974
	CMTK B	3.80	2.81	1.22	3.24	6.71	1415636

Table S57: AL_L : adult antennal lobe

Template	Algorithm	Mean	Std dev	10th perc	median	90th perc	N
FCWB	ANTs A	5.01	4.45	1.58	4.24	8.77	3183810
	ANTs B	5.48	4.72	1.58	4.69	9.51	3063022
	ANTs C	6.04	4.63	2.00	5.20	10.70	3139250
	CMTK A	6.42	5.41	1.73	5.15	12.25	3092300
	CMTK C	6.47	5.42	2.00	5.34	11.51	2966210
	CMTK B	6.10	5.18	1.73	5.00	11.25	3118278
JFRC2013	ANTs A	4.90	4.45	1.58	4.12	8.54	3117410
	ANTs B	5.35	4.71	1.58	4.53	9.33	2892702
	ANTs C	5.63	4.82	1.58	4.74	9.95	3018516
	CMTK A	6.79	7.51	1.73	5.00	11.85	2609038
	CMTK C	6.09	4.47	2.12	5.34	10.46	2663474
	CMTK B	7.04	8.26	1.73	5.05	11.94	2576206
Tefor	ANTs A	4.75	4.25	1.41	4.06	8.31	3107898
	ANTs B	5.06	4.67	1.58	4.18	8.86	2912902
	ANTs C	5.75	5.05	1.58	4.74	10.12	3115598
	CMTK A	6.85	7.16	1.58	4.74	14.25	2831230
	CMTK C	6.57	7.25	1.58	4.74	11.87	2736262
	CMTK B	6.86	7.12	1.58	4.74	14.30	2839816
JRC2018	ANTs A	4.78	4.23	1.58	4.06	8.34	3135938
	ANTs B	5.04	4.50	1.58	4.24	8.77	3102894
	ANTs C	5.55	4.65	1.58	4.58	10.00	3145260
	CMTK A	4.83	4.37	1.58	4.12	8.34	3073602
	CMTK C	4.91	4.37	1.58	4.18	8.51	3136598
	CMTK B	4.82	4.43	1.58	4.12	8.31	3085844
JFRC2010	ANTs A	6.21	5.69	1.58	4.95	11.73	3208676
	ANTs B	5.10	4.60	1.58	4.30	8.86	2887600
	ANTs C	5.41	4.47	1.58	4.58	9.51	3165268
	CMTK A	6.17	5.53	1.58	4.95	11.42	3100936
	CMTK C	6.27	5.21	1.73	5.15	11.20	2840876
	CMTK B	5.86	5.42	1.58	4.69	10.61	3023396

Table S58: ME_L : medulla

Template	Algorithm	Mean	Std dev	10th perc	median	90th perc	N
FCWB	ANTs A	5.03	5.25	0.71	3.46	11.07	560066
	ANTs B	5.34	5.45	0.71	3.61	12.39	493738
	ANTs C	5.29	5.46	0.71	3.54	12.23	574654
	CMTK A	5.32	5.64	0.71	3.54	12.45	535526
	CMTK C	4.92	5.02	0.71	3.24	11.45	526058
	CMTK B	5.21	5.47	0.71	3.54	12.02	544466
JFRC2013	ANTs A	4.13	4.72	0.71	2.35	10.07	580284
	ANTs B	5.68	5.77	0.71	3.81	13.42	500620
	ANTs C	5.34	5.58	0.71	3.46	12.77	558630
	CMTK A	5.03	4.66	1.00	3.61	10.91	493046
	CMTK C	5.83	5.23	1.00	4.24	12.65	486968
	CMTK B	5.03	4.58	1.00	3.67	10.82	514176
Tefor	ANTs A	3.82	4.39	0.71	2.12	9.22	579900
	ANTs B	4.55	4.82	0.71	2.92	10.77	584556
	ANTs C	4.99	5.10	0.71	3.32	11.42	631596
	CMTK A	5.64	7.63	0.71	2.45	15.91	586094
	CMTK C	5.30	5.94	0.71	3.16	13.06	631288
	CMTK B	5.65	7.38	0.71	2.65	15.18	581586
JRC2018	ANTs A	3.77	4.29	0.71	2.12	9.08	568444
	ANTs B	4.29	5.01	0.71	2.24	10.82	565658
	ANTs C	4.53	5.18	0.71	2.65	11.00	601494
	CMTK A	3.82	4.19	0.71	2.24	9.06	573080
	CMTK C	4.09	4.71	0.71	2.24	9.95	575064
	CMTK B	3.79	4.27	0.71	2.24	9.08	560844
JFRC2010	ANTs A	5.48	6.14	0.71	3.32	13.23	606516
	ANTs B	4.67	4.99	0.71	2.92	11.07	542156
	ANTs C	4.85	5.32	0.71	2.92	11.62	587638
	CMTK A	5.89	6.81	0.71	3.16	15.39	642956
	CMTK C	6.18	6.99	0.71	3.24	16.26	566916
	CMTK B	6.57	7.61	0.71	3.61	17.52	698112

Table S59: SLP_L : superior lateral protocerebrum

Template	Algorithm	Mean	Std dev	10th perc	median	90th perc	N
FCWB	ANTs A	6.75	5.69	1.22	5.10	14.59	108758
	ANTs B	5.04	4.82	1.00	3.61	10.72	101844
	ANTs C	5.00	4.61	1.00	3.61	10.61	115356
	CMTK A	6.31	5.14	1.58	5.00	12.67	78828
	CMTK C	5.46	4.73	1.00	4.18	11.42	108796
	CMTK B	6.12	5.07	1.58	4.80	12.04	80406
JFRC2013	ANTs A	4.92	4.25	1.00	3.81	9.99	99962
	ANTs B	6.26	5.08	1.41	4.95	13.23	101214
	ANTs C	5.38	4.40	1.22	4.24	10.82	105364
	CMTK A	5.67	4.62	1.00	4.47	12.10	110080
	CMTK C	5.86	4.37	1.41	4.95	11.51	105472
	CMTK B	5.76	4.72	1.22	4.53	12.39	109792
Tefor	ANTs A	4.83	4.16	1.00	3.67	9.72	95462
	ANTs B	5.12	4.49	1.00	3.81	10.63	96784
	ANTs C	5.53	4.55	1.41	4.36	11.07	118818
	CMTK A	6.36	5.75	1.00	4.53	15.00	103720
	CMTK C	6.19	5.00	1.41	4.74	13.13	129028
	CMTK B	6.22	5.35	1.22	4.58	13.95	103650
JRC2018	ANTs A	4.82	4.15	1.00	3.67	9.85	99134
	ANTs B	5.16	4.57	1.00	3.87	10.82	90884
	ANTs C	5.30	4.63	1.00	4.06	10.89	93564
	CMTK A	4.76	4.11	1.00	3.61	9.67	102790
	CMTK C	4.98	4.31	1.00	3.81	10.32	91042
	CMTK B	4.78	4.21	1.00	3.61	9.85	97670
JFRC2010	ANTs A	8.20	5.96	2.12	6.96	15.95	157422
	ANTs B	5.01	4.55	1.00	3.67	10.54	99662
	ANTs C	5.42	4.87	1.00	4.00	11.53	100246
	CMTK A	5.63	4.72	1.00	4.36	12.04	93114
	CMTK C	6.37	5.29	1.22	4.80	14.00	89592
	CMTK B	5.57	4.76	1.00	4.24	12.04	91852

Table S60: SIP_L : superior intermediate protocerebrum

Template	Algorithm	Mean	Std dev	10th perc	median	90th perc	N
FCWB	ANTs A	2.78	2.84	0.71	2.00	6.00	1993800
	ANTs B	3.34	2.97	0.71	2.55	6.96	1546890
	ANTs C	3.26	2.97	0.71	2.45	6.86	1817190
	CMTK A	3.28	3.13	0.71	2.35	7.00	1760952
	CMTK C	3.24	2.99	0.71	2.35	7.00	1673578
	CMTK B	3.16	3.02	0.71	2.24	6.67	1789962
JFRC2013	ANTs A	2.55	2.52	0.71	1.73	5.43	1978286
	ANTs B	2.86	2.80	0.71	2.12	6.08	1878714
	ANTs C	2.79	2.79	0.71	2.00	6.00	1961782
	CMTK A	2.86	2.84	0.71	2.12	6.08	1808334
	CMTK C	3.24	2.86	0.71	2.45	6.86	1874888
	CMTK B	2.97	2.90	0.71	2.12	6.40	1785804
Tefor	ANTs A	2.54	2.54	0.71	1.73	5.34	1953734
	ANTs B	2.70	2.53	0.71	2.12	5.70	1875044
	ANTs C	2.76	2.62	0.71	2.12	5.83	1996512
	CMTK A	3.52	3.77	0.71	2.24	7.91	1744916
	CMTK C	3.09	2.97	0.71	2.24	6.56	1797932
	CMTK B	3.50	3.82	0.71	2.24	7.81	1736936
JRC2018	ANTs A	2.56	2.57	0.71	1.73	5.43	1956318
	ANTs B	2.67	2.61	0.71	2.00	5.66	1819568
	ANTs C	2.64	2.64	0.71	2.00	5.57	1914416
	CMTK A	2.55	2.46	0.71	2.00	5.20	1955892
	CMTK C	2.67	2.58	0.71	2.00	5.57	1853804
	CMTK B	2.60	2.49	0.71	2.00	5.34	1883916
JFRC2010	ANTs A	4.49	4.76	0.71	2.92	10.22	2048810
	ANTs B	2.87	2.69	0.71	2.12	6.08	1844162
	ANTs C	2.88	2.82	0.71	2.12	6.12	1905962
	CMTK A	3.98	4.46	0.71	2.55	8.80	1538652
	CMTK C	4.04	4.26	0.71	2.65	9.22	1457268
	CMTK B	3.60	3.65	0.71	2.45	8.03	1604384

Table S61: SMP_L : superior medial protocerebrum

Template	Algorithm	Mean	Std dev	10th perc	median	90th perc	N
FCWB	ANTs A	5.63	4.53	1.41	4.53	11.00	675074
	ANTs B	6.54	4.68	1.73	5.52	12.83	548688
	ANTs C	6.57	4.86	1.58	5.43	13.15	595164
	CMTK A	6.05	4.46	1.58	5.00	11.70	656072
	CMTK C	6.35	4.55	1.58	5.34	12.27	568660
	CMTK B	5.88	4.45	1.58	4.95	11.38	650172
JFRC2013	ANTs A	4.99	3.98	1.22	4.12	9.49	712030
	ANTs B	6.91	4.97	1.73	5.74	13.58	560778
	ANTs C	6.43	4.97	1.58	5.15	12.83	630090
	CMTK A	5.87	4.37	1.58	4.95	11.42	667434
	CMTK C	6.65	4.64	1.73	5.57	12.90	526864
	CMTK B	5.96	4.40	1.58	5.00	11.60	647920
Tefor	ANTs A	4.98	3.94	1.22	4.12	9.41	732900
	ANTs B	5.71	4.35	1.58	4.69	11.16	671192
	ANTs C	6.29	4.68	1.58	5.20	12.37	718464
	CMTK A	6.74	7.06	1.41	4.64	14.51	742970
	CMTK C	6.57	5.97	1.58	5.00	13.32	669718
	CMTK B	6.74	7.00	1.41	4.64	14.65	728246
JRC2018	ANTs A	4.95	3.93	1.22	4.12	9.33	718986
	ANTs B	5.34	4.18	1.41	4.36	10.39	698242
	ANTs C	5.57	4.27	1.58	4.53	10.72	736770
	CMTK A	4.95	3.89	1.22	4.12	9.25	713194
	CMTK C	5.17	4.01	1.41	4.30	9.72	688070
	CMTK B	4.98	3.92	1.41	4.12	9.30	698056
JFRC2010	ANTs A	7.82	6.24	1.73	5.87	17.39	698640
	ANTs B	5.94	4.43	1.58	5.00	11.51	648902
	ANTs C	6.32	4.71	1.58	5.20	12.41	734882
	CMTK A	6.25	4.86	1.58	5.00	12.67	858926
	CMTK C	6.58	4.77	1.73	5.52	12.90	798272
	CMTK B	6.12	4.78	1.58	4.95	12.37	847098

Table S62: AVLP_L : anterior ventrolateral protocerebrum

Template	Algorithm	Mean	Std dev	10th perc	median	90th perc	N
FCWB	ANTs A	6.04	5.00	1.22	4.53	13.08	157390
	ANTs B	7.11	5.37	1.73	5.74	14.39	156264
	ANTs C	7.10	5.52	1.58	5.70	14.28	154378
	CMTK A	6.89	5.18	1.58	5.74	13.32	152632
	CMTK C	6.80	5.18	1.58	5.43	13.89	152840
	CMTK B	6.70	5.21	1.58	5.52	13.06	151664
JFRC2013	ANTs A	5.29	4.31	1.22	4.12	11.18	160822
	ANTs B	6.86	5.05	1.58	5.74	13.51	146820
	ANTs C	6.68	5.16	1.58	5.39	13.58	147114
	CMTK A	6.05	4.70	1.58	4.74	12.53	170840
	CMTK C	6.50	4.79	1.58	5.34	13.02	145374
	CMTK B	6.04	4.73	1.58	4.74	12.55	167216
Tefor	ANTs A	5.35	4.32	1.22	4.18	11.20	158444
	ANTs B	6.16	4.73	1.58	5.00	12.29	146406
	ANTs C	6.60	5.08	1.58	5.39	13.00	156388
	CMTK A	7.42	6.98	1.41	5.05	17.22	148962
	CMTK C	7.19	6.04	1.58	5.29	16.02	157190
	CMTK B	7.39	6.92	1.41	5.05	17.18	148222
JRC2018	ANTs A	5.32	4.35	1.22	4.12	11.18	160018
	ANTs B	5.64	4.67	1.22	4.36	11.87	154582
	ANTs C	5.62	4.47	1.22	4.36	11.60	157128
	CMTK A	5.48	4.42	1.22	4.18	11.60	151870
	CMTK C	5.40	4.40	1.22	4.18	11.27	155220
	CMTK B	5.46	4.46	1.22	4.18	11.60	152622
JFRC2010	ANTs A	9.11	6.66	2.00	7.42	19.12	187494
	ANTs B	6.46	4.85	1.58	5.29	12.83	147296
	ANTs C	6.65	5.10	1.58	5.52	13.00	152126
	CMTK A	9.76	7.61	1.73	7.58	21.79	202130
	CMTK C	9.66	7.31	2.12	7.52	21.07	231152
	CMTK B	9.15	7.12	1.73	7.14	19.92	197878

Table S63: PVLP_L : posterior ventrolateral protocerebrum

Template	Algorithm	Mean	Std dev	10th perc	median	90th perc	N
FCWB	ANTs A	5.39	3.50	1.73	4.74	9.64	175478
	ANTs B	5.71	3.83	1.73	5.00	10.22	172314
	ANTs C	5.59	3.65	1.73	4.95	9.95	178622
	CMTK A	6.00	4.27	1.73	5.05	11.09	199722
	CMTK C	5.38	3.44	1.73	4.80	9.51	176718
	CMTK B	5.74	4.16	1.73	4.95	10.20	184238
JFRC2013	ANTs A	5.07	3.54	1.58	4.47	8.97	170302
	ANTs B	5.35	3.43	1.73	4.74	9.27	201282
	ANTs C	5.18	3.44	1.58	4.53	9.08	205812
	CMTK A	5.15	3.63	1.58	4.47	9.22	173202
	CMTK C	5.40	3.66	1.73	4.69	9.49	196884
	CMTK B	5.10	3.60	1.58	4.36	9.11	175770
Tefor	ANTs A	5.01	3.44	1.58	4.47	8.72	172432
	ANTs B	5.35	3.49	1.73	4.74	9.30	193554
	ANTs C	5.77	3.94	1.73	5.00	10.22	199872
	CMTK A	5.98	4.55	1.58	5.00	11.27	200804
	CMTK C	5.84	3.84	2.00	5.10	10.51	201972
	CMTK B	6.25	4.82	1.73	5.15	11.83	198428
JRC2018	ANTs A	5.05	3.50	1.58	4.36	8.86	168292
	ANTs B	5.15	3.51	1.58	4.53	9.11	176482
	ANTs C	5.17	3.41	1.58	4.53	8.97	189348
	CMTK A	5.12	3.48	1.58	4.53	8.97	164240
	CMTK C	5.16	3.54	1.58	4.53	9.19	164222
	CMTK B	5.13	3.51	1.58	4.53	9.06	161266
JFRC2010	ANTs A	6.17	4.57	1.73	5.15	11.94	195518
	ANTs B	5.51	3.67	1.73	4.80	9.64	186276
	ANTs C	5.56	3.74	1.73	4.80	9.90	193810
	CMTK A	5.67	3.87	1.58	4.95	10.22	191244
	CMTK C	5.69	3.86	1.73	5.00	10.02	204724
	CMTK B	5.39	3.71	1.58	4.74	9.33	195038

Table S64: IVLP_L : wedge

Template	Algorithm	Mean	Std dev	10th perc	median	90th perc	N
FCWB	ANTs A	3.60	4.51	0.71	2.00	9.06	475416
	ANTs B	4.14	4.62	0.71	2.45	10.00	424340
	ANTs C	4.23	4.60	0.71	2.65	9.92	420268
	CMTK A	5.87	6.77	0.71	3.54	13.96	366682
	CMTK C	4.26	4.90	0.71	2.55	10.51	398244
	CMTK B	5.52	6.42	0.71	3.32	12.90	352618
JFRC2013	ANTs A	3.31	4.10	0.71	1.73	8.09	445348
	ANTs B	4.34	4.21	0.71	3.00	9.54	434152
	ANTs C	4.10	4.12	0.71	2.83	9.11	446134
	CMTK A	3.94	4.22	0.71	2.55	9.11	414136
	CMTK C	4.39	4.29	0.71	3.00	9.85	405546
	CMTK B	4.02	4.28	0.71	2.55	9.25	404460
Tefor	ANTs A	3.30	4.09	0.71	1.73	8.09	464996
	ANTs B	3.83	4.21	0.71	2.35	8.97	452548
	ANTs C	3.92	4.25	0.71	2.45	9.06	482426
	CMTK A	4.35	6.38	0.71	2.00	11.70	443760
	CMTK C	4.64	5.55	0.71	2.65	11.40	446180
	CMTK B	4.44	6.38	0.71	2.12	12.10	442604
JRC2018	ANTs A	3.29	4.08	0.71	1.73	8.09	455796
	ANTs B	3.43	4.03	0.71	2.12	8.12	465462
	ANTs C	3.58	4.01	0.71	2.12	8.34	474688
	CMTK A	3.28	4.04	0.71	1.73	8.03	446974
	CMTK C	3.32	4.07	0.71	2.00	7.94	434284
	CMTK B	3.24	4.03	0.71	1.73	7.91	441626
JFRC2010	ANTs A	6.06	6.08	0.71	3.81	15.07	425196
	ANTs B	4.34	4.46	0.71	2.92	10.07	412812
	ANTs C	4.62	4.69	0.71	3.00	10.44	373646
	CMTK A	6.86	7.38	0.71	3.61	18.11	583892
	CMTK C	7.07	6.97	0.71	4.36	17.73	485036
	CMTK B	5.41	6.13	0.71	2.83	14.59	487112

Table S65: PLP_L : posterior lateral protocerebrum

Template	Algorithm	Mean	Std dev	10th perc	median	90th perc	N
FCWB	ANTs A	11.51	7.48	2.92	10.30	21.92	33530
	ANTs B	6.66	7.30	1.00	3.81	17.96	15710
	ANTs C	6.12	6.35	1.00	4.12	14.56	24774
	CMTK A	9.34	7.22	2.12	7.42	19.35	14154
	CMTK C	7.19	6.62	1.22	5.05	16.64	24994
	CMTK B	9.45	7.08	2.24	7.55	19.51	14176
JFRC2013	ANTs A	8.40	7.37	1.58	5.83	18.17	13596
	ANTs B	8.36	6.60	1.58	6.48	18.01	31014
	ANTs C	7.39	6.61	1.22	5.20	16.87	30028
	CMTK A	12.45	8.89	2.12	11.38	25.16	19976
	CMTK C	9.56	7.41	2.12	7.55	20.59	16956
	CMTK B	12.12	8.75	2.00	10.89	24.55	20068
Tefor	ANTs A	8.63	7.95	1.58	5.52	20.01	14782
	ANTs B	8.46	7.39	1.58	6.04	19.15	16114
	ANTs C	7.99	6.19	1.73	6.36	16.46	31686
	CMTK A	11.92	8.93	1.73	10.82	24.03	18692
	CMTK C	7.86	7.18	1.22	5.52	18.87	30052
	CMTK B	11.29	8.86	1.73	8.86	23.67	19294
JRC2018	ANTs A	8.89	8.13	1.58	5.79	20.91	13630
	ANTs B	8.60	8.03	1.58	5.34	20.81	12338
	ANTs C	8.76	7.56	1.58	6.36	19.72	14006
	CMTK A	8.80	7.94	1.58	5.87	19.96	13928
	CMTK C	8.81	7.96	1.58	5.74	20.11	12312
	CMTK B	9.00	8.06	1.58	5.92	20.44	13452
JFRC2010	ANTs A	16.33	9.44	4.58	15.33	29.28	80554
	ANTs B	8.68	7.33	1.58	6.24	19.61	14514
	ANTs C	8.93	6.97	2.00	7.00	18.79	17056
	CMTK A	12.81	10.30	1.73	10.22	29.03	17914
	CMTK C	13.05	9.56	2.55	10.82	27.29	16882
	CMTK B	13.30	10.06	2.12	11.42	28.78	22412

Table S66: AOTU_L : anterior optic tubercle

Template	Algorithm	Mean	Std dev	10th perc	median	90th perc	N
FCWB	ANTs A	5.35	3.65	1.58	4.58	10.05	346104
	ANTs B	6.27	4.08	2.00	5.43	11.68	267224
	ANTs C	6.37	4.30	1.73	5.43	12.10	293326
	CMTK A	6.10	4.05	1.73	5.20	11.60	289148
	CMTK C	6.31	4.46	1.73	5.29	12.19	278118
	CMTK B	5.86	3.92	1.58	5.00	11.27	297822
JFRC2013	ANTs A	5.11	3.58	1.58	4.36	9.62	318536
	ANTs B	5.92	4.02	1.58	5.10	11.27	259806
	ANTs C	6.06	4.16	1.58	5.15	11.60	314784
	CMTK A	5.55	3.98	1.58	4.53	11.05	351580
	CMTK C	5.42	4.16	1.22	4.47	11.07	340114
	CMTK B	5.46	3.87	1.58	4.53	10.84	350916
Tefor	ANTs A	4.83	3.46	1.22	4.12	9.22	326606
	ANTs B	5.29	3.64	1.58	4.53	9.92	301662
	ANTs C	5.55	3.92	1.58	4.74	10.51	332776
	CMTK A	7.51	7.92	1.41	4.74	19.31	276804
	CMTK C	6.62	6.75	1.58	4.69	13.34	282262
	CMTK B	7.83	8.48	1.41	4.74	21.24	266390
JRC2018	ANTs A	4.86	3.42	1.41	4.18	9.17	327132
	ANTs B	5.21	3.48	1.58	4.53	9.64	315620
	ANTs C	5.36	3.55	1.58	4.64	10.05	338732
	CMTK A	4.93	3.42	1.41	4.24	9.25	326348
	CMTK C	4.95	3.45	1.41	4.24	9.30	311878
	CMTK B	4.89	3.42	1.41	4.18	9.19	316248
JFRC2010	ANTs A	6.26	4.81	1.58	5.00	12.67	306006
	ANTs B	5.44	3.68	1.58	4.69	10.22	269522
	ANTs C	5.90	4.15	1.58	5.00	11.36	304562
	CMTK A	5.67	4.17	1.41	4.69	11.34	295072
	CMTK C	6.29	4.90	1.58	5.00	12.59	258870
	CMTK B	5.61	4.39	1.41	4.53	11.20	282530

Table S67: LH_R : lateral horn

Template	Algorithm	Mean	Std dev	10th perc	median	90th perc	N
FCWB	ANTs A	3.23	2.59	0.71	2.55	6.71	82426
	ANTs B	3.87	3.10	1.00	3.08	7.65	90258
	ANTs C	3.64	2.77	1.00	2.92	7.35	90864
	CMTK A	7.47	7.19	1.22	4.69	19.61	56578
	CMTK C	3.82	3.24	0.71	2.92	8.06	88790
	CMTK B	6.59	6.54	1.22	4.27	16.82	67432
JFRC2013	ANTs A	3.29	2.51	0.71	2.65	6.71	86924
	ANTs B	4.30	3.43	0.71	3.46	9.11	89722
	ANTs C	4.52	3.52	1.00	3.61	9.62	86652
	CMTK A	3.38	2.80	0.71	2.65	7.11	75820
	CMTK C	4.01	3.14	1.00	3.24	7.91	89236
	CMTK B	3.47	2.86	0.71	2.65	7.21	77116
Tefor	ANTs A	3.32	2.57	0.71	2.65	6.86	85508
	ANTs B	3.77	2.93	0.71	3.00	7.81	87320
	ANTs C	3.75	2.94	0.71	3.00	7.84	83340
	CMTK A	4.08	4.37	0.71	2.65	8.86	68066
	CMTK C	3.97	3.40	0.71	3.00	8.09	88896
	CMTK B	4.00	4.07	0.71	2.65	8.63	69704
JRC2018	ANTs A	3.30	2.50	0.71	2.65	6.71	87562
	ANTs B	3.52	2.70	0.71	2.92	7.14	87832
	ANTs C	3.41	2.71	0.71	2.65	7.07	80968
	CMTK A	3.35	2.71	0.71	2.65	7.14	71502
	CMTK C	3.42	2.60	0.71	2.83	7.00	84368
	CMTK B	3.34	2.69	0.71	2.65	7.11	73202
JFRC2010	ANTs A	5.60	4.18	1.41	4.53	11.42	87290
	ANTs B	4.03	3.40	0.71	3.00	8.75	88176
	ANTs C	4.59	3.90	0.71	3.46	10.22	72964
	CMTK A	5.30	5.32	0.71	3.24	12.90	82058
	CMTK C	4.54	4.27	0.71	3.16	10.25	72248
	CMTK B	4.87	5.09	0.71	3.00	11.49	76474

Table S68: GOR_L : gorget

Template	Algorithm	Mean	Std dev	10th perc	median	90th perc	N
FCWB	ANTs A	4.46	3.04	1.22	3.81	8.54	310260
	ANTs B	5.15	3.71	1.41	4.36	9.85	250986
	ANTs C	4.78	3.47	1.22	4.06	9.22	304398
	CMTK A	5.40	4.31	1.22	4.24	11.18	354154
	CMTK C	5.45	4.03	1.41	4.53	10.70	226302
	CMTK B	5.09	3.90	1.22	4.18	10.02	353338
JFRC2013	ANTs A	4.46	2.96	1.22	3.81	8.51	319094
	ANTs B	4.94	3.47	1.41	4.18	9.46	322084
	ANTs C	4.93	3.37	1.41	4.18	9.43	320916
	CMTK A	3.86	2.36	1.22	3.54	7.04	255508
	CMTK C	5.12	3.19	1.58	4.53	9.54	196572
	CMTK B	4.04	2.49	1.22	3.61	7.28	250828
Tefor	ANTs A	3.57	2.32	1.00	3.08	6.75	390314
	ANTs B	4.78	3.53	1.22	4.06	9.08	266852
	ANTs C	4.94	3.73	1.22	4.06	9.72	328196
	CMTK A	5.22	5.36	1.00	3.61	10.42	352240
	CMTK C	5.25	4.12	1.41	4.30	10.00	261764
	CMTK B	5.39	5.50	1.22	3.81	10.86	337534
JRC2018	ANTs A	3.62	2.36	1.00	3.08	6.86	393546
	ANTs B	4.27	3.01	1.00	3.61	8.06	369874
	ANTs C	4.07	2.74	1.00	3.54	7.65	394530
	CMTK A	3.85	2.47	1.00	3.32	7.28	413950
	CMTK C	4.11	2.58	1.22	3.61	7.65	382438
	CMTK B	3.91	2.50	1.00	3.46	7.42	401238
JFRC2010	ANTs A	4.60	3.06	1.41	4.00	8.66	386392
	ANTs B	5.16	3.80	1.41	4.36	9.85	282626
	ANTs C	4.70	3.34	1.22	4.06	8.97	359548
	CMTK A	4.70	3.43	1.22	3.87	9.11	366014
	CMTK C	5.13	3.61	1.41	4.36	9.87	275910
	CMTK B	4.52	3.05	1.22	3.87	8.51	386536

Table S69: MB_CA_L : calyx of adult mushroom body

Template	Algorithm	Mean	Std dev	10th perc	median	90th perc	N
FCWB	ANTs A	4.69	3.96	1.00	3.61	9.62	405374
	ANTs B	5.13	4.09	1.22	4.06	10.39	423360
	ANTs C	4.79	3.67	1.22	3.81	9.59	415376
	CMTK A	6.76	6.92	1.41	4.64	14.65	293282
	CMTK C	5.47	5.27	1.22	3.81	11.51	374896
	CMTK B	6.17	6.60	1.22	4.18	12.90	327190
JFRC2013	ANTs A	4.28	3.57	1.00	3.24	8.77	386086
	ANTs B	5.28	4.15	1.22	4.18	10.79	423082
	ANTs C	5.15	4.12	1.22	4.06	10.51	413470
	CMTK A	4.51	3.72	1.00	3.54	9.06	356370
	CMTK C	5.22	4.37	1.22	4.06	10.65	425034
	CMTK B	4.56	3.70	1.00	3.61	9.19	363436
Tefor	ANTs A	4.22	3.52	1.00	3.24	8.60	397556
	ANTs B	4.96	4.02	1.22	3.87	10.15	424108
	ANTs C	5.22	3.93	1.41	4.30	10.27	393994
	CMTK A	5.36	5.15	1.00	3.81	11.40	340272
	CMTK C	5.13	4.46	1.22	3.87	10.61	447014
	CMTK B	5.43	5.18	1.00	3.81	11.53	340788
JRC2018	ANTs A	4.20	3.54	1.00	3.24	8.60	390572
	ANTs B	4.68	3.78	1.00	3.61	9.54	376408
	ANTs C	4.66	3.68	1.00	3.67	9.30	357000
	CMTK A	4.67	3.86	1.00	3.61	9.33	330466
	CMTK C	4.44	3.73	1.00	3.54	8.94	327862
	CMTK B	4.58	3.82	1.00	3.61	9.25	321912
JFRC2010	ANTs A	7.31	6.16	1.58	5.43	16.28	494082
	ANTs B	5.33	4.21	1.22	4.24	10.82	451332
	ANTs C	5.23	3.98	1.22	4.24	10.44	481422
	CMTK A	6.76	6.10	1.22	4.69	15.56	310332
	CMTK C	6.59	6.31	1.22	4.53	15.52	465200
	CMTK B	6.43	5.86	1.22	4.47	14.75	335610

Table S70: SPS_L : superior posterior slope

Template	Algorithm	Mean	Std dev	10th perc	median	90th perc	N
FCWB	ANTs A	6.60	4.79	1.58	5.43	13.44	197364
	ANTs B	7.00	4.75	2.00	6.04	13.30	162610
	ANTs C	6.93	4.80	2.00	5.87	13.44	157050
	CMTK A	9.01	6.14	2.24	7.78	17.61	247140
	CMTK C	7.85	5.54	2.00	6.44	16.02	189734
	CMTK B	8.81	6.14	2.24	7.42	17.36	216198
JFRC2013	ANTs A	6.60	5.14	1.58	5.20	13.87	188088
	ANTs B	7.08	4.71	2.12	6.08	13.67	176902
	ANTs C	7.01	4.67	2.12	5.92	13.58	186466
	CMTK A	6.74	4.97	1.58	5.57	13.34	169248
	CMTK C	7.36	4.96	2.12	6.16	14.47	189470
	CMTK B	6.84	5.03	1.58	5.70	13.66	165164
Tefor	ANTs A	6.10	4.77	1.41	4.80	12.67	184588
	ANTs B	7.18	4.73	2.12	6.20	13.82	185350
	ANTs C	7.42	4.87	2.24	6.36	14.25	173904
	CMTK A	7.82	5.97	1.73	6.36	16.00	207344
	CMTK C	7.28	5.38	1.73	6.08	14.25	219074
	CMTK B	8.04	6.17	1.73	6.48	16.58	199956
JRC2018	ANTs A	6.00	4.82	1.41	4.58	12.37	185274
	ANTs B	7.11	5.05	1.73	5.92	14.07	172736
	ANTs C	7.17	4.98	2.00	6.04	14.09	171534
	CMTK A	6.51	4.92	1.58	5.20	13.29	167674
	CMTK C	6.90	5.24	1.58	5.57	14.05	158340
	CMTK B	6.58	4.99	1.58	5.34	13.42	161066
JFRC2010	ANTs A	10.21	7.50	2.55	8.49	19.87	209044
	ANTs B	7.29	4.89	2.12	6.20	14.16	183132
	ANTs C	7.08	4.81	2.12	6.00	13.62	193510
	CMTK A	9.10	5.86	2.35	7.94	17.73	167668
	CMTK C	8.03	5.76	2.00	6.44	16.57	213410
	CMTK B	8.03	5.57	2.12	6.86	15.91	166860

Table S71: IPS_L : inferior posterior slope

Template	Algorithm	Mean	Std dev	10th perc	median	90th perc	N
FCWB	ANTs A	3.33	3.60	0.71	2.00	8.19	319986
	ANTs B	3.42	3.76	0.71	2.12	8.34	291926
	ANTs C	3.35	3.61	0.71	2.12	8.25	304426
	CMTK A	3.99	4.81	0.71	2.24	9.85	252984
	CMTK C	3.02	3.57	0.71	1.73	7.11	311560
	CMTK B	3.97	4.56	0.71	2.35	9.62	258242
JFRC2013	ANTs A	2.50	2.65	0.71	1.58	5.83	330144
	ANTs B	3.35	3.48	0.71	2.12	8.12	306500
	ANTs C	3.03	3.19	0.71	1.73	7.25	325802
	CMTK A	3.16	2.93	0.71	2.24	6.96	308818
	CMTK C	3.73	3.27	0.71	2.83	7.94	296110
	CMTK B	3.17	2.98	0.71	2.24	7.00	309956
Tefor	ANTs A	2.47	2.61	0.71	1.58	5.74	332778
	ANTs B	2.82	2.96	0.71	1.73	6.67	318136
	ANTs C	3.08	3.17	0.71	2.00	7.25	337976
	CMTK A	2.94	4.01	0.71	1.58	6.96	320210
	CMTK C	3.01	3.52	0.71	1.73	6.86	323594
	CMTK B	2.96	4.03	0.71	1.58	7.00	317748
JRC2018	ANTs A	2.49	2.64	0.71	1.58	5.79	333308
	ANTs B	2.67	2.82	0.71	1.58	6.36	328600
	ANTs C	2.70	2.77	0.71	1.73	6.40	328444
	CMTK A	2.45	2.60	0.71	1.58	5.70	326512
	CMTK C	2.49	2.66	0.71	1.58	5.74	323692
	CMTK B	2.43	2.60	0.71	1.58	5.70	326858
JFRC2010	ANTs A	5.45	6.30	0.71	3.16	13.29	365908
	ANTs B	3.06	3.23	0.71	2.00	7.31	310344
	ANTs C	3.26	3.51	0.71	2.00	8.06	287574
	CMTK A	3.27	4.04	0.71	1.73	8.66	316734
	CMTK C	4.37	4.87	0.71	2.35	11.60	354038
	CMTK B	4.49	5.10	0.71	2.24	12.29	378216

Table S72: SCL_L : superior clamp

Template	Algorithm	Mean	Std dev	10th perc	median	90th perc	N
FCWB	ANTs A	5.23	4.08	1.22	4.12	11.20	10960
	ANTs B	6.99	5.39	1.73	5.52	14.23	11730
	ANTs C	7.27	6.43	1.58	5.00	17.12	10192
	CMTK A	6.68	6.66	1.58	4.53	14.18	5850
	CMTK C	5.27	5.93	1.00	3.54	10.39	7818
	CMTK B	7.74	6.83	1.73	5.74	16.23	7096
JFRC2013	ANTs A	4.77	3.64	1.00	3.67	9.92	11272
	ANTs B	9.05	6.85	2.35	6.86	19.91	8706
	ANTs C	9.88	7.18	2.12	7.84	20.63	8176
	CMTK A	4.65	3.55	1.00	3.61	9.85	7850
	CMTK C	5.58	5.37	1.00	3.81	11.86	8396
	CMTK B	4.74	3.66	1.00	3.67	9.85	7898
Tefor	ANTs A	4.50	3.44	1.00	3.54	9.43	10886
	ANTs B	7.67	6.47	1.58	5.52	17.77	8006
	ANTs C	8.40	7.11	1.58	5.87	19.31	6976
	CMTK A	5.39	6.92	1.00	3.00	11.40	5952
	CMTK C	7.15	6.19	1.41	5.52	15.48	10986
	CMTK B	5.38	6.77	1.00	3.16	11.83	6314
JRC2018	ANTs A	4.71	3.60	1.00	3.67	9.87	11212
	ANTs B	5.37	4.39	1.00	4.12	11.60	10352
	ANTs C	6.86	5.46	1.58	5.43	12.92	9650
	CMTK A	4.18	3.20	1.00	3.24	9.00	7242
	CMTK C	4.37	3.30	1.00	3.54	8.97	9412
	CMTK B	4.27	3.17	1.00	3.46	8.96	8104
JFRC2010	ANTs A	8.47	6.13	1.73	6.86	17.26	20800
	ANTs B	9.97	8.12	1.73	7.65	23.59	5310
	ANTs C	13.09	9.89	2.65	10.02	28.27	5350
	CMTK A	8.00	7.30	1.22	4.74	19.42	7936
	CMTK C	14.07	8.65	3.16	13.23	26.09	8348
	CMTK B	8.87	7.74	1.41	5.70	20.54	8882

Table S73: EPA_L : epaulette

Template	Algorithm	Mean	Std dev	10th perc	median	90th perc	N
FCWB	ANTs A	7.72	3.92	2.65	7.38	13.15	4658
	ANTs B	7.15	4.44	2.00	6.48	13.06	5524
	ANTs C	7.91	3.77	3.24	7.65	13.06	5910
	CMTK A	7.53	3.86	2.65	7.21	13.09	5108
	CMTK C	8.76	3.76	4.18	8.28	14.23	3826
	CMTK B	7.68	3.94	2.92	7.25	13.42	4854
JFRC2013	ANTs A	7.33	3.69	2.65	7.00	12.51	4904
	ANTs B	8.97	4.46	3.46	8.54	15.15	3702
	ANTs C	7.55	4.32	2.12	7.07	13.95	3488
	CMTK A	8.72	4.34	3.16	8.51	14.47	5628
	CMTK C	8.18	4.18	3.16	7.42	13.96	4600
	CMTK B	8.51	4.35	3.00	8.15	14.47	6310
Tefor	ANTs A	7.28	3.80	2.45	6.86	12.77	5312
	ANTs B	7.38	3.78	2.74	7.00	12.61	5956
	ANTs C	8.36	4.23	3.04	8.03	13.96	6816
	CMTK A	8.65	4.42	3.08	8.19	14.58	4492
	CMTK C	9.73	4.80	3.54	9.30	16.55	4354
	CMTK B	9.25	4.82	3.16	9.30	15.18	3766
JRC2018	ANTs A	7.19	3.76	2.35	6.71	12.53	5298
	ANTs B	7.43	3.86	2.45	7.11	12.83	5168
	ANTs C	7.36	3.79	2.65	6.86	12.71	6022
	CMTK A	7.32	3.82	2.55	6.86	12.77	4962
	CMTK C	7.40	4.02	2.24	7.11	13.08	5154
	CMTK B	7.28	3.86	2.35	6.86	12.93	4570
JFRC2010	ANTs A	9.79	6.88	2.92	8.28	19.30	6906
	ANTs B	7.66	3.98	2.65	7.14	13.30	5612
	ANTs C	8.22	4.27	3.00	7.66	14.03	6166
	CMTK A	8.41	4.06	3.08	8.28	13.67	4720
	CMTK C	8.29	4.46	2.65	8.03	14.37	7384
	CMTK B	8.17	4.24	2.54	7.84	13.95	7860

Table S74: GA_L : gall

Template	Algorithm	Mean	Std dev	10th perc	median	90th perc	N
FCWB	ANTs A	6.64	5.69	1.22	4.80	14.92	50220
	ANTs B	5.84	4.11	1.58	4.90	11.40	133492
	ANTs C	6.72	4.68	1.73	5.70	13.29	105324
	CMTK A	10.19	6.57	2.35	9.19	19.97	113524
	CMTK C	7.42	5.57	1.73	6.00	15.57	74432
	CMTK B	9.80	6.40	2.35	8.60	18.95	71940
JFRC2013	ANTs A	4.99	5.34	1.00	3.16	11.79	47072
	ANTs B	5.08	3.93	1.41	4.00	10.32	158968
	ANTs C	5.85	4.35	1.58	4.69	11.70	130506
	CMTK A	6.40	5.85	1.41	4.53	14.02	37398
	CMTK C	6.53	4.82	1.73	5.29	12.92	82804
	CMTK B	6.53	5.59	1.58	4.95	13.44	41744
Tefor	ANTs A	5.09	5.42	1.00	3.32	12.04	46480
	ANTs B	5.72	4.60	1.41	4.53	11.79	46570
	ANTs C	7.08	5.22	1.73	5.70	13.87	61358
	CMTK A	10.62	6.53	2.55	9.85	19.70	80892
	CMTK C	10.54	7.22	2.24	9.30	20.88	81748
	CMTK B	10.68	6.66	2.55	9.82	19.97	77374
JRC2018	ANTs A	5.15	5.55	1.00	3.24	12.19	46336
	ANTs B	5.76	4.82	1.22	4.53	11.60	53168
	ANTs C	5.79	4.12	1.58	4.95	10.72	75474
	CMTK A	5.81	5.89	1.00	3.81	13.73	33196
	CMTK C	5.93	5.92	1.22	4.06	13.65	35616
	CMTK B	5.85	5.90	1.00	3.87	13.74	32616
JFRC2010	ANTs A	11.57	7.57	2.35	10.46	22.11	176308
	ANTs B	5.99	5.23	1.41	4.53	12.77	53780
	ANTs C	6.01	5.24	1.41	4.53	12.67	48400
	CMTK A	9.96	6.65	2.35	8.66	19.67	95702
	CMTK C	8.47	5.69	2.12	7.25	16.75	102936
	CMTK B	10.80	7.19	2.35	9.54	21.38	84010

Table S75: LAL_R : lateral accessory lobe

Template	Algorithm	Mean	Std dev	10th perc	median	90th perc	N
FCWB	ANTs A	4.69	3.69	1.22	3.87	8.54	751334
	ANTs B	4.77	3.93	1.41	4.00	8.54	846026
	ANTs C	4.75	3.80	1.41	4.00	8.51	855024
	CMTK A	5.09	3.87	1.58	4.30	9.17	831892
	CMTK C	4.92	3.64	1.58	4.18	8.75	781292
	CMTK B	4.99	3.84	1.58	4.24	8.97	819294
JFRC2013	ANTs A	4.61	3.76	1.22	3.81	8.51	796100
	ANTs B	5.15	4.08	1.58	4.36	9.19	790572
	ANTs C	5.10	4.18	1.58	4.24	9.19	820998
	CMTK A	4.90	3.86	1.41	4.12	9.06	746112
	CMTK C	5.12	3.79	1.58	4.36	9.25	766278
	CMTK B	4.91	3.81	1.41	4.12	9.00	741396
Tefor	ANTs A	4.57	3.66	1.22	3.81	8.28	756640
	ANTs B	5.02	3.75	1.58	4.30	9.00	811812
	ANTs C	5.19	3.92	1.58	4.36	9.41	828668
	CMTK A	5.29	4.18	1.41	4.36	10.07	769982
	CMTK C	5.24	4.07	1.58	4.36	9.46	783740
	CMTK B	5.27	4.06	1.41	4.36	10.07	761656
JRC2018	ANTs A	4.57	3.85	1.22	3.81	8.28	757694
	ANTs B	4.89	3.77	1.58	4.12	8.77	783234
	ANTs C	5.05	3.89	1.58	4.24	9.08	815800
	CMTK A	4.60	3.88	1.22	3.81	8.40	751242
	CMTK C	4.63	3.70	1.41	3.81	8.40	733568
	CMTK B	4.57	3.77	1.22	3.81	8.37	739994
JFRC2010	ANTs A	5.97	5.35	1.58	4.53	11.62	815870
	ANTs B	4.85	3.71	1.58	4.12	8.63	856040
	ANTs C	4.95	3.89	1.58	4.18	8.86	901644
	CMTK A	5.16	4.13	1.58	4.18	9.62	867552
	CMTK C	5.13	4.05	1.58	4.24	9.19	846840
	CMTK B	5.00	3.96	1.58	4.12	9.17	846594

Table S76: SAD : saddle